Comparative Valuation Dynamics in Production Economies:

Long-run Uncertainty, Heterogeneity, and Market Frictions*

Lars Peter Hansen
University of Chicago
lhansen@uchicago.edu

Paymon Khorrami
Duke Unversity
paymon.khorrami@duke.edu

Fabrice Tourre
Baruch College, City University of New York
fabrice.tourre@gmail.com

June 12, 2024

Abstract

We compare and contrast production economies exposed to long-run uncertainty with investors that have possibly different preferences and/or access to financial markets. We study the macroeconomic and asset pricing properties of these models, identify common features and highlight areas where these models depart from each other. Our framework allows us to investigate more fully the impact of investor heterogeneity, capital heterogeneity, and fluctuations of the growth components to the capital evolution as they affect the dynamics of macroeconomic quantities and asset prices. In our comparisons, we employ an array of diagnostic tools to explore time-variation and state-dependencies in nonlinear environments.

*First draft February 2018. We thank Joseph Huang, Chun Hei Hung, Haomin Qin, Han Xu for excellent research assistance, and Amy Boonstra and Diana Petrova for their support. We would like to gratefully acknowledge the Macro-Finance Modeling initiative for their generous financial support. We thank Manav Chaudary, Hui Chen (the editor), Elisabeth Proehl, Simon Scheidegger, Panagiotis Souganidis, Judy Yue, and an anonymous referee for their constructive feedback. In addition, we thank conference participants at the 2nd MMCN, PASC18, University of Zurich, Northwestern University, CFE-CMStatistics and participants at the Economic Dynamics and Financial Markets Working Group at the University of Chicago.

1 Introduction

Beware the person of one ~~book~~ model. Thomas Aquinas (almost)

An under-appreciated task in the study of dynamic macroeconomics is model comparison. This is especially true for models requiring numerical methods to solve and analyze. While journals seemingly embrace publications that target specific models, there is much to be gained by looking formally across models.

One strategy for making comparisons across models is to nest models within a common framework in which each model of interest is a special case. At this juncture, we could turn things over to a statistician to test which model within this nesting best fits the data. This strategy makes the most sense when we could plausibly view one of the models within the family as being "correctly specified," given data. But in many cases, we see models as providing valuable insights even when they are not designed to fit some agreed upon list of favorite facts. As we explore nonlinear models more fully, this nesting-testing approach becomes all the more challenging. But even for examples when linearized approximations work well, the fitting all or some predesignated facts can lead to black box outcomes when driven by the simplistic ambitions of "full" empirical success. Models end up with multiple pieces often clouding the ability to isolate and understand better particular economic mechanisms.

In this paper, we develop a framework and diagnostic tools for comparing and contrasting dynamic macroeconomic models. The models that interest us require special attention relative to most dynamic stochastic equilibrium models because of the important role played by nonlinearity in the implied dynamic evolution. This nonlinearity has notable implications for both economic and financial market outcomes. Given these ambitions, our analysis is explicitly numerical and not limited to "paper and pencil" style analyses. It is necessary that we solve such models using global solution methods as the competitive equilibrium is typically characterized by a set of highly nonlinear second-order elliptic partial differential equations. Moreover, even with the option of numerical solutions, we find it revealing to explore and compare highly stylized models featuring particular economic mechanisms. In accompanying notebooks and user-friendly software, we propose and explore quantitative methods that expose salient features of the macroeconomic and valuation dynamics of the models we investigate. This essay provides illustrations of possible computations.

While we explore two different classes of models, a common feature in all of them is a long-run process altering investment opportunities. Our technologies can be viewed as

production-based specifications inclusive of long-run risk. Analogous to Bansal and Yaron (2004), we capture this risk with a continuous-time version of a first-order autoregressive process. The process is meant to be a simple proxy for uncertainty of such phenomenon as secular stagnation, technological progress or other forms of long-term uncertainty.

The first class of models have no market frictions. While including stochastic growth following in the footsteps of Lucas and Prescott (1971) and Brock and Mirman (1972), these models include single investor type and we start by consider a model with single capital stock with a long-run risk contribution to the investment opportunities. While we provide some sensitivity analyses that are of interest in their own right, understanding these initial models sets the stage for our subsequent investigations.

We give two extensions, one in which the representative or stand-in investor has concerns about model ambiguity captured by uncertainty in growth rate persistence along with overall model misspecification concerns. The other extension considers specifications with two capital stocks differentially exposed to macroeconomic shocks. Capital movements are sluggish in the sense that there are adjustment costs in both capital technologies. This class of models extend those of Eberly and Wang (2009) and Eberly and Wang (2011). We investigate the consequences of heterogeneous technological exposure to long-run risk in conjunction with motives for diversification. Including production in which the two capital stocks are not perfect substitutes adds an additional economic channel with interesting nonlinear impacts.

The second class of models, motivated in part by financial crises like 2008, considers two heterogeneous investor types. These agents can differ in skill, preferences, or contractual and regulatory constraints. Dynamic trading between these heterogeneous investors induces potentially dramatic economic and financial market outcomes in some states of the world, especially those in which constraints are binding. Our exercise is motivated by a substantial literature with a variety of different modeling ingredients. These include, for instance, the models in Basak and Cuoco (1998), He and Krishnamurthy (2011), Brunnermeier and Sannikov (2014), and Gârleanu and Panageas (2015). Recently, several papers have exposed a more complex representation of the role of financial intermediation than that captured by the stylized models we consider here. It is not our aim in this essay to survey this literature. The models we consider, however, do have mechanisms that enhance our understanding of nonlinear linkages between financial markets and the macroeconomy, even if they miss some of the actual complexities that limit financial intermediaries or other such specialists.

2 Investor Preferences

In this essay we use a continuous-time specification of a Kreps and Porteus (1978) utility recursion as in Duffie and Epstein (1992a) in connection with an information structure generated expressed in terms of a vector standard Brownian motion $B \stackrel{\text{def}}{=} \{B_t : t \geqslant 0\}$ of dimension d. Thus we are imposing "local normality". While shocks are normally distributed, we entertain nonlinear transition mechanisms that permit endogenously determined variables to possess transition probabilities and stationary distributions that are not even approximately normal. In this section, we provide a heuristic link between the continuous-time and discrete-time representation of preferences since the discrete-time formulation has been used extensively in the quantitative asset pricing literature. The local normality does allow for some simplicity when we study continuous-time limiting economies. We do not ask the reader to be knowledgeable of the subtleties associated with the continuous-time mathematics.

2.1 Discrete-time

Continuation values provide a convenient way to specify recursive preferences. With this is in mind, let $V \stackrel{\text{def}}{=} \{V_t : t \geqslant 0\}$ be the continuation utility process where V_t is a date-t utility index that summarizes current and future prospective contributions to preferences. In discrete time with a time interval ϵ, we use two CES, homogeneous of degree one recursions to represent the evolution of continuation values:

$$\begin{aligned} V_t &= \left[\left[1-\exp(-\delta\epsilon)\right](C_t)^{1-\rho} + \exp(-\delta\epsilon)\mathbb{R}(V_{t+\epsilon} \mid \mathfrak{F}_t)^{1-\rho}\right]^{\frac{1}{1-\rho}} \\ \mathbb{R}(V_{t+\epsilon} \mid \mathfrak{F}_t) &= \left(\mathbb{E}\left[(V_{t+\epsilon})^{1-\gamma} \mid \mathfrak{F}_t\right]\right)^{\frac{1}{1-\gamma}} \end{aligned} \tag{1}$$

where $\mathfrak{F}_t$ is the time-t information set. Notice that the second equation computes a certainty equivalent with parameter γ. If the continuation utility $V_{t+\epsilon}$ is known at t, then γ has no impact on the recursion since $\mathbb{R}(V_{t+\epsilon} \mid \mathfrak{F}_t) = V_{t+\epsilon}$ implying that this contribution is indeed an adjustment for risk. Taking the two equations together, this is a forward looking-recursion whereby we start with a terminal specification of the continuation utility and work backwards. We consider infinite horizon counterparts in our computations. Notice that this recursive specification is governed by three underlying parameters:

i) δ – the subjective discount rate;

ii) ρ – the inverse of the intertemporal elasticity of substitution (the "IES");

iii) γ – the risk aversion.

In some later examples, we will have two investor types with possibly heterogenous specifications of the preference parameters (δ, ρ, γ).

Two special cases of these preferences are: $\rho = \gamma$ and $\rho = 1$. When $\rho = \gamma$, this utility recursion defines preferences that are equivalent to those implied by discounted, time-separable, power utility. Specifically, when $\gamma = \rho$, by solving the recursion forward, it follows that:

$$V_t = \left(\mathbb{E} \left[\frac{1}{1 - \exp(-\delta\epsilon)} \sum_{j=0}^{\infty} \exp(-\delta j \epsilon) \left(C_{t+j\epsilon} \right)^{1-\gamma} \mid \mathfrak{F}_t \right] \right)^{\frac{1}{1-\gamma}}, \quad \text{if} \quad \rho = \gamma. \tag{2}$$

Imposing $\rho = 1$ implies a unitary IES, and the limiting recursion has a Cobb-Douglas representation:

$$V_t = (C_t)^{[1-\exp(-\delta\epsilon)]} \left[\mathbb{R}(V_{t+\epsilon} \mid \mathfrak{F}_t) \right]^{\exp(-\delta\epsilon)}, \quad \text{if} \quad \rho = 1.$$

Continuation values are only defined up to increasing transformations. Numerical and conceptual convenience lead us to use $\widehat{V}_t = \log V_t$. (We will always use the notation "$\widehat{X}$" to designate the logarithm of a variable X.) The logarithmic counterparts to the underlying recursions are given by:

$$\begin{aligned} \widehat{V}_t &= \frac{1}{1-\rho} \log \left[[1 - \exp(-\delta\epsilon)] \left(C_t \right)^{1-\rho} + \exp(-\delta\epsilon) \exp \left[(1-\rho) \widehat{\mathbb{R}}(\widehat{V}_{t+\epsilon} \mid \mathfrak{F}_t) \right] \right] \\ \widehat{\mathbb{R}} \left(\widehat{V}_{t+\epsilon} \mid \mathfrak{F}_t \right) &= \frac{1}{1-\gamma} \log \left(\mathbb{E} \left[\exp[(1-\gamma)\widehat{V}_{t+\epsilon}] \mid \mathfrak{F}_t \right] \right). \end{aligned} \tag{3}$$

For this representation, $\rho = \gamma = 1$ is a relevant benchmark whereby the recursions become:

$$\begin{aligned} \widehat{V}_t &= [1 - \exp(-\delta\epsilon)] \log C_t + \exp(-\delta\epsilon) \widehat{\mathbb{R}}(\widehat{V}_{t+\epsilon} \mid \mathfrak{F}_t) \\ \widehat{\mathbb{R}}(\widehat{V}_{t+\epsilon} \mid \mathfrak{F}_t) &= \mathbb{E}[\widehat{V}_{t+\epsilon} \mid \mathfrak{F}_t], \end{aligned} \tag{4}$$

which has discounted logarithmic utility scaled by $[1 - \exp(-\delta\epsilon)]$ as the solution.

2.2 Robustness to model misspecification

Our motivation so far for the recursive utility formulation relies of uncertainty aversion as applying to risk, a situation in which investors have complete confidence in their probability assignments. In many applications, this narrow notion of uncertainty seems like a strain. This especially could be a concern when considering uncertainty in long-term macroeconomic growth rates. See, for instance, discussions in Hansen (2007) and Chen et al. (2024). Concerns about ambiguity as to which among a family of potential models is one that governs data generation or concerns about potential model misspecification may come into play as reflecting broader notions of uncertainty concerns.[1] We now show how to reinterpret the recursive utility formulation (1) as a preference for robustness to model uncertainty. Later in this essay, we also consider implications of aversion to ambiguity over how to weight alternative models. See Section 4.5.

Using the lens of robust control theory, consider a positive random variable $L_{t+\epsilon}$ with unit conditional expectation — a convenient mathematical device pertinent to models of subjective beliefs that are distinct from those implied by the data generating process:

$$\mathbb{E}\left(L_{t+\epsilon} \mid \mathfrak{F}_t\right) = 1.$$

Think of $L_{t+\epsilon}$ as a relative density (likelihood ratio) that alters the transition probability from t to $t+\epsilon$. To obtain the implied subjective conditional expectations, multiply the next-period random variables by $L_{t+\epsilon}$ prior to forming the conditional expectations. For instance, the implied subjective expectation of next period's continuation value is $\mathbb{E}(L_{t+\epsilon}\widehat{V}_{t+\epsilon} \mid \mathfrak{F}_t)$.

While a subjective belief specification allows for departures from a "rational expectations" assumption that investors know the data generating process, we use the modeling approach differently. Suppose that the investor has a benchmark model of the transition probabilities without *full confidence* in that specification. This skepticism is expressed by entertaining other models, with a particular interest in ones that are "statistically close" to the benchmark model. This approach has antecedents in the robust control literature.[2] Formally, solve

$$\min_{\substack{L_{t+\epsilon}\geqslant 0 \\ \mathbb{E}(L_{t+\epsilon}|\mathfrak{F}_t)=1}} \mathbb{E}\left(L_{t+\epsilon}\widehat{V}_{t+\epsilon} \mid \mathfrak{F}_t\right) + \xi\mathbb{E}\left(L_{t+\epsilon}\log L_{t+\epsilon} \mid \mathfrak{F}_t\right) = -\xi\log\mathbb{E}\left[\exp\left(-\frac{1}{\xi}\widehat{V}_{t+\epsilon}\right) \mid \mathfrak{F}_t\right], \quad (5)$$

[1] See Hansen and Sargent (2023) and Cerreia-Vioglio et al. (2024) for some recent discussions of axiomatic rationales.

[2] See, for instance, Jacobson (1973), Whittle (1981), James (1992), and Petersen et al. (2000).

which is familiar from applied probability theory. This minimization problem investigates the expected utility consequences of altering the probability distribution subject to a conditional relative entropy penalty used as a Kullback-Leibler measure of statistical divergence. The parameter ξ penalizes the search over alternative probabilities. Setting $\xi = \infty$ implements expected logarithmic utility. Small values of the penalty imply a large aversion to uncertainty about the transition probabilities.

The minimizing solution to problem (5) is:

$$L^*_{t+\epsilon} = \frac{\exp\left(-\frac{1}{\xi}\widehat{V}_{t+\epsilon}\right)}{\mathbb{E}\left[\exp\left(-\frac{1}{\xi}\widehat{V}_{t+\epsilon}\right)|\mathfrak{F}_t\right]}, \tag{6}$$

provided that the denominator is well defined. This formulation gives an example of what Maccheroni et al. (2006) call variational preferences designed to confront broader notions of uncertainty other than risk. The minimizing probability displays what is called exponential tilting as the probabilities and slanted towards more adverse continuation values in an exponential manner. The implied minimizer is also of interest for the reasons articulated by the robust Bayesian, Good (1952), as a way to assess plausibility. Also, the implied measure of statistical divergence is revealing as a measure of statistical challenges implicit in the choice of the penalty parameter ξ.

This construction is an alternative interpretation for the large risk aversion often imposed in recursive utility models. The mathematical equivalence can be seen by letting $\xi = \frac{1}{\gamma - 1}$. The economic interpretation, however, is very different as is the assessment of what are plausible calibrations of the uncertainty adjustment in the utility recursion.

2.3 Continuous-time limit

To depict the continuous-time counterpart to equation (1), suppose that the continuation utility evolves as:[3]

$$d\widehat{V}_t = \hat{\mu}_{v,t}dt + \sigma_{v,t} \cdot dB_t.$$

where $\hat{\mu}_{v,t}$ is the local mean and $|\sigma_{v,t}|^2$ is local variance. In positing this evolution we are using local normality induced by the Brownian increments to deduce the local normality of the continuation utility increments.

[3]Starting with V instead of $\widehat{V}$, we would write $dV_t = V_t[\mu_{v,t}dt + \sigma_{v,t} \cdot dB_t]$ where $\hat{\mu}_{v,t} = \mu_{v,t} - \frac{1}{2}|\sigma_{v,t}|^2$.

The limiting version of recursion (1) gives the following restriction on $(\hat{\mu}_{v,t}, |\sigma_{v,t}|^2)$:

$$0 = \left(\frac{\delta}{1-\rho}\right)\left[(C_t/V_t)^{1-\rho} - 1\right] + \hat{\mu}_{v,t} + \left(\frac{1-\gamma}{2}\right)|\sigma_{v,t}|^2. \tag{7}$$

For the unitary IES case ($\rho = 1$), equation (7) becomes:

$$0 = \delta\left(\widehat{C}_t - \widehat{V}_t\right) + \hat{\mu}_{v,t} + \left(\frac{1-\gamma}{2}\right)|\sigma_{v,t}|^2 \tag{8}$$

Equations (7)-(8) provide an expression for the local mean $\hat{\mu}_{v,t}$ as a function of $\widehat{C}_t - \widehat{V}_t$ and the local variance $|\sigma_{v,t}|^2$.[4]

Consider once again the robust interpretation of our recursive preferences and the minimization problem (5). This problem has a simplified version in the case of a Brownian motion information structure. Let L be a positive martingale or likelihood ratio used to induce an alternative probability distribution. From the Girsanov Theorem, under the probability measure induced by L, the process B becomes a Brownian motion with a drift $H \stackrel{\text{def}}{=} \{H_t : t \geqslant 0\}$. Locally, the Brownian increment dB_t inherits a drift $H_t dt$. The evolution of L thus takes the form

$$dL_t = L_t H_t \cdot dB_t$$

and in logarithms:

$$d\widehat{L}_t = -\frac{1}{2}|H_t|^2 dt + H_t \cdot dB_t$$

with normalization $L_0 = 1$ or equivalently $\widehat{L}_0 = 0$. Under the implied change of probability measure, the drift of $\widehat{L}$ is $-\frac{1}{2}|H_t|^2$ — a local measure of Kullback-Leibler divergence or relative entropy. The continuous-time formulation of (5) then becomes

$$\min_{H_t} \hat{\mu}_{v,t} + \sigma_{v,t} H_t + \frac{\xi}{2}|H_t|^2.$$

[4]We find this representation to be both pedagogically revealing with a direct heuristic link to familiar discrete-time specifications. Continuation values are only well defined up to a strictly increasing transformation as emphasized by Duffie and Epstein (1992a). For mathematical reasons, often a different ordinally equivalent representation, $(V_t)^{1-\gamma}/(1-\gamma)$, is used in many papers constructed to remove the volatility contribution to the recursion.

The minimizing H_t is

$$H_t^* = -\frac{1}{\xi}\sigma_{v,t}{}' \tag{9}$$

with a minimized objective given by:

$$\widehat{\mu}_{v,t} - \frac{1}{2\xi}|\sigma_{v,t}|^2. \tag{10}$$

The negative of local exposure vector, $\sigma_{v,t}$, of the continuation value to Brownian risk determines the direction of the drift adjustment to the stochastic state evolution. Comparing this result to the limiting recursion (7), the parameter γ can be viewed as a form of uncertainty aversion, instead of a measure of risk aversion, when using $\gamma - 1 = 1/\xi$. Not suprisingly, this agrees with our discrete-time discussion of section 2.2.

2.4 Stochastic discount factor process

We deduce a representation for the shadow stochastic discount factor (SDF) process in discrete and continuous time. For economies with a single agent type, this shadow SDF provides a convenient representation of equilibrium asset prices. In heterogeneous agent economies with financing frictions, the shadow SDFs are typically not equalized across agents types but they can be used to represent commonly traded assets. Moreover, their differences reflect the absence of full risk sharing induced by market frictions.

Think of the SDF process S as providing a way to depict shadow prices over any investment horizon. In particular, $S_{t+\epsilon}/S_t$ in conjunction with the transition probabilities associated with an underlying probability measure give date-t prices for a payoff at date $t+\epsilon$. Deduce the shadow SDF process by computing the intertemporal marginal rate of substitution across different possible realized states in the future. By differentiating through the utility recursion, the evolution over a period of length ϵ, expressed in logarithms, is

$$\widehat{S}_{t+\epsilon} - \widehat{S}_t = -\epsilon\delta - \rho\left(\widehat{C}_{t+\epsilon} - \widehat{C}_t\right) + (1-\gamma)\left[\widehat{V}_{t+\epsilon} - \widehat{\mathbb{R}}(\widehat{V}_{t+\epsilon} \mid \mathfrak{F}_t)\right] + (\rho-1)\left[\widehat{V}_{t+\epsilon} - \widehat{\mathbb{R}}(\widehat{V}_{t+\epsilon} \mid \mathfrak{F}_t)\right].$$

Of particular interest, the term $(1-\gamma)[\widehat{V}_{t+\epsilon} - \widehat{\mathbb{R}}(\widehat{V}_{t+\epsilon} \mid \mathfrak{F}_t)]$ adjusts for risk or robustness. Its exponential has conditional expectation equal to unity and is equal to the minimizer $L_{t+\epsilon}^*$ in (6). Thus, this particular contribution to the SDF induces a change in the probability distribution motivated explicitly by robustness considerations. More generally, the difference between $\widehat{V}_{t+\epsilon}$ and its certainty equivalent $\widehat{R}_t$ is forward looking and depends on the

decision maker's perspective of the future. This contribution vanishes when $\gamma = \rho$. When $\rho = 1$, only the contribution captured by the change in probability measure is forward looking.

Consider next the local evolution of the SDF. Write:

$$dS_t = -r_t S_t dt - S_t \pi_t \cdot dB_t$$

With this representation, r_t is the instantaneous risk-free rate and π_t is the vector of local prices of exposure to the Brownian increment dB_t, also called "risk prices". Similarly, write the local consumption evolutions as:

$$d\widehat{C}_t = \hat{\mu}_{c,t} dt + \sigma_{c,t} \cdot dB_t.$$

Then, in terms of the dynamics of $\widehat{C}$ and $\widehat{V}$ (above), we have the following riskless rate and risk prices

$$\begin{aligned} r_t &= \delta + \rho \hat{\mu}_{c,t} - \frac{1}{2}|\pi_t|^2 + \frac{(\gamma - 1)(\gamma - \rho)}{2}|\sigma_{v,t}|^2 \\ \pi_t &= \rho \sigma_{c,t} + (1 - \rho)\sigma_{v,t} + (\gamma - 1)\sigma_{v,t}. \end{aligned}$$

Notice that the third contribution to the "risk-price vector" is negative of the robustness adjustment, H_t^*, to the drift of the vector Brownian motion as depicted in formula (9). The second contribution vanishes when the intertemporal elasticity, $\frac{1}{\rho}$ is unity.

3 Local measures of exposures and prices

In all the models we consider, the logarithms of several quantities of interest will grow or decay stochastically over time with increments that are stationary Markov processes. Let M be such a process and $\widehat{M}$ its logarithm. Restrict the process $\widehat{M}$ to display linear, stochastic growth or decay. Write

$$\widehat{M}_{t+\epsilon} - \widehat{M}_t = \epsilon \hat{\mu}_m(X_t) + \sigma_m(X_t) \cdot (B_{t+\epsilon} - B_t) \tag{11}$$

where X is an asymptotically stationary Markov process. Examples of such $\widehat{M}$ processes in our models are the log SDF $\widehat{S}$ and log consumption $\widehat{C}$.

3.1 Shock elasticities

Shock elasticities are constructed using local changes in the exposure to shocks. For instance, consider a shock, $B_\epsilon - B_0$ that is distributed as a multivariate standard normal. We introduce a parameterized family of random variables $H_\epsilon(\mathsf{r})$ where

$$\log H_\epsilon(\mathsf{r}) = \mathsf{r}\nu(X_0)\cdot(B_\epsilon - B_0) - \frac{\mathsf{r}^2}{2}\epsilon|\nu(X_0)|^2.$$

where we normalize the row vector ν so that $\mathbb{E}\left[|\nu(X_0)|^2\right] = 1$. In our applications, ν is state independent and selects one of the components of $B_\epsilon - B_0$. Notice that $H_\epsilon(\mathsf{r})$ is positive and has conditional expectation equal to one. Consider:

$$\frac{d}{d\mathsf{r}}\log\mathbb{E}\left[\left(\frac{M_t}{M_0}\right)H_\epsilon(\mathsf{r})\mid X_0\right]\Big|_{\mathsf{r}=0} = \frac{\nu(X_0)\cdot\mathbb{E}\left[\left(\frac{M_t}{M_0}\right)(B_\epsilon - B_0)\mid X_0\right]}{\mathbb{E}\left[\left(\frac{M_t}{M_0}\right)\mid X_0\right]}. \tag{12}$$

We refer to the outcome as a shock elasticity because we differentiate a logarithm with respect to an argument $H_\epsilon(\mathsf{r})$ which is equal to one at $\mathsf{r} = 0$. This elasticity depends on the state X_0 and horizon t. When scaled by $\frac{1}{\epsilon}$, it has a well defined limit as ϵ declines to zero.

In formula (12), notice that the essential input is:

$$\frac{\mathbb{E}\left[\left(\frac{M_t}{M_0}\right)(B_\epsilon - B_0)\mid X_0\right]}{\epsilon\mathbb{E}\left[\left(\frac{M_t}{M_0}\right)\mid X_0\right]}. \tag{13}$$

The numerator is vector of conditional regression coefficients of $\frac{M_t}{M_0}$ onto $B_\epsilon - B_0$ since the regressors have a conditional covariance matrix that scales an identity matrix by ϵ. In the language of empirical macroeconomics, these vectors are conditional counterparts to local projections.[5] The denominator of (13) is included because of our interest in characterization involving M instead of $\widehat{M}$ as is often done by empirical macroeconomists and because we are interested in measuring elasticities. The continuous-time limits can be computed

[5]The continuous-time limits are related to constructs from stochastic process theory. The Haussmann-Clark-Ocone formula gives continuous time, moving-average representations of general processes constructed from underlying Brownian motion information structures. The counterparts to moving-average coefficients are stochastic and interpreted as conditional expectations of so-called Malliavin derivatives. The limiting version of numerator (13) can be viewed as an approximation to the coefficient on dB_0 in such a representation. These types of computations also play an important role in characterizing derivative claims pricing. See Fournié et al. (1999). Borovička et al. (2014) for a more complete development and discussion of the connections to various continuous-time representations.

numerically in a straightforward way for the Markovian economies of the type we consider here. See Borovička et al. (2014) for further discussion.

The scaling by H_ϵ in formula (12) (or its continuous-time limit) has two distinct interpretations depending on the application:

i) it changes the distribution of B_ϵ by giving it a conditional mean $\epsilon \mathsf{r} \nu(X_0)$

ii) it changes the exposure of $\widehat{M}_t - \widehat{M}_0$, and hence M_t/M_0, to the shock $B_\epsilon - B_0$ through the addition of $\mathsf{r}\nu(X_0) \cdot (B_\epsilon - B_0)$.

The first of these interpretations provides a distributional version of an impulse response function. It matches exactly for the linear, log-normal model, in which case X is a multivariate, Gaussian vector autoregression, that is when μ is affine in x, and ν and σ_m are vectors of constants. Once we include nonlinearities, the state x can matter along with the time horizon t. See Gallant et al. (1993) and Koop et al. (1996) for related constructs of nonlinear impulse responses. For intertemporal asset pricing applications, the second interpretation will help us understand shock elasticities as implied compensations for changes in the exposures. We discuss this asset pricing application next.

3.2 Compensations for exposure to uncertainty

Let $\widehat{Y}$ denote the logarithm of a cash flow process, and let $\widehat{S}$ denote the equilibrium log SDF process both of which have stochastic evolutions of the form (11). Compute:

i) exposure elasticity

$$\frac{\nu(X_0) \cdot \mathbb{E}\left[\left(\frac{Y_t}{Y_0}\right)(B_\epsilon - B_0) \mid X_0\right]}{\epsilon \mathbb{E}\left[\left(\frac{Y_t}{Y_0}\right) \mid X_0\right]};$$

ii) value elasticity

$$\frac{\nu(X_0) \cdot \mathbb{E}\left[\left(\frac{S_t Y_t}{S_0 Y_0}\right)(B_\epsilon - B_0) \mid X_0\right]}{\epsilon \mathbb{E}\left[\left(\frac{S_t Y_t}{S_0 Y_0}\right) \mid X_0\right]};$$

iii) price elasticity (exposure minus value)

$$\frac{\nu(X_0) \cdot \mathbb{E}\left[\left(\frac{Y_t}{Y_0}\right)(B_\epsilon - B_0) \mid X_0\right]}{\epsilon \mathbb{E}\left[\left(\frac{Y_t}{Y_0}\right) \mid X_0\right]} - \frac{\nu(X_0) \cdot \mathbb{E}\left[\left(\frac{S_t Y_t}{S_0 Y_0}\right)(B_\epsilon - B_0) \mid X_0\right]}{\epsilon \mathbb{E}\left[\left(\frac{S_t Y_t}{S_0 Y_0}\right) \mid X_0\right]};$$

These all have well defined continuous-time limits as $\epsilon \downarrow 0$. As mentioned above, one can interpret the price elasticity as the expected excess return required for a marginal increase in risk exposure to Y.

There is one additional calculation of interest. Suppose that $L = \exp(\widehat{M})$ is a martingale. This is of interest when we entertain beliefs that differ from the data generating process and study their value contribution. From the Law of Iterated Expectations,

$$\frac{\nu(X_0) \cdot \mathbb{E}\left[\left(\frac{L_t}{L_0}\right)(B_\epsilon - B_0) \mid X_0\right]}{\epsilon \mathbb{E}\left[\left(\frac{L_t}{L_0}\right) \mid X_0\right]} = \left(\frac{1}{\epsilon}\right) \nu(X_0) \cdot \mathbb{E}\left[\left(\frac{L_\epsilon}{L_0}\right)(B_\epsilon - B_0) \mid X_0\right],$$

and does not depend on the horizon t. In this circumstance (and perhaps others as well), we find it revealing to change the date of the Brownian increment by reporting the small ϵ limit of

$$\frac{1}{\epsilon}\mathbb{E}\left[\left(\frac{L_t}{L_0}\right)\nu(X_{t-\epsilon}) \cdot (B_t - B_{t-\epsilon}) \mid X_0\right] \tag{14}$$

as a term structure of "uncertainty prices." These prices will be horizon dependent.

4 Economies with a representative investor

For pedagogical purposes, we begin our exposition by focusing on a "representative investor" with recursive preferences in a complete-market production economy featuring long-run-risk shocks. We may view the economy as a production-based counterpart to that in the seminal paper by Bansal and Yaron (2004). In part we share a similar ambition to that of Jermann (1998) in describing a production-based model with asset pricing, but we also use this class of models as a benchmark for model classes that include heterogeneous capital or heterogeneous investors. We follow Bansal and Yaron (2004) by focusing on recursive utility in contrast to Jermann (1998), who features habit persistence preferences.

Since our benchmark model features complete markets, we study the planner problem to characterize equilibrium quantities and prices in the economy. A decentralized version of the model allows for a rich set of assets locally spanning the Brownian increments along with a riskless security. Risk prices are embedded in the stochastic discount factor evolution.

Even for a model with a single capital stock, the introduction of production and investment turns out to be important relative to endowment economies when we change preference parameters. Much of the asset pricing literature features endowment economies

in which changes in the intertemporal elasticity of substitution (IES) have only a pricing impact. As we will illustrate, in a production economy changing the IES has a substantial impact on the investment/capital ratio and hence growth in the underlying economy.

4.1 Exogenous stochastic inputs

We presume that there are two underlying exogenous processes that evolve as solutions to stochastic differential equations

$$dZ_t^1 = -\beta_1 Z_t^1 dt + \sqrt{Z_t^2}\sigma_1 \cdot dB_t \tag{15}$$

$$dZ_t^2 = -\beta_2 (Z_t^2 - \mu_2) dt + \sqrt{Z_t^2}\sigma_2 \cdot dB_t \tag{16}$$

where $\beta_1 > 0$, $\beta_2 > \frac{1}{2}|\sigma_2|^2$, and $\mu_2 > 0$. In addition, σ_1, σ_2, are d-dimensional vectors of real numbers. The Z^1 process governs the conditional mean of the stochastic component to technology growth and the process Z^2 captures the exogenous component to aggregate stochastic volatility. Notice that $\sqrt{Z^2}$ scales the Brownian increment to both of the processes. The local variance of the exogenous technology shifter is $Z_t^2|\sigma_1|^2$, and the local variance for the stochastic volatility process is $Z_t^2|\sigma_2|^2$.

The stochastic variance process Z^2 is a special case of a Feller square root process. The exogenous stochastic technology growth process, Z^1, is a continuous-time version of an autoregression with innovations that are conditionally heteroskedastic. The autoregressive coefficients for discrete-time counterparts are $\exp(-\beta_1)$, $\exp(-\beta_2)$. Values of β_1 and β_2 that are close to zero imply a large amount of persistence. The unconditional mean of Z^1 is normalized to be zero, and the unconditional mean of Z^2 in a stochastic steady state is μ_2. In what follows, we let

$$Z_t \stackrel{\text{def}}{=} \begin{bmatrix} Z_t^1 \\ Z_t^2 \end{bmatrix} \quad \mu_z(Z_t) \stackrel{\text{def}}{=} \begin{bmatrix} -\beta_1 Z_t^1 \\ -\beta_2 (Z_t^2 - \mu_2) \end{bmatrix} \quad \sigma_z \stackrel{\text{def}}{=} \sqrt{Z_t^2} \begin{bmatrix} \sigma_1{}' \\ \sigma_2{}' \end{bmatrix}.$$

4.2 Technology

We use a so-called AK technology with adjustment costs to represent production.[6] Let K_t be the stock of capital, I_t the investment rate, and C_t the consumption rate at date t. The technology consists of two equations: an output and a capital evolution equation. Output

[6] See, e.g., Cox et al. (1985), Merton (1973), Jones and Manuelli (1990) and Brock and Magill (1979).

is constrained by:

$$C_t + I_t = \alpha K_t, \tag{17}$$

where α is a fixed productivity parameter. Our capital accumulation equation features aggregate shocks as follows:

$$dK_t = K_t \left[\Phi \left(\frac{I_t}{K_t} \right) + \beta_k Z_t^1 - \eta_k \right] dt + K_t \sqrt{Z_t^2} \sigma_k \cdot dB_t, \tag{18}$$

where η_k embeds an adjustment for depreciation and σ_k is a $d \times 1$ vector quantifying the importance of the Brownian motion in generating stochastic returns to investment. The function Φ, called the installation function by Hayashi (1982), is an increasing and concave function. A leading example of Φ in our essay is

$$\Phi(i) = \frac{1}{\phi} \log (1 + \phi i) . \tag{19}$$

where i is a stand-in for a realization of the investment-capital ratio. The small i quadratic approximation is:

$$\Phi(i) \approx i - \frac{\phi}{2} i^2$$

We note this relationship since quadratic specifications are often imposed in the investment literature.

By design, the technology is homogeneous of degree one in investment, capital and consumption. This model has stochastic shocks that i) alter the physical returns to investment; ii) shift the conditional mean of that investment; and iii) shift the aggregate volatility of the technology. For such a stylized model, capital should be interpreted very broadly and potentially should include human, organizational, and intangible contributions. The shock to physical returns to investment is sometimes referred to as a "capital quality shock" or a "technology shock."[7]

4.3 Value function

Given the homogeneity properties of both preferences and technology, the value function scales linearly with the capital stock. It will be most convenient to work with the logarithm

[7] Our model is isomorphic to an AK model where productivity (instead of capital K_t) is being hit by Brownian shocks, and in which adjustment costs also scale up and down with such shock.

of the value function, which we posit takes the following form:

$$\widehat{V}_t = \widehat{K}_t + \upsilon(Z_t). \tag{20}$$

We combine the evolutions of $\upsilon(Z_t)$ and $\widehat{K}_t$ to deduce a Hamilton-Jacobi-Bellman equation for the function υ:

$$\begin{aligned} 0 = \max_{c+i=\alpha} \Bigg\{ \left(\frac{\delta}{1-\rho}\right) \left(c^{1-\rho} \exp\left[(\rho-1)\upsilon\right] - 1\right) + \Phi(i) + \beta_k z_1 - \eta_k - \frac{1}{2} z_2 |\sigma_k|^2 \\ + \mu_z \cdot \frac{\partial \upsilon}{\partial z} + \frac{z_2}{2} \mathrm{trace}\left\{ \sigma_z{}' \frac{\partial^2 \upsilon}{\partial z \partial z'} \sigma_z \right\} + \frac{(1-\gamma) z_2}{2} \left| \sigma_k + \sigma_z{}' \frac{\partial \upsilon}{\partial z} \right|^2 \Bigg\}, \end{aligned} \tag{21}$$

where c is the consumption-to-capital ratio and i is the investment-to-capital ratio. The first-order condition for the optimal consumption-capital ratio, c^*, is:

$$\delta \left[c^*(z)\right]^{-\rho} \exp\left[(\rho-1)\upsilon(z)\right] = \Phi'\left[\alpha - c^*(z)\right]. \tag{22}$$

Capital provides the sole source of wealth in this economy. Total wealth is given by the continuation value divided by the marginal utility of consumption, evaluated at equilibrium outcomes:[8]

$$\frac{1}{\delta} \left[c^*(z)\right]^{\rho} \exp[(1-\rho)\upsilon(z)] k.$$

The implied price of capital is given by $Q_t = q(Z_t)$ where

$$q(z) = \frac{1}{\delta} \left[c^*(z)\right]^{\rho} \exp[(1-\rho)\upsilon(z)] = \frac{1}{\Phi'\left[\alpha - c^*(z)\right]} = 1 + \phi i^*(z). \tag{23}$$

The instantaneous capital return in this economy has an exposure to the vector, dB_t, of Brownian increments given by

$$\sigma_{r,t} = \sqrt{Z_t^2}\sigma_k + \sqrt{Z_t^2} \frac{\partial \ln q}{\partial z'}(Z_t)\sigma_z$$

where the first term captures the exposure of capital to the Brownian increments and the second one reflects the exposure of valuation to these same increments.

[8] The two recursions in (1) are both homogeneous of degree one. From an infinite-dimensional version of Euler's Theorem, the continuation value divided by the marginal utility of consumption is the current period shadow price of current and future consumption which equals wealth in equilibrium.

4.4 Single capital stock economies

In contrast to the other economies that we study, this economy can be well approximated by log-quadratic approximations. We use this as a benchmark to the study of economies that are more explicitly nonlinear. We imagine a family of economies indexed by $(\rho, \gamma, \delta, \alpha)$. Of course other parameter sensitivity could also be explored. Our use of a production economy provides a revealing contrast to the familiar Lucas (1978) endowment economy.

In consumption-based models with endowment specifications, the preference parameter ρ has a substantial impact on the risk-free rate. In models with production, like the ones we explore here, changing ρ while holding other parameters of preferences and technology fixed, has a substantial impact on production and savings. Table 1 gives parameter values that we hold fixed in these computations, and Table 2 reports the steady state investment- and consumption-to-output ratios along with the steady state growth rate. The IES has a dramatic impact on all these average macroeconomic aggregates.

η_k	ϕ	β_k	β_1	β_2	μ_2
.04	8	.04	.056	.194	6.3×10^{-6}

	Upper triangular	Lower triangular
σ_k	$\sqrt{12}[.92 \;\; .40 \;\; 0]$	$\sqrt{12}[1 \;\; 0 \;\; 0]$
σ_1	$\sqrt{12}[0 \;\; 5.7 \;\; 0]$	$\sqrt{12}[2.3 \;\; 5.2 \;\; 0]$
σ_2	$\sqrt{12}[0 \;\; 0 \;\; .00031]$	

Table 1: Parameter values that we hold fixed for the one-capital model. The numbers for η_k, ϕ, β_1, σ_k and σ_1 are such that, when multiplied by stochastic volatility, they match the parameters from Hansen and Sargent (2021). In particular, the constant Z^2 which scales our σ_k to match HS 2020 is 7.6×10^{-6}. This is the 67th percentile of our Z^2 distribution. While Hansen and Sargent (2021) use a lower triangular representation for the two-by-two right block of $\left[\begin{smallmatrix}\sigma_k \\ \sigma_1\end{smallmatrix}\right]$, we use an observationally equivalent upper triangular representation for most of the results. Both versions are listed here. Finally, the numbers for β_2 and σ_2 come from Schorfheide et al. (2018), but they are adjusted for approximation purposes as described in Appendix A. In both cases, we use the medians of their econometric evidence as input into our analysis.

ρ	0.67	1	1.5
consumption-output ratio	0.012	0.175	0.279
investment-output ratio	0.988	0.825	0.721
steady state growth rate	0.028	0.019	0.013

Table 2: Steady states for alternative specifications of ρ for $\alpha = .092$ and $\delta = .01$. These are computed by setting shock variances to zero.

To diminish this impact, we change the productivity parameter α to pin down a common growth rate in consumption. Table 3 reports the results. There is still a noticeable impact of ρ on investment- and consumption-to-output ratios, but not nearly as dramatic. The subjective discount rate also impacts these steady states by increasing the consumption-to-output ratios as also seen by Table 3.

	$\delta = .01$		
ρ	0.67	1	1.5
consumption-output ratio	0.071	0.175	0.296
investment-output ratio	0.929	0.825	0.704
productivity (α)	0.082	0.092	0.108
growth rate	0.019	0.019	0.019
	$\delta = .015$		
ρ	0.67	1	1.5
consumption-output ratio	0.155	0.242	0.346
investment-output ratio	0.845	0.758	0.654
productivity (α)	0.090	0.100	0.116
growth rate	0.019	0.019	0.019

Table 3: Steady states adjusting the productivity parameter α to match a specific growth rate. These are computed by setting the shock variances to zero.

We next consider shock exposure and shock price elasticities. We focus on the growth-rate shock. The capital evolution shock is also quantitatively important. In contrast, the impact of the stochastic volatility shock is quantitatively small.[9] Stochastic volatility does induce state dependence in the other shock elasticities as we will illustrate.

[9]The quantitative magnitudes could be amplified by pushing the mean reversion parameter β_2 even closer to zero, as is done in calibrations of asset pricing models.

Consider the shock exposure elasticity, or equivalently the local impulse response function, for the investment-to-output ratio. Since output is proportional to capital, formula (23) implies these are also approximately the elasticities for the price of capital (which is affine in the investment-to-capital ratio). As Figure 1 shows, the responses to a growth rate shock are positive when $\rho < 1$ and negative when $\rho > 1$. The elasticities are only modestly sensitive to changing the risk aversion parameter γ, while they increase notably when the subjective discount rate δ is increased.

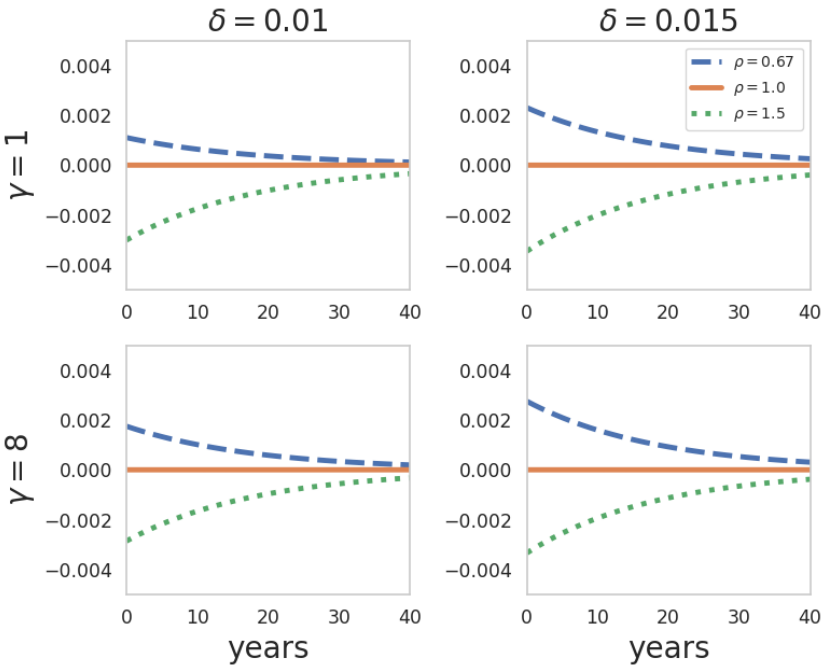

Figure 1: Investment-output ratio exposure elasticities to a growth-rate shock. The elasticities are initialized by setting the stochastic growth rate state to zero.

Finally, we consider both the shock exposure and price elasticities of consumption in Figure 2. The consumption elasticity to a growth rate shock builds over time, as expected given investment adjustment costs. The $\rho = 1$ elasticities imitate those of an endowment economy like the Bansal and Yaron (2004) economy (without stochastic volatility). The risk aversion parameter γ has very little impact on these exposure elasticities, in contrast to the price elasticities. As revealed by Figure 2, the shock price elasticities are very sensitive, as expected, to the choice of γ. Recall the robustness interpretation of recursive utility, where misspecification concerns contribute a martingale component to valuation. This component comes to dominate as γ becomes larger and this leads to a relatively flat shock

price elasticity trajectory.

Figure 3 shows how the elasticities depend on the initial level of volatility. The key takeaway is that stochastic volatility provides exogenous fluctuations in risk pricing, in contrast to some of the more endogenous mechanisms that we explore going forward. In addition, as is well understood, a shock to exogenous volatility itself is priced under these preferences, as shown via its shock price elasticity in the right panel.

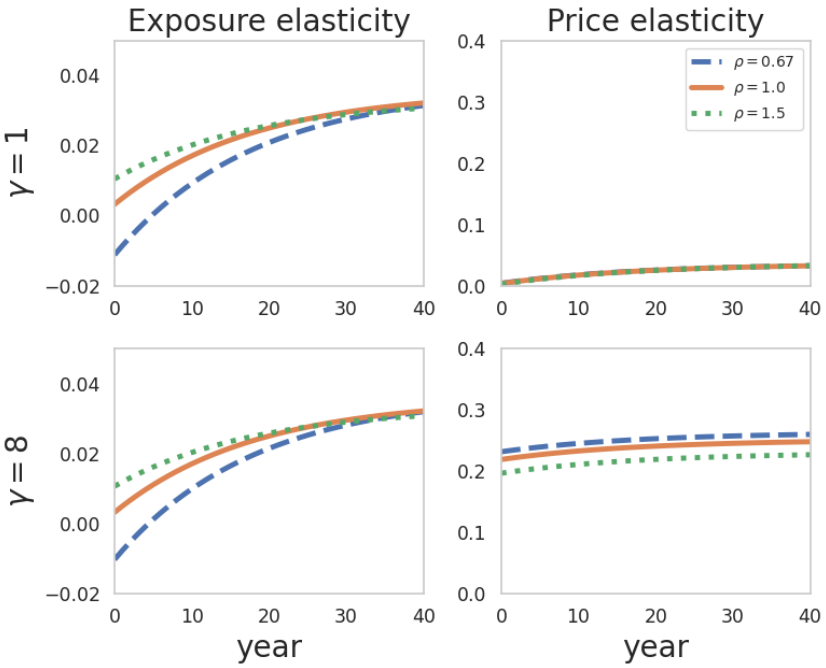

Figure 2: Exposure and price elasticities for the growth rate shock. Perturbations are relative to the equilibrium consumption process. The growth and volatility states are set to their medians.

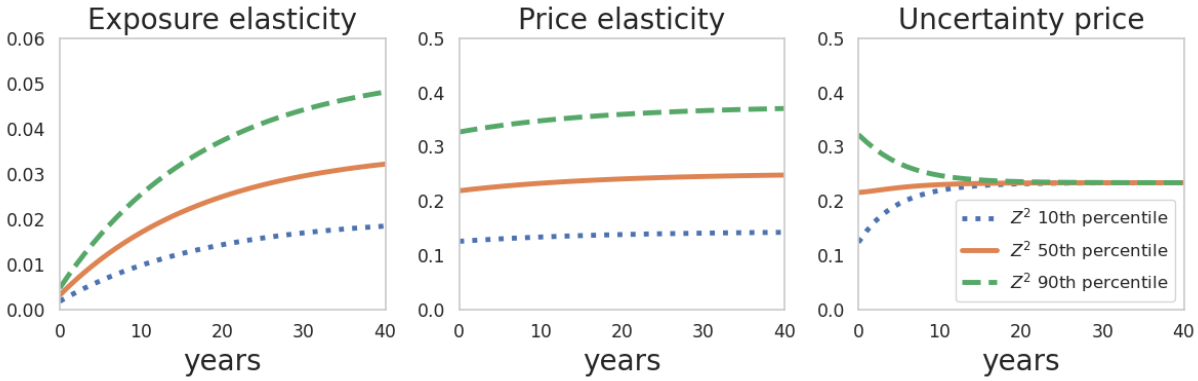

Figure 3: Shock exposure and price elasticities for $\gamma = 8$, $\rho = 1$, and for alternative volatility quantiles. The shock elasticities apply to the growth-rate shock.

4.5 Endogenous fluctuations in valuation

Here we illustrate an endogenous channel induced by ambiguity aversion by building on ideas from Chen and Epstein (2002), Hansen (2007), Andrei et al. (2019), and, in particular, Hansen and Sargent (2021). As we will show, this adds a form of state dependence in valuation. For this illustration we focus exclusively on the case in which $\rho = 1$. To feature the endogeneity of fluctuations in valuation, we abstract from exogenously specified stochastic volatility in this subsection (by setting $\sigma_2 = 0$). In addition, we impose that

$$\sigma_k = \begin{bmatrix} .0087 & 0.0038 & 0 \end{bmatrix}$$
$$\sigma_1 = \begin{bmatrix} 0 & .055 & 0 \end{bmatrix}$$

We follow Hansen and Sargent (2022) by considering both model ambiguity and potential model misspecification. Recall that recursive utility provides a direct link to the latter, an approach that we continue to use here. For model ambiguity, we proceed differently. Given a parameterized family of models, the investor is unsure how much weight should be given to each. For a Bayesian decision maker, this would be addressed with subjective inputs in the form of a prior. Our investor is unsure which such prior to impose. Formally, we use a framework for diffusion processes that is consistent with Chen and Epstein (2002) to entertain a rich family of what Hansen and Sargent (2022) refer to as "structured" models.

In our application we start with a four-dimensional space of unknown parameters in the drifts of capital K and the growth rate Z^1. We modify the evolution of Z^1 to be:

$$dZ_t^1 = \left(\psi_1 - \beta_1 Z_t^1\right) dt + \sigma_1 \cdot dB_t$$

where the parameter ψ_1, which we have taken to be zero so far, allows for a shift in the local drift dynamics that does not scale with Z^1. In the long-term, $\psi_1 \neq 0$ could induce a nonzero unconditional mean in Z^1 process. The unknown parameters are $\eta_k, \beta_k, \psi_1, \beta_1$. Recall that η_k governs depreciation and β_k the exposure to long-term growth rate uncertainty. Our investors take uncertainty in these parameters as a starting point, but they entertain a so-called time varying parameter perspective without imposing a prior on the form of the time variation. Instead, the parameters are constrained to be in an ambiguity set using a recursive measure of relative entropy or Kullback-Leibler divergence as described in Hansen and Sargent (2021).

We consider two specifications. One limits the ambiguity to be over the two slope

parameters, (β_k, β_1), and the other also includes the constant terms, (η_k, ϕ_1). Figure 4 plots both the two-dimensional and four-dimensional ambiguity sets. By construction, the projection of the slope coefficients for the four-dimensional set is contained within the two-dimensional ambiguity set as depicted in the right panel of Figure 4.[10] By design, this approach entertains misspecification relative to a benchmark in a much more structured way than that embedded in the robust interpretation of Kreps and Porteus (1978) utility.

Recall that in the standard continuous-time recursive formulation of dynamic programming, the decision-maker maximizes the expected value-function increment by choice of a control. In our recursive formulation of ambiguity, algorithmically a fictitious second-agent minimizes the expected value function increment over the respective sets of parameter values, instant-by-instant. The minimizer will reside somewhere on the boundary and its location will depend on the realized growth-rate state, z^1. The problem is made tractable in part because the minimization problem is quadratic. We also include potential model misspecification in the same manner as described previously. As we have shown, $\gamma = 1$ abstracts from misspecification concerns while larger values of γ enhance these concerns.

We illustrate the nonlinear outcome by reporting the implied uncertainty-adjusted (minimizing) drift for the long-run growth process in Figure 5. The downward slope of the line in the baseline model governs the pull towards zero in the conditional mean dynamics for Z^1. The dashed and dot-dashed curves are the uncertainty-adjusted nonlinear counterparts. The dot-dashed curve includes misspecification concerns in addition to parameter ambiguity. The left panel shows implications when the ambiguity consideration is limited to the slope coefficients while the right panel illustrates outcomes when the ambiguity is four-dimensional.

Observe that these curves are flatter for negative growth rates and steeper for positive growth rates. This is to be expected because investors fear persistence when growth is sluggish and the lack of persistence when growth is brisk. This outcome emerges in the computations in part because of how the minimizing choice of β_1 over the ambiguity set displayed in Figure 4 depends on Z^1. The investor is exploring the other parameters as well, and the outcome of minimization also impacts a counterpart for drift specification for capital.

While the one-capital model without ambiguity concerns can be approximately solved using log-quadratic specification, the model with ambiguity requires a global alternative to

[10] We constructed these sets using, in the notation of Hansen and Sargent (2021), $q = 0.2$ with $\rho_1 = 0$ and $\rho_2 = \frac{q^2}{|\sigma_1|^2}$ for the two parameter case, and $\rho_2 = \frac{q^2}{2|\sigma_1|^2}$ for the four parameter case.

capture the potential nonlinearities that are entertained by the decision maker.

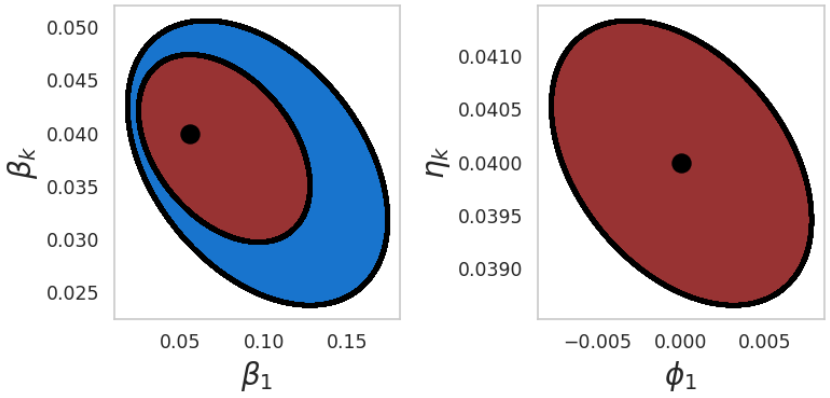

Figure 4: Ambiguity parameter sets constrained by a flow measure of relative entropy developed in Hansen and Sargent (2021). The left panel of the plot depicts the ambiguity in the slope coefficients for the state Z_t^1 in the capital evolution and the state evolution. The blue region plots two-dimensional ambiguity set and red region gives two-dimensional projection for the four-dimensional ambiguity set. The red region in the right panel gives the two-dimensional projection of the constant terms in the capital and state evolution for the four parameter ambiguity set. Baseline values for the four parameters are recorded as black dots.

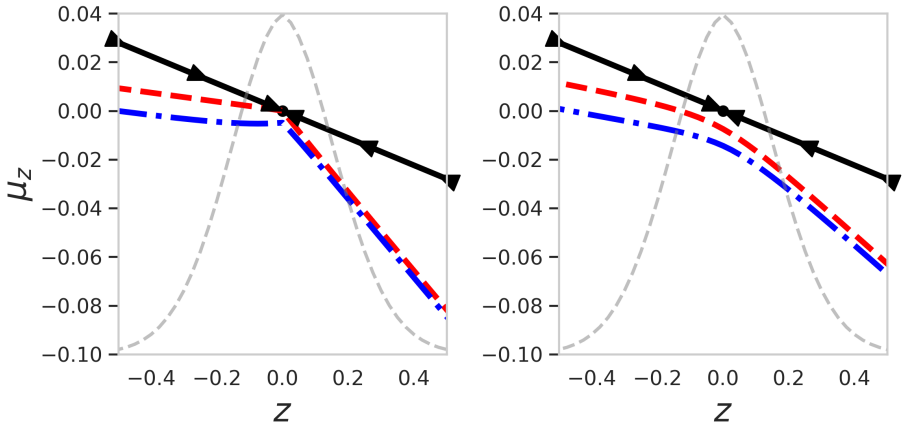

Figure 5: Uncertainty-adjusted growth rate drift and baseline stationary density for Z^1. The left panel explores ambiguity over slope parameters only and the right panel includes the constant terms as well. Black solid: baseline model; red dashed: $\gamma = 1$; blue dot-dashed: $\gamma = 3$ for the left panel and $\gamma = 4$ for the right panel. The lower value of γ in the left panel relative to the right panel is imposed to so that the magnitudes of the misspecification adjustments are approximately the same. The gray dashed curve depicts the stationary density for Z^1 stationary density.

The two forms of uncertainty aversion we consider introduce a composite martingale component to valuation. We explore its properties by looking at the implied uncertainty price elasticities using the formula (14). The results are reported in Figure 6. We represent

state dependence by exploring not only the median, but also the 10th and 90th percentiles. While the 90th percentile prices start higher than the others, this gets reversed as we go out to longer horizons. This reflects the decrease in persistence in the uncertainty-adjusted probability measure for relatively high realized values of the growth state Z_t^1. As is evident from the right column in Figure 6, misspecification concerns contribute to the asymmetry in the responses in an important way. This is particularly true for the two-dimensional specification of ambiguity aversion.

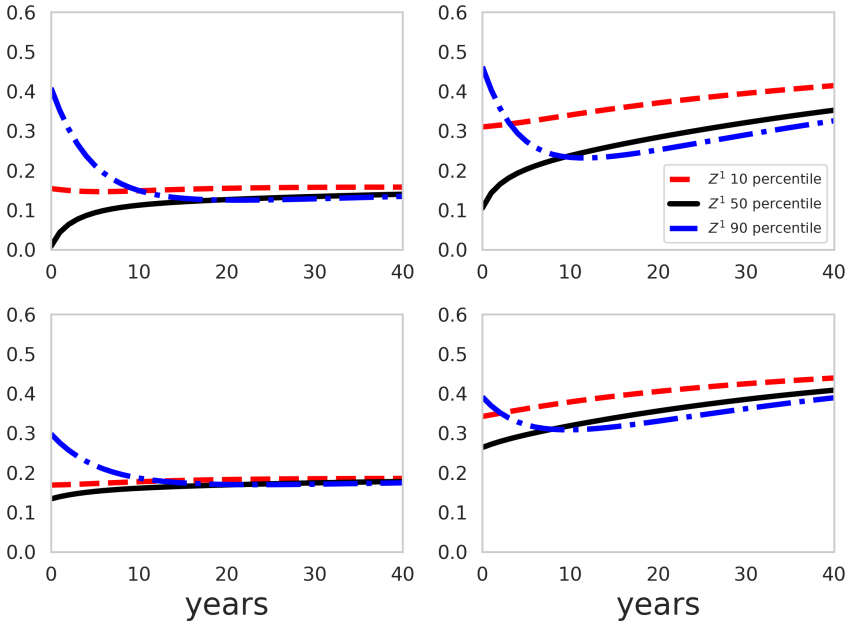

Figure 6: Shock price elasticities for the martingale contribution induced by uncertainty aversion. Black solid: median of the Z^1 stationary distribution; red dashed: .1 decile; and dot-dashed: .9 decile. The top row gives results for $\gamma = 1$ (left panel) and $\gamma = 3$ (right panel) when the ambiguity set is two dimensional. The bottom row gives results for $\gamma = 1$ (left panel) and $\gamma = 4$ (right panel) for the four dimensional ambiguity set.

In summary, we induce changes in asset values by investors' altering their perspectives on what models are most concerning within the constrained ambiguity set. These fluctuations prevail in large part because of uncertainty in the persistence of the process Z^1. In low growth states investors are concerned about being "stuck in a rut" whereas in good times they worry that "brisk growth" will end soon. This type of mechanism was noted in Hansen (2007) in a distinct but related modeling framework. That paper uses a different specification of ambiguity aversion and entertains explicit learning. In the example here, learning is off the table because of potential time or state variation in parameters. Relatedly, learning about persistence was also featured in Andrei et al. (2019) as a mechanism

for fluctuations over time in valuation.

4.6 Sluggish heterogeneous capital stocks

We now explore two capital models with growth rate uncertainty. Precursors of these models are the multiple tree models of Cochrane et al. (2008) and Martin (2013). These models do not entertain capital movements from one production source to another. Here we follow Eberly and Wang (2009), Eberly and Wang (2012), Hansen et al. (2020), and Kozak (2022) by allowing capital mobility subject to adjustment costs. In this sense, capital movements are sluggish. We extend the capital evolution in Eberly and Wang (2009), Eberly and Wang (2012), and Kozak (2022) by introducing exposures to an exogenously specified growth rate uncertainty consistent with our previous examples, similar to Hansen et al. (2020). We allow for the exposure to this uncertainty to be heterogeneous.

Formally, consider a family of models with two capital stocks and adjustment costs.

$$dK_t^j = K_t^j \left[\Phi^j \left(\frac{I_t^j}{K_t^j} \right) + \beta_k^j Z_t^1 - \eta^j \right] dt + K_t^j \sqrt{Z_t^2} \sigma_k^j \cdot dB_t,$$

for $j = 1, 2$. Suppose that the output equation is now

$$C_t + I_t^1 + I_t^2 = \alpha K_t^a$$

where aggregate capital is a CES aggregator of the two capital stocks:

$$K_t^a = \left[(1-\zeta) \left(K_t^1 \right)^{(1-\tau)} + \zeta \left(K_t^2 \right)^{(1-\tau)} \right]^{\frac{1}{1-\tau}}$$

for $0 \leqslant \zeta < 1$ and $\tau \geqslant 0$. For characterization and computation, we form two state variables: one is $\widehat{Y}_t = \log(K_t^2/K_t^1)$ and the other is $\widehat{K}_t^a$. For this class of models, the value function has the separable form:

$$\widehat{V}_t = \widehat{K}_t^a + \upsilon(\widehat{Y}_t, Z_t).$$

Eberly and Wang (2009), Eberly and Wang (2012), Hansen et al. (2020) and Kozak (2022) feature the case in which the two capital stocks are perfect substitutes ($\tau = 0, \zeta = .5$). In the illustrations that follow, we also impose this restriction as a featured special case. Our computational software allows for production curvature among the two capital stocks,

and as we will illustrate, this opens the door to an even richer collection of examples. With perfect substitutability, the deterministic limit of this model has a continuum of steady states. This makes locally linear-quadratic approximations inoperative. Even with production curvature, local methods can be unreliable. Thus we find global solutions' approaches to be important for this class of examples.

Parameters common across the two capitals				
η_k	ϕ	α, ρ	β_1	β_2	σ_1, σ_2
.04	8	$\alpha =$ .16 .18 .22 $\rho =$ .67 1 1.5	.056	0.194	$\sigma_1 = \sqrt{12}\begin{bmatrix}0 & 0 & 5.7 & 0\end{bmatrix}$ $\sigma_2 = \sqrt{12}\begin{bmatrix}0 & 0 & 0 & .00031\end{bmatrix}$
symmetric		asymmetric			capital volatilities
$\beta_k^1 = .04$		$\beta_k^1 = 0$			$\sigma_k^1 = \sqrt{12}\begin{bmatrix}\sqrt{2}(.92) & 0 & .4 & 0\end{bmatrix}$
$\beta_k^2 = .04$		$\beta_k^2 = .08$			$\sigma_k^2 = \sqrt{12}\begin{bmatrix}0 & \sqrt{2}(.92) & .4 & 0\end{bmatrix}$

Table 4: Parameter values for the two capital model. We include a separate capital shock for each technology. The coefficients on the two capital stocks are given by the first two entries of the σ's. We doubled α for the two capital because K_t^a is the average capital stock for each of the three specifications of ρ. To maintain comparability with the single capital model, we scale the first two entries of σ_k^1 and σ_k^2 by $\sqrt{2}$, since a fictitious social planner can now diversify across the two capital shocks. The specification "symmetric" presumes symmetric exposure to growth uncertainty, while the specification "asymmetric" presumes that only the second capital is exposed to growth uncertainty.

The parameter values that we use in this section are recorded in Table 4. We consider two different specifications of the exposures. One specification is "symmetric." While each capital stock has its own shock, the relative importance of long-term uncertainty to each K^j is the same. The other specification is "asymmetric." The first capital stock is not exposed to long-run uncertainty while the second one is. Table 4 gives some additional explanations and details. For these economies, we abstract from parameter ambiguity.

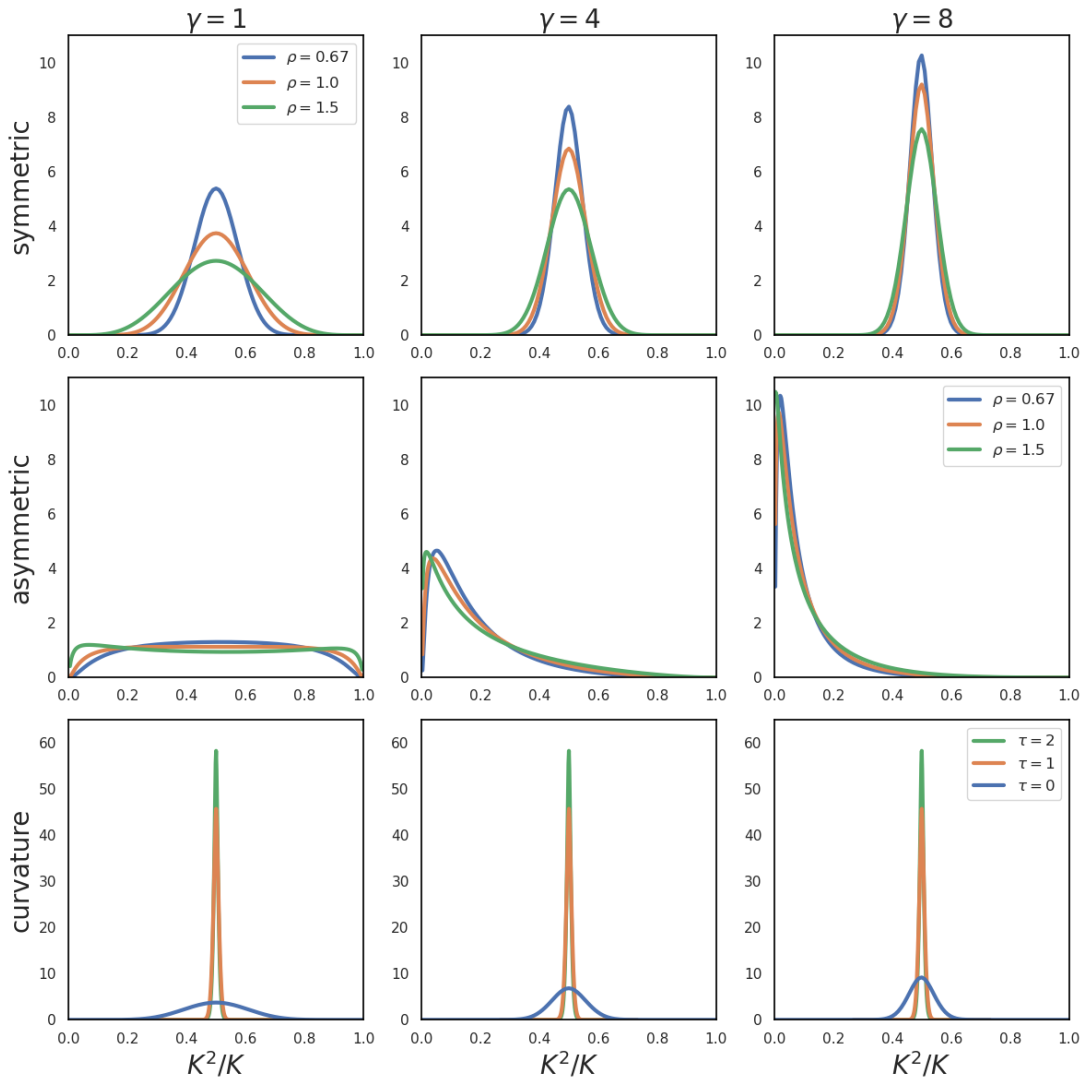

Figure 7: Stationary densities for the second capital stock as share of total capital. For the "asymmetric" row, only the second capital stock is exposed to growth-rate uncertainty. Finally, for the "curvature" row, the $\tau = 1$ specification assumes a unitary substitution elasticity across the two types of capital, and the $\tau = 2$ specification assumes a substitution elasticity equal to $1/2$. The results in the third row impose $\rho = 1$ and the same exposure to long-term uncertainty for both capital stocks.

We start by reporting stationary densities in Figure 7 for the fraction of the capital that is allocated to the second technology. Initially, consider the case of symmetric exposures. We see some sensitivity to the IES with the plots for $\rho = .67$ being more peaked. As Eberly and Wang (2012) emphasize, increasing risk aversion through changing γ (or increasing the concern for misspecification) makes diversification all the more attractive giving rise to densities that are much more sharply peaked. It is noteworthy that when $\gamma = 1$,

the asymmetric parameterization flattens out the allocation densities. But arguably more interesting is that for $\gamma = 8$ the second capital stock becomes much less attractive and even more so as we decrease ρ. The mode of the density is now centered near .2 instead of .5 as investors seek to avoid exposure to long-term uncertainty. For the model specifications discussed so far, the two capital stocks are perfect substitutes in the production of output.

So far, the only heterogeneity in the capital stock is in the exposure to shocks and long-term uncertainty. We next illustrate the impact of production function curvature by making the elasticity of substitution across the two types of capital one ($\tau = 1$) and one-half ($\tau = 2$). See the third row of Figure 7. This decrease in elatisticity of substitution in production makes the stationary densities more peaked. This is to be expected given the more central role played by both capital stocks in the production of output. We include this computation as an illustration only, as there are alternative substantive motivations for multiple capital stocks with differential impacts on production. For example, intangible, organizational or human capital contribute to production in arguably distinct ways. While incorporation of these components could lead to even richer models, the force on display in Figure 7 will still be present.[11]

Figure 8 plots the shock elasticity or local impulse responses for the aggregate investment-to-capital ratio. We only depict these for $\gamma = 12$ as the $\gamma = 1$ responses are very similar. The elasticities for the symmetric case are very similar to those we computed for the one-capital model. In contrast, for the asymmetric case the responses are more muted consistent with the flatter densities reported in Figure 7. Figure 9 depicts the shock price elasticities for the growth shock. We report only the case in which $\gamma = 12$ as the $\gamma = 1$ results are unsurprisingly small. The price elasticities are very flat reflecting a dominant martingale component to the SDF. Recall we used robustness concerns to model misspecification as an important contributor to this martingale. The magnitude of the growth-rate shock price elasticities are very close to those we reported for the single-capital model. In the asymmetric case, the prices are significantly smaller because capital is reallocated to reduce the exposure to growth rate uncertainty.

[11] See Crouzet et al. (2022) for a recent discussion of modeling and measuring intangible capital.

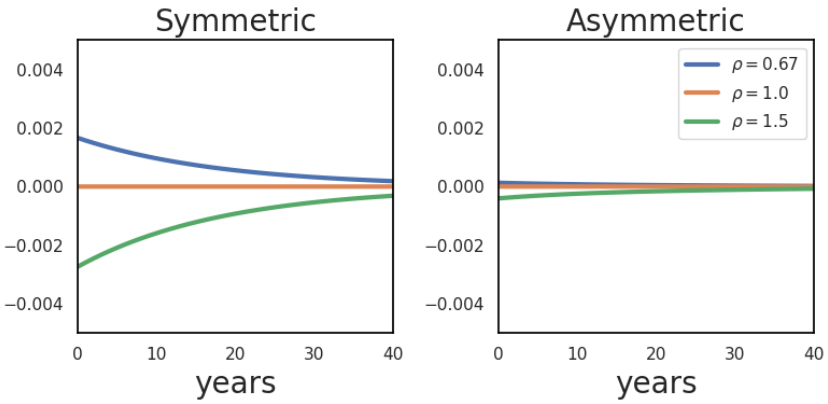

Figure 8: Investment-output ratio exposure elasticities for growth-rate shock when $\gamma = 8$. The reported elasticities condition on the medians of the state variables.

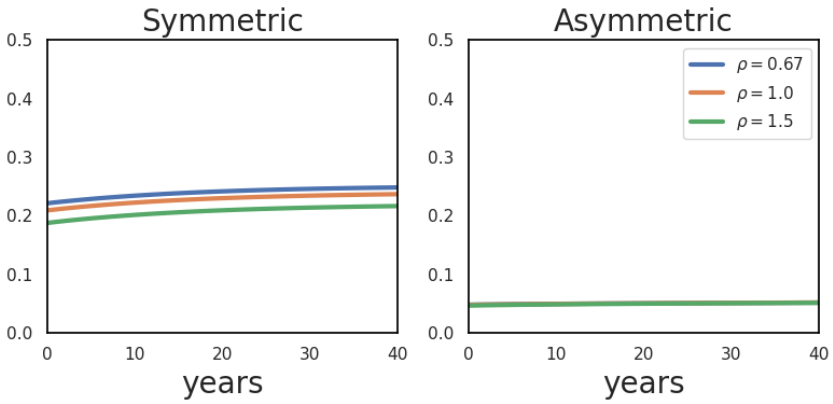

Figure 9: Consumption price elasticities for the growth-rate shock when $\gamma = 8$. The reported elasticities condition on the medians of the state variables.

5 Heterogeneous agents and financial frictions

We now explore a different form of heterogeneity. We alter our one-capital baseline model in Section 4 to include (ex-ante) agent heterogeneity and financial frictions. Agents will be heterogeneous in both their preferences, productivities, and financial market access. We think of the baseline economy as one in which multiple economic agents have homogeneous preferences and homogeneous access to the production technology. In this case, consumption and wealth are proportional over time, making aggregation immediate. This simple aggregation will not be true in the class of economies that we explore in this section. With various forms of market impediments, we can no longer focus on the planner problem as has

been true in our previous examples. Instead we study a competitive equilibrium in which wealth heterogeneity matters. As in our previous economies, we entertain the possibility of growth-rate uncertainty in the production technology. We feature model comparisons within a conveniently nested class of models.

5.1 Environment, equilibrium, and solution overview

There are two agent types in the economy: "experts" and "households", indexed by e and h, respectively. Both agents have recursive preferences, but their preference parameters (δ, γ, ρ) can differ. There is a single capital accumulation technology, but the productivity of this capital stock may differ in the hands of each of the agents, with $\alpha_e \geqslant \alpha_h$. Capital trades freely amongst agents, with price Q_t that follows endogenous diffusive dynamics.

Several financial instruments also trade: risk-free short term debt at an interest rate r_t, and various financial claims exposed to aggregate risk: (a) derivatives contracts traded amongst households at vector π_t per unit of Brownian increment risk exposure; and (b) equity contracts issued by experts with payoff proportional to the return on capital they hold. In some of our economies, experts face a financial restriction: they must remain exposed to at least a fraction $\underline{\chi}$ of the total capital they hold. Experts therefore cannot issue unlimited equity nor can they trade freely in hedging contracts.

Let N_t^j be the date-t net worth of type-j agent for $j = h, e$. Then,

$$\frac{dN_t^j}{N_t^j} = \left(\mu_{n,t}^j - C_t^j/N_t^j\right) dt + \sigma_{n,t}^j \cdot dB_t, \tag{24}$$

where the local mean $\mu_{n,t}^j$ net of consumption and the shock exposure vector $\sigma_{n,t}^j$ are

$$\mu_{n,t}^j = r_t + \frac{Q_t K_t^j}{N_t^j}\left[\mu_{R,t}^j - r_t\right] + \theta_t^j \cdot \pi_t \qquad\qquad \sigma_{n,t}^j = \frac{Q_t K_t^j}{N_t^j}\sigma_{R,t} + \theta_t^j,$$

and where K_t^j and θ_t^j denote the capital and hedging positions chosen by the type-j agent. A hedging position θ_t^j implies an exposure $N_t^j \theta_t^j \cdot dB_t$ to Brownian risk. As capital is also exposed to Brownian risk, $\sigma_{n,t}^j$ reflects both exposures. Due to productivity differences, the expected excess return on capital $\mu_{R,t}^j - r_t$ is type-specific (see Online Appendix B for the expression for $\mu_{R,t}^j$). The risk exposure vector, $\sigma_{R,t}$, for capital is common for households and experts and has a direct contribution from capital-quality shocks and a contribution from the market price Q_t of capital.

Market incompleteness is encoded via a constraint on the hedging vector θ_t^e of experts. While households are unconstrained, experts have restrictions on their exposure to aggregate risk. Suppose experts choose θ_t^e to reduce their exposure to capital risk by a fraction χ_t. To achieve this reduction,

$$\theta_t^e = (\chi_t - 1)\frac{Q_t K_t^e}{N_t^e}\sigma_{R,t}.$$

Imposing a so-called "skin-in-the-game constraint": $\chi_t \geqslant \underline{\chi}$ restricts the ability of the experts to hedge their risk to the capital that they own:

$$\theta_t^e \in \left\{(\chi_t - 1)\frac{Q_t K_t^e}{N_t^e}\sigma_{R,t} \;\; : \;\; \chi_t \geqslant \underline{\chi}\right\}, \tag{25}$$

Notice that even in the limit, relaxing this constraint still limits the type of hedging that can be done by experts, since the portfolio weights remain constrained to be proportional to $\sigma_{R,t}$. For the purpose of making model comparisons, the structure just described embeds three types of heterogeneity. First, there is preference heterogeneity. In addition to heterogeneous subjective discounting, we allow for $\gamma_h \geqslant \gamma_e$, which can reflect either an enhanced aversion to risk on the part of households or less confidence in the probability model. Second, we allow for experts to use capital more productively than households ($\alpha_e \geqslant \alpha_h$). Finally, we entertain heterogeneity in financial market access: the skin-in-the-game restriction (25) limits experts' ability to offset their capital risk exposure via equity issuance. These alternative forms of heterogeneity allow revealing comparisons across alternative model specifications.

Our definition of a competitive equilibrium is standard: it is a set of price processes (Q, π, r) and allocation processes $(C^e, C^h, N^e, N^h, K^e, K^h, \chi, \theta^e, \theta^h)$, such that agents solve their constrained optimization problems, taking price processes as given, and all markets—the goods market, the market for capital, and the market for derivatives (which are in zero net supply)—clear. By Walras' law, the risk-free debt market will also clear.

We look for a Markovian equilibrium in which the state variables are the wealth distribution, the aggregate stock of capital, as well as the driving processes Z^1, Z^2. Given the homogeneity properties of our model, (i) the wealth distribution can be summarized by the experts' wealth share $W_t \stackrel{\text{def}}{=} N_t^e / \left(N_t^e + N_t^h\right)$, and (ii) all growing processes scale with K_t, which means that $X_t' \stackrel{\text{def}}{=} (W_t, Z_t^1, Z_t^2)$ can serve as a state vector for our economy. While (Z^1, Z^2) are specified exogenously, the wealth share W evolves endogenously.

The log continuation value of each type-j agent takes the additively separable form, analogous to the value function for benchmark economy given by (20):

$$\widehat{V}_t^j = \widehat{N}_t^j + v^j(X_t),$$

where $\widehat{N}^j = \log N^j$. We construct a Hamilton-Jacobi-Bellman equation analogous to that given in (21) for the social planner in the benchmark economy. (See Online Appendix B for these HJB equations.) The homogeneity properties of our model allow us to derive agents' optimal consumption and portfolio choices as a function of v^j. For instance, the optimal consumption-wealth ratio for each agent type is

$$c^j(x) = \delta^{1/\rho} \exp\left[(1 - 1/\rho)v^j(x)\right],$$

and their portfolio choice solves a familiar problem that includes both a mean-variance and a hedging component:

$$\max_{K^j, \theta^j} \Big\{ \underbrace{\mu_n^j - \frac{1}{2}\gamma_j |\sigma_n^j|^2}_{\text{mean-variance}} + \underbrace{(1-\gamma_j)(\sigma_x \sigma_n^j) \cdot \frac{\partial v^j}{\partial x}}_{\text{hedging}} \Big\}. \tag{26}$$

The outcome of this portfolio problem is a set of Euler equations (when constraints are non-binding) and inequalities (when constraints are binding). For instance, households will hold strictly positive amounts of capital if and only if their expected excess return $\mu_{R,t}^h - r_t$ is sufficiently high to match the market compensation they could otherwise obtain through derivatives markets. Similarly, experts have an incentive to issue as much equity as possible (and their financial constraint will then bind) when their expected return on capital $\mu_{R,t}^e - r_t$ is greater than the market compensation $\pi_t \cdot \sigma_{R,t}$ they need to pay to holders of their equity. Their issuance constraint does not bind otherwise. Since experts are more productive than households, it is efficient for them to hold all the capital in the economy and exhaust their equity-issuance capacity. In fact, one can show that whenever households hold positive amounts of capital, experts' equity issuance constraint must be binding.

The consumption and portfolio choice of the various agent types leads to endogenous dynamics for the experts' wealth share W_t; its drift rate depends on the consumption-to-wealth ratio of households relative to that of experts, on experts' leverage and their expected excess return on capital relative to its required market compensation and finally the differential aggregate risk exposure between households and experts. The diffusion

coefficient of W_t only depends on this latter force. The wealth share dynamics depend on asset prices, which themselves depend on wealth share dynamics—generating a two-way feedback loop that amplifies capital return volatility (Brunnermeier and Sannikov, 2014). While this section only provides an overview of the model solution, its full details are contained in Online Appendix B.

The remainder of this section explores this heterogeneous agent model in a series of "model comparisons," offering some general takeaways. In Section 5.2, we specify four different economic environments that differ in terms of market opportunities and productivities of the two agent types. Section 5.3 then explores parameter sensitivity within each of these environments to help elucidate the economic forces at work. Section 5.4 then makes comparisons across environments by discussing outcomes that both unite and distinguish these models. Finally, we provide some discussion of the extant literature.

5.2 Alternative economic environments

We explore four different types of economic environments. These are motivated by some prior contributions, but they differ in the actual modeling inputs, including a stochastic technology that includes long-run risk. The first environment is motivated by the Basak and Cuoco (1998) model (specification RF for "risk-free") in which households can only engage in risk-free exchange in security markets in an environment extended to include long-term uncertainty. Production is done by experts. The second setup allows for unrestricted trade in the equity market, but this remains a "partial risk sharing" environment (specification PR) since our model accommodates a three-dimensional specification of the Brownian motion. In the case of only a single shock, our risk-sharing limitation becomes inconsequential, making this setup very similar to that of Dumas et al. (2000) and Gârleanu and Panageas (2015).[12] Our third setup adds a skin-in-the-game constraint on the productive experts along the lines of He and Krishnamurthy (2013), enforced by setting $0 < \underline{\chi} < 1$ on the productive experts (specification SG for "skin-in-the-game"). Finally, motivated by Brunnermeier and Sannikov (2014), we also allow households to be productive, but less

[12] Gârleanu and Panageas (2015) impose exponentially distributed death probabilities in conjunction with an exogenous allocation of agent types at birth. The finite life feature enhances the subjective discounting and pulls the expert wealth fraction towards a pre-specified level interpreted as the wealth fraction of experts at birth. See Appendix D of Gârleanu and Panageas (2015) for an elaboration. Under our reinterpretation of risk aversion, the death probabilities are known with full confidence in contrast to the uncertainty induced by the vector Brownian motion. By design, this finite life feature ensures a stationary wealth distribution. In the reported examples we do not impose this finite-life aspect, although our computer code and the full model details in Online Appendix B accommodate it.

so than experts (specification IP for "inefficient production"). Here, experts do not trade equity claims (so the skin-in-the-game constraint is maximally tight). The specifications for these four environments are summarized in Table 5.

In the reported examples $\rho_h = \rho_e = 1$, and $\delta_h = .01$. Furthermore, experts will always be less patient than households, in order to accommodate a stationary wealth distribution. Sensitivity to these choices are also interesting and straightforward to explore. When we explore sensitivity to γ_e, we shall refer to this as "expert risk aversion," but as we have argued previously, this could equivalently be interpreted as a lack of confidence in the stochastic specification. Specifically, when $\gamma_e < \gamma_h$, experts are more confident in the stochasic specifications of technology than households.

economy	pneumonic	household productivity	market access	risk aversion
RF	"risk-free"	$\alpha_h = -\infty$	$\underline{\chi} = 1$	$\gamma_e \leqslant \gamma_h$
PR	"partial risk-sharing"	$\alpha_h = -\infty$	$\underline{\chi} = 0$	$\gamma_e \leqslant \gamma_h$
SG	"skin-in-the-game"	$\alpha_h = -\infty$	$0 < \underline{\chi} < 1$	$\gamma_e \leqslant \gamma_h$
IP	"inefficient production"	$-\infty < \alpha_h < \alpha_e$	$\underline{\chi} = 1$	$\gamma_e = \gamma_h$

Table 5: Parameters settings for the four different economic environments. We use the capital accumulation parameters and the parameters governing the exogenous stochastic dynamics given in Table 1.

5.3 Comparisons within each economic environment

We explore the implications of altering the expert risk aversion or the household productivity through four economic environments. Heterogeneity in risk preferences and productivity are two of the key channels to modulate risk price dynamics in this class of models.

5.3.1 Environment RF

We first consider an economic environment in which experts and households only trade a risk-free asset. We explore the pricing implications of the shadow price for return-on-capital shocks $\sigma_R \cdot dB$. This is the risk price that would clear a stock market populated only by experts. The results are reported in Figure 10. A key force in all the models we explore is the importance of expert wealth: when w falls, risk prices rise, potentially dramatically.[13] In this particular environment, experts must directly absorb all risks, and so their demand for risk compensation rises when w falls. The effect of γ_e depicts a tension between the

[13]See Section 2.3 of Panageas (2020) for a derivation of this "countercyclical risk price" property in a class of one-shock heterogeneous-agent models.

level and variability of risk prices. When we increase γ_e, we see an upward shift in risk price levels; at the same time, the state dependence in these prices is pushed further into the left tail of the stationary distribution. Intuitively, experts accumulate more wealth for precautionary reasons as γ_e increases. (These plots hold fixed household risk aversion $\gamma_h = 8$, but there is little sensitivity to this choice because households can only trade in a risk-free security market.) In this environment and the following ones, stochastic volatility contributes importantly to the risk compensations, as is evident by comparing the .1 and .9 percentiles of Z^2 in Figure 10.

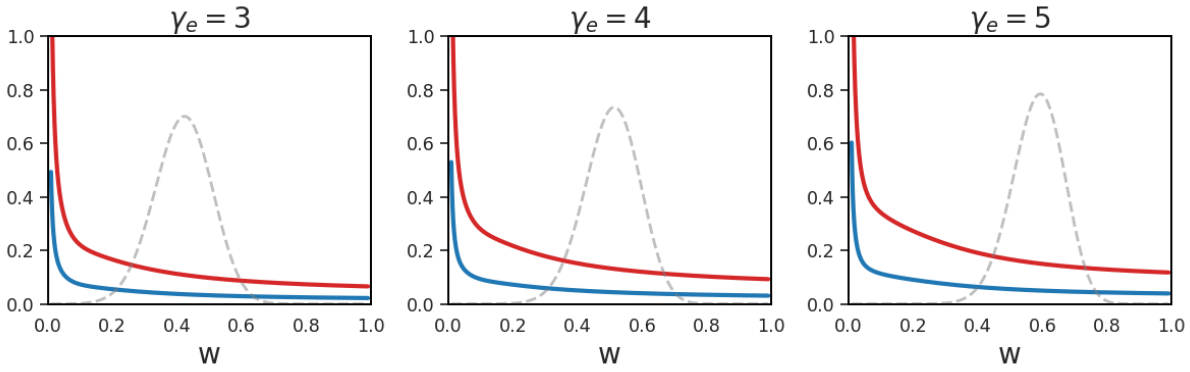

Figure 10: Equity return risk prices for the experts in environment RF. The prices are expressed as functions of the relative wealth of experts for alternative specifications of expert risk aversion. Household risk aversion is set at $\gamma_h = 8$. The subjective discount rates are $\delta_e = .0115$ and $\delta_h = .01$. Stationary densities for the expert wealth share are in the background. For the plots, $Z_t^1 = 0$ and Z_t^2 is set to either the tenth percentile (blue) or the ninetieth percentile (red).

5.3.2 Environment PR

We next consider an environment in which there is frictionless trading in the equity claim. In this case we explore implications for both the equity risk price and the equity retention by the experts. The results are displayed in Figure 11. Given that households now have access to equity, its risk price has very limited sensitivity to γ_e. In contrast, the stationary density for experts' relative wealth is sensitive to γ_e. For instance, wealth is very concentrated at zero when $\gamma_e = 6$. Indeed, as γ_e approaches γ_h, the only prominent heterogeneity remaining is experts higher consumption rate due to their larger subjective discounting, $\delta_e > \delta_h$, which tends to erode experts' relative wealth.

With the homothetic preferences we feature, risk-taking is typically monotonic in wealth,

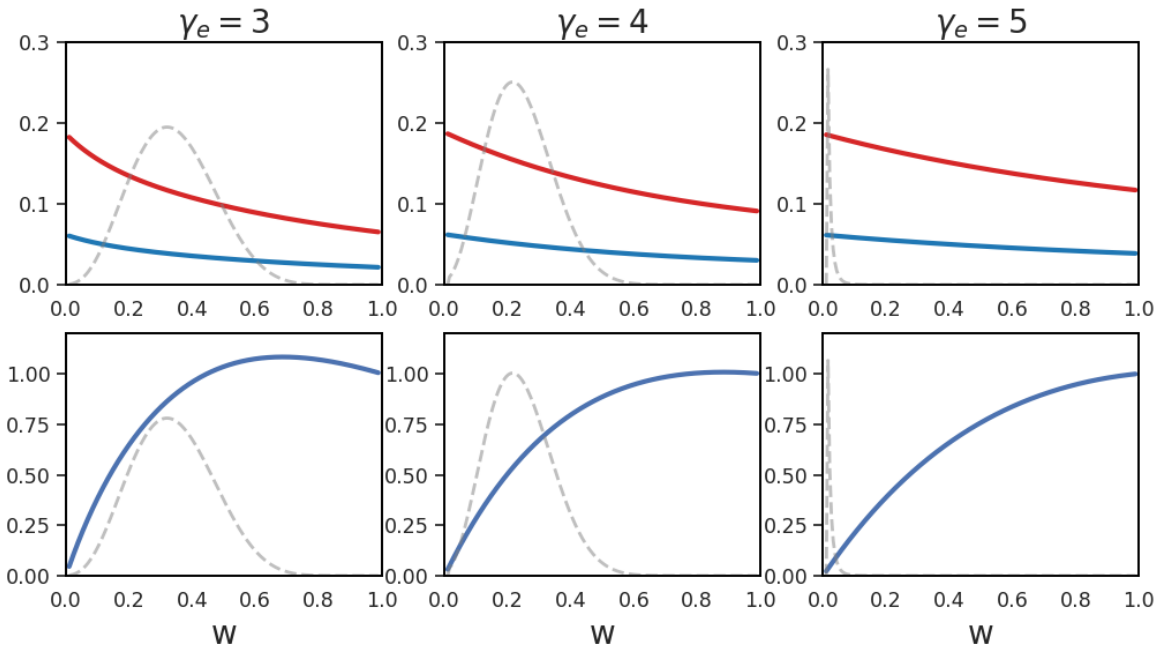

Figure 11: Equity return risk prices (top row) and expert equity retention (bottom row) for environment PR. The objects of interest are expressed as functions of the relative wealth of experts for alternative specifications of expert risk aversion. Household risk aversion is set at $\gamma_h = 8$. The subjective discount rates are $\delta_e = .0115$ and $\delta_h = .01$. Stationary densities for the expert wealth share are in the background. The axis of the stationary density for $\gamma_e = 5$ is scaled down twenty times relative to $\gamma_e = 3, 4$. For the plots, $Z_t^1 = 0$ and Z_t^2 is set to either the tenth percentile (blue) or the ninetieth percentile (red). The equity retention is not sensitive to changes in stochastic volatility.

because absolute risk aversion is decreasing with wealth. In contrast to this conventional result, Figure 11 shows that, particularly when γ_e is small relative to γ_h, the equity retention χ by experts is not monotonic in their relative wealth. Moreover, χ exceeds one for some values of w, more prominently when γ_e is particularly small. Why does this occur?

In this PR environment, risk sharing is limited, and the two agents only trade equity returns. A key force at play in the equity retention figures is households' desire to hedge long-term uncertainty induced by stochastic growth Z^1. Since we have imposed a unitary EIS, the Brownian exposure of the return-on-equity is $\sigma_{R,t} = \sqrt{Z_t^2}\sigma_k$ in this environment. The composite shock $\sigma_k \cdot dB_t$ not only has a direct contribution to the stochastic evolution of capital dK_t, but it also alters the long-term growth prospects through dZ_t^1 (i.e., growth and capital-quality shocks are correlated). Households, being more risk averse than experts, are more concerned about this growth uncertainty. Absent direct integrated hedging markets,

households use capital to obtain partial insurance against growth-rate fluctuations from experts leading them to short expert equity for some realizations of the relative wealth share.[14] This same mechanism plays a central role in the determination of a non-degenerate stationary distribution for W. Typically, complete-markets models with heterogeneous preferences would, except in knife-edge cases, feature degenerate stationary distributions at $w = 0$ or $w = 1$; here, a broad range of preference parameters can produce non-degenerate wealth distributions.[15]

5.3.3 Environment SG

We next explore the impact of adding a skin-in-the-game constraint requiring $\chi \geqslant \underline{\chi} = .2$. This constraint binds for low values of the expert wealth share, and is "occasionally binding" in dynamic simulations. We report results in Figure 12. Increasing γ_e expands the region in which the constraint binds. Figure 12 also illustrates the connection between the binding equity constraint and the nonlinear dependence of experts' equity risk price on w; this extreme nonlinearity is why researchers sometimes refer to binding equity constraints as "financial crises."[16]

The occasionally-binding phenomenon on display in Figure 12 arises because less averse experts retain more risk than their wealth (i.e. $\chi > w$), so the unconstrained region remains "stochastic" (in the sense that $\sigma_w \neq 0$ even when $\chi > \underline{\chi}$). This is essentially what drives the occasionally-binding equilibrium of He and Krishnamurthy (2013): they restrict households to always invest a fixed positive fraction of their wealth in risk-free assets, which makes them act more risk-averse than experts (see their Parameter Assumption 1). In fact, we prove for a very general set of cases that the skin-in-the-game constraint is either always-binding or never-binding when risk aversions are equalized. In this sense, heterogeneous risk-preferences are critical to occasionally binding skin-in-the-game constraints.[17]

[14] As further confirmation of this mechanism, unreported results for $\gamma_e = 2$ and $\gamma_h = 8$ show that households' shadow risk prices for exposure to the growth rate shock range between .25 and .31 when evaluated at the medians of the exogenous state variables, whereas experts' shadow growth risk price ranges between .09 and .15. Risk-aversion heterogeneity is critical to this discrepancy in growth risk prices.

[15] We include the dependence between the direct shock to the capital evolution and the shock to exogenous changes in growth-rate opportunities in our examples because of the empirical calibration reported in Hansen and Sargent (2022). Absent this correlation, χ is monotone increasing in the expert wealth share, and the stationary distribution becomes a point mass at either $w = 0$ or $w = 1$ (depending on the parameters $\delta_e, \delta_h, \gamma_e, \gamma_h$).

[16] Note that in this environment, the potentially-binding constraint implies we must distinguish experts' and households' shadow risk prices for equity exposure. When $\chi > \underline{\chi}$ the two agree; but when $\chi = \underline{\chi}$, the two diverge. We are plotting experts' shadow risk price.

[17] See Online Appendix B (Proposition B.3) for analysis of the case when $\gamma_e = \gamma_h$. For a large set of

On one hand, our results here provide a partial justification for the procedure, performed by many DSGE models with financial frictions, that consists in log-linearizing equilibrium equations assuming constraints are always binding. On the other hand, this exercise illustrates that some models with occasionally-binding risk-sharing constraints may be standing on, perhaps hidden, assumptions about risk aversion heterogeneity.

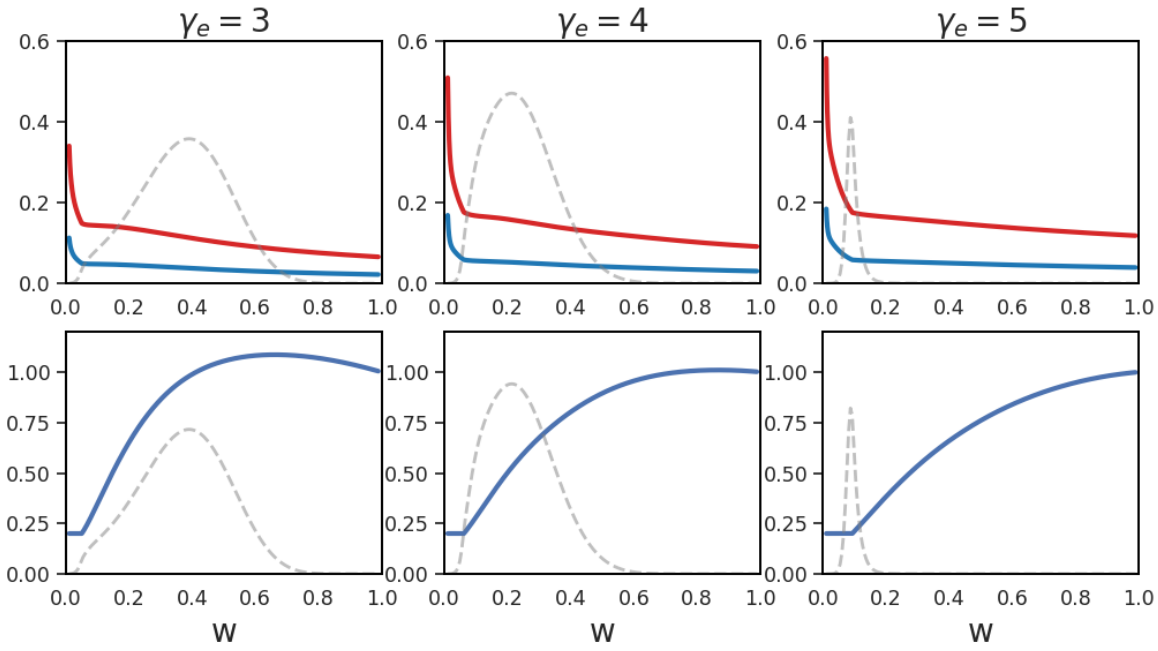

Figure 12: Expert equity return risk prices (top row) and expert equity retention (bottom row) for environment SG. The objects of interest are expressed as functions of the relative wealth of experts for alternative specifications of expert risk aversion. Household risk aversion is set at $\gamma_h = 8$. The subjective discount rates are $\delta_e = .0115$ and $\delta_h = .01$. Stationary densities for the expert wealth share are in the background. The axis of the stationary density for $\gamma_e = 5$ is scaled down eight times relative to $\gamma_e = 3, 4$. For the plots, $Z_t^1 = 0$ and Z_t^2 is set to either the tenth percentile (blue) or the ninetieth percentile (red).

5.3.4 Environment IP

Finally, we explore an environment in which households sometimes engage in production even though experts are more skilled at it. To isolate the role of productive heterogeneity, we eliminate risk aversion heterogeneity here. In financial markets, households and experts trade in a risk-free security, but there is no trade in equities as enforced by setting $\underline{\chi} = 1$.

parameters, either $\chi_t = \underline{\chi}$ for all t or $\chi_t > \underline{\chi}$ for all t, almost surely.

When both agents manage capital, however, they face the same exposure to stochastic capital evolution along with growth-rate risk. For computational reasons, we eliminate stochastic volatility for this environment and set Z^2 equal to mean, μ_2, under the stationary distribution.

In Figure 13, we plot experts' shadow capital risk price and their capital share. For low values of the wealth share, households are active producers even though they have lower productivity. In this region, experts demand high shadow compensations for exposure to capital evolution uncertainty. Increasing household productivity increases the likelihood of inefficient household production but decreases the shadow risk price conditional on inefficiency.

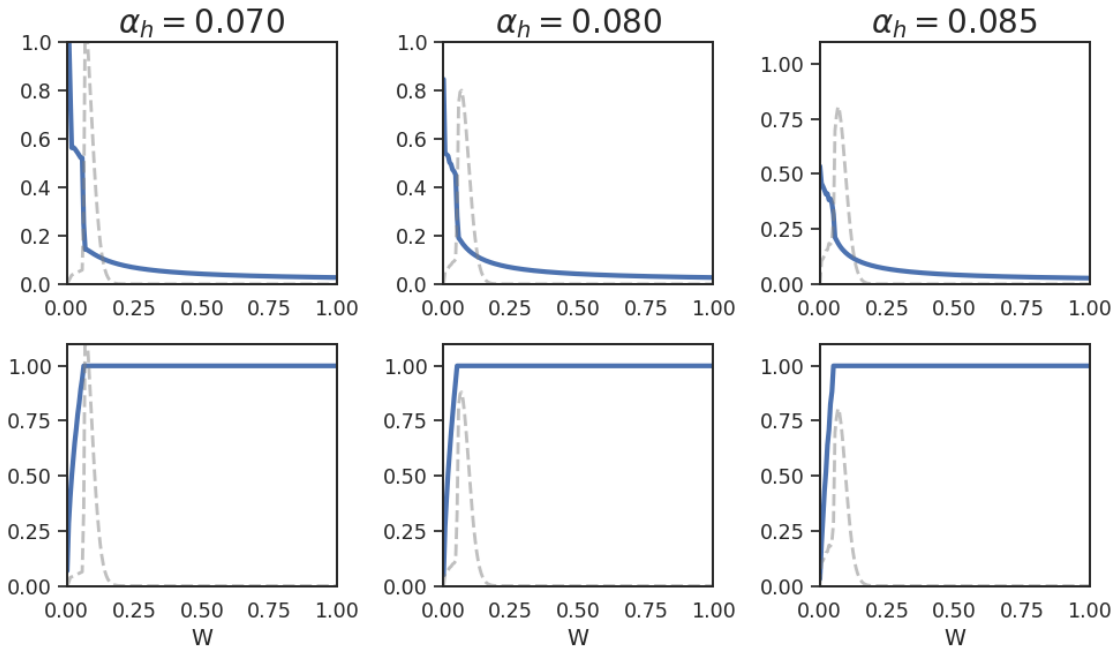

Figure 13: Expert's risk prices (top row) and expert capital share for environment IP. The objects of are interest are expressed as functions of the relative wealth of experts. Household and expert risk aversion are the same, $\gamma_h = \gamma_e = 2$. The subjective discount rates are $\delta_e = .03$ and $\delta_h = .01$. Stationary densities for the expert wealth share are in the background. For the plots, $Z_t^1 = 0$.

5.4 Comparisons across environments

In this subsection we note some interesting comparisons that emerge when we look across environments. Of course, such comparisons may well be sensitive particular parameter

configurations. Our computational methods allow for more comprehensive comparisons done in thoughtful ways.

5.4.1 Deleveraging

Among the four economic environments, we distinguish those that allow "deleveraging" from those that do not—this demarcation represents a significant divide in the nature of model dynamics.

To explore deleveraging, we consider how the "risk share" of experts behaves relative to their wealth share. The expert risk share is given by the product $\chi\kappa$ where χ is equity retention fraction and κ is the fraction of capital held by experts. We think of deleveraging occurring when $\chi\kappa$ falls. This is a reasonable definition to consider, since $\chi\kappa$ falling entails either experts selling capital or issuing additional equity.[18]

By this definition, environments RF and SG do not allow deleveraging. In both cases, all capital is held by experts ($\kappa = 1$) and a financial constraint prevents χ from ever falling to zero. Thus, $\chi\kappa$ is bounded away from zero for RF and SG. This feature implies that as the wealth share of experts declines to zero, experts risk exposure per unit of their wealth grows without bound, which in turn implies experts require unbounded risk compensation as $w \to 0$. See Figures 10 and 12. High risk prices allow experts to earn high profits and recapitalize their balance sheets.

Environments PR and IP do allow deleveraging. In PR, while all capital is held by experts ($\kappa = 1$), there is no constraint on equity issuance (so χ can fall). In IP, experts can deleverage by directly selling capital to households (so κ can fall). Whether through χ or κ, these two environments feature $\chi\kappa$ tending to zero at the same rate as $w \to 0$. Due to deleveraging, experts' risk prices remain bounded even as $w \to 0$; see Figures 11 and 13.

Online Appendix B.9 conducts a formal asymptotic analysis as $w \to 0$. We show analytically how the deleveraging behavior of $\chi\kappa$, through its effect on equilibrium risk compensations, governs the tail shape of the stationary wealth distribution. Looking back at Figures 10-13, one can see how the models with deleveraging can permit substantially more mass near $w = 0$.

[18] In all models we explore, it is true that expert leverage rises as their wealth falls. However, we refer to deleveraging as the *active* decision to reduce risk exposure ($\chi\kappa$) given leverage has risen. Thus, the models that we dub "deleveraging" will have more muted leverage dynamics.

5.4.2 Relative wealth dynamics

In Figure 14 we report the elasticities for experts' wealth share W_t to an initial capital exposure shock. We document the differential nature of the responses depending on the initial relative wealth position which demonstrates a form of nonlinearity. With the exception of environment IP, the responses are very flat suggesting that the shocks have a very persistent impact on the wealth distribution. When we condition on the median wealth share, the responses are lower than when we initialize W_0 at lower percentiles. This is evidence of some reversion in these nonlinear settings since "escapes" become more likely with enhanced volatility. Initializing at even smaller quantities than we report will reveal more decay in the elasticities as there will eventually be pull away from the $w = 0$ boundary.[19]

Recall that in environments RF and IP, households only trade in risk-free securities. In environment IP, however, households obtain risk exposure from directly holding capital, in contrast to environments RF. As is evident from the top row of the figures, the shock responses are initially much larger with notable reversion to zero for IP environment than for the others. This decay in the shock elasticities to zero, as we increase the horizon, is much more substantial for the low quantiles than for the median of the relative expert share of the wealth distribution.

5.4.3 Uncertainty prices

Households and experts share risk in environments PR and SG, but they do not engage in full risk-sharing. Thus we expect differences in the implied shadow prices for experts and households. Recall that these uncertainty prices use the interpretation of recursive preferences as "aversion to model mispecification."[20] Figure 15 explores differences in the implied uncertainty shadow prices for growth-rate shocks for the two agent types. First

[19]The finite-life imposition as described in footnote 12 would provide an additional mechanism for reversion away from the boundaries of the wealth distribution.

[20]In environments like RF and SG, limited expert deleveraging creates an asymptote for local "risk pricing" at $w = 0$. While the shadow stochastic discount factors play a role in representing intertemporal budget constraints, they may only determine what Hugonnier (2012) refers to as fundamental prices. Since equilibrium wealths are constrained to be positive at all dates, Hugonnier's insightful paper notes the possibility of bubbles, i.e., equilibrium security prices above their fundamental values. He characterizes the bubbles in terms of local martingales that fail to be global martingales in the stochastic discount factor processes. From a numerical perspective, this can potentially create subtle issues in computing shock price elasticities that need to be examined on a case-by-case basis, including the proper treatment of boundary conditions. That being said, this subsection studies the uncertainty prices to growth rate shocks, as opposed to shocks hitting the level of capital. Since local uncertainty prices for these shocks do not feature such an asymptote at $w = 0$, we conjecture such local martingale issues are not critical to the calculations here.

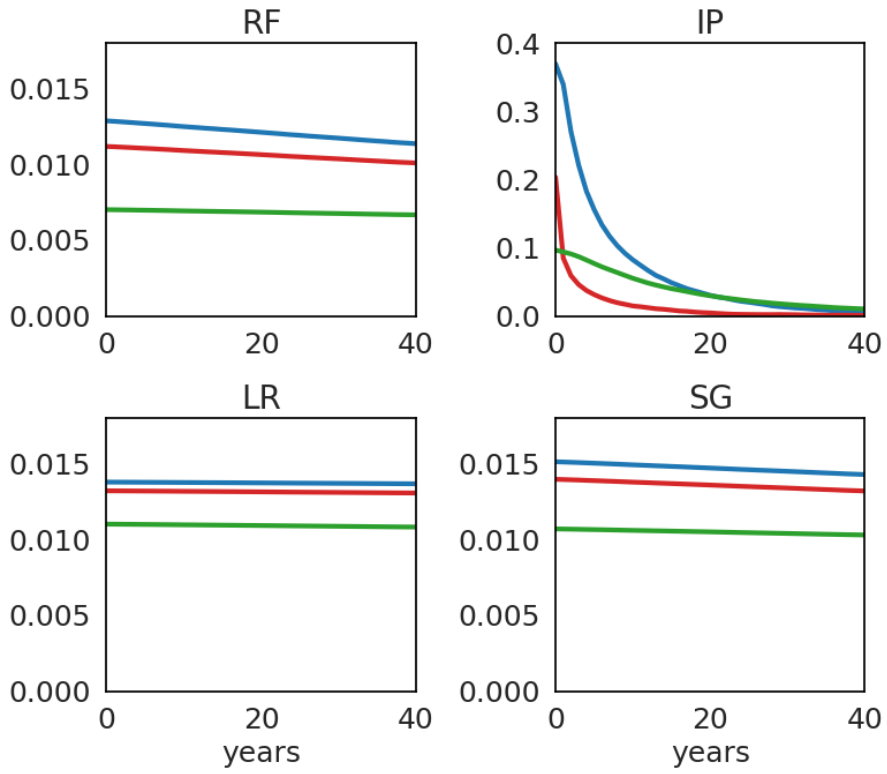

Figure 14: Relative wealth response elasticities to an initial period capital shock for the four environments. We use $\gamma_e = 4$ and $\delta_e = 0.0115$ for environments RF, PR, and SG. For environment IP, we set $\gamma_e = 2$, $\delta_e = 0.03$ and $\alpha_h = .08$. For all environments, $\gamma_h = 8$ and $\delta_h = 0.01$. We restrict the initial exogenous state variables to be at their medians. The blue curve gives elasticities when W is initialized at the .05 percentile of the relative wealth distribution, the red curve at the .1 percentile, and the green curve at the median.

of all, we see sizable shadow compensation for exposure to growth rate uncertainty. In addition, the significant difference between experts' and households' shadow prices reflects the preference inequality $\gamma_h > \gamma_e$ along with the incomplete risk sharing. Third, by looking at the differences within each of the four panels, we see the impact of the initial stochastic volatility. Finally, while the shadow price differences are very different between households and experts, the differences across environments are quite modest.[21]

[21] We found little sensitivity of the uncertainty price shock to the initial wealth share for these calculations.

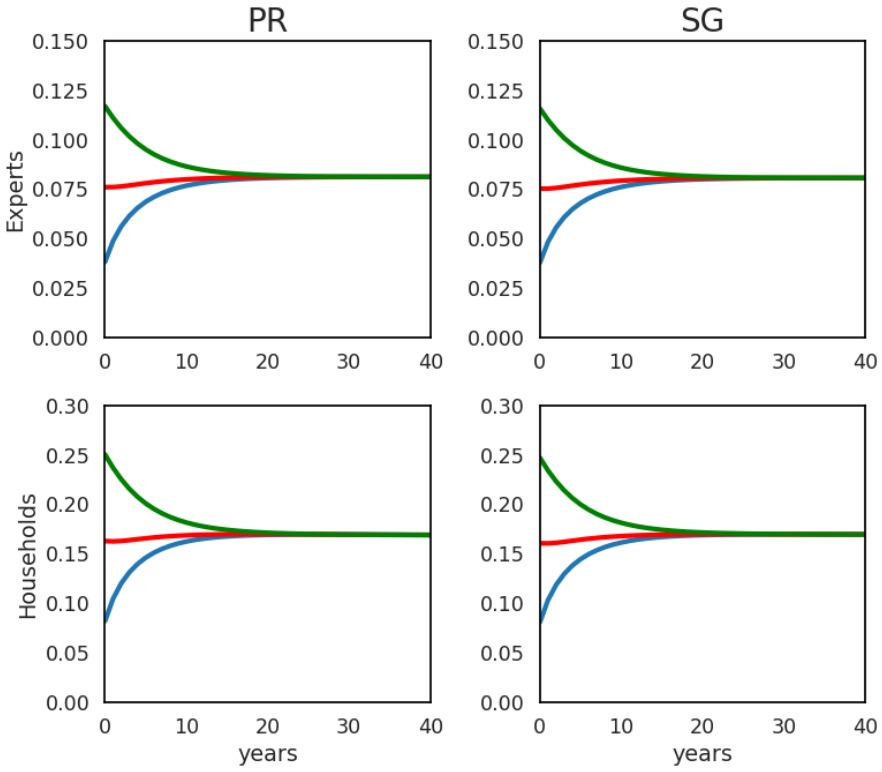

Figure 15: Uncertainty price elasticities for a growth-rate shock for environments PR and SG. We use risk aversions $\gamma_e = 4$ and $\gamma_h = 8$ for both models. We initialize W and Z^1 at their medians. The blue curve gives elasticities when Z^2 is initialized at the .1 percentile of its distribution, the red curve at the median, and the green curve at the .9 percentile.

5.5 Discussion of related literature

The models we have explored in this section highlight the role of ex-ante agent heterogeneity and risk-sharing. The literature studying this class of models is voluminous, and we do not attempt to survey all of it here. However, we will comment briefly on which existing mechanisms we have covered and which we have not, along with what we see as the challenges for future research in this area.

As mentioned above, the models closest to ours include Basak and Cuoco (1998), He and Krishnamurthy (2011, 2013, 2019), Brunnermeier and Sannikov (2014, 2016), and Gârleanu and Panageas (2015). All of these are models where pricing dynamics become interesting either because risk-sharing is constrained or because of the trading dynamics induced by attempts to share risks. Our framework essentially nests these models, pairing them with a setup that features long-run uncertainty in the macroeconomic growth.

These core frameworks have been extended to think about a variety of substantive issues. While our framework does not nest these extensions, we collect some of them here to illustrate the wide range of possibilities: capital requirements and leverage restrictions (Phelan, 2016, Klimenko et al., 2016); margin constraints (Gromb and Vayanos, 2002, Garleanu and Pedersen, 2011); shadow banking (Moreira and Savov, 2017); liquidity premia and monetary policy (Drechsler et al., 2018); unconventional monetary policy (Silva, 2016); international capital flows (Brunnermeier and Sannikov, 2015); the link between idiosyncratic and aggregate risk-sharing (Di Tella, 2017, 2019); financial innovation driven boom-bust cycles (Khorrami, 2020); and entry into the intermediation sector (Haddad, 2014, Khorrami, 2021). While we work in continuous time, related issues have been explored in discrete-time frameworks (Gertler and Karadi, 2011, Gertler and Kiyotaki, 2010, Mendoza, 2010, Bianchi, 2011, Gertler and Kiyotaki, 2015, Christiano et al., 2014).

While this class of models is rich enough to feature some interesting insights, there are reasons to expand their scope. First, financial crises are often more sudden and extreme than the models we explore here would predict. Second, large booms in credit and asset prices have some predictive power for a subsequent bust and financial crisis. Modeling additional amplification mechanisms like bank runs is one way to generate more realistically extreme crises (Mendo, 2018, Krishnamurthy and Li, 2021). Modeling investor "sentiment," both via non-rational beliefs (Maxted, 2024, Krishnamurthy and Li, 2021) and rational fear (Khorrami and Mendo, 2023), are extensions that can generate crisis predictability.

As an intriguing analogy to our long-run uncertainty framework, Maxted (2024) considers extrapolative sentiment as the belief in a persistent stochastic growth rate that, in fact, does not exist. We could capture such impacts in our framework by supposing that the state variable Z^1 is "only in the heads of the investors and households" and not in the actual dynamic evolution. We can analyze such a model in same manner as we currently do by including the Z^1 dynamics in the model solution, but omitting it from the simulations, stationary distributions, and elasticity computations. In this way, there is a wedge between beliefs and the actual data generation. We find this alternative perspective on long-term risk to be intriguing; but as we have seen in Section 4.5, an alternative to subjective belief models are ones that acknowledge the measurement challenge of identifying a long-run risk component in data. This challenge seems pertinent not only to econometricians but also economic agents.[22]

The class of models we explored, by design, nests alternative forms of heterogeneity,

[22]See Hansen (2014) and Chen et al. (2024) for related discussions.

albeit a rather stark form with two types of investors. For all of the alternatives we investigate, a natural question is "who are the so-called experts?" Should we identify them with insiders at productive firms, or managers of banks, or specialist investors more broadly? The answers to these questions influences the type of market frictions that are reasonable to consider, as well as the calibrations one should adopt.

One related empirical literature explores intermediary asset pricing implications by seeking to identify new pricing factors. Models of the type featured here, when applied to financial intermediaries, highlight forms of state dependence in valuation that could be important. Exposures and market compensations fluctuate as functions of state variables, suggesting a more dynamic approach to empirical investigation.

6 Conclusions

Our essay explores alternative macro-finance models, including many with explicit nonlinearities. The models are highly stylized and perhaps best thought of a devices to engage in "quantitative story telling." The models are not designed to provide fully comprehensive accounting of empirical facts, but rather they offer characterizations of alternative mechanisms for linkages between financial markets and the macroeconomy. We feature model comparisons rather than deep probes into one specific mechanism. While the latter is clearly valuable, we also believe in value of making model comparisons, something that is less common in journal publication. In effect, we are engaged in "quantitative story telling with multiple stories." In this sense, we share a common ambition with Dou et al. (2020), although the class of models we feature is different as are the tools we use. Related ambitions are also reflected in the comprehensive Macro Model Data Base (MMB, https://www.macromodelbase.com), although many the models we entertain require special computational challenges because of their nonlinear structure. Moreover, our essay focuses on the substantive comparisons.

Computational methods are required to support this type of analyses. As we explain in our Online Appendix C, this is a nontrivial component to our investigation. In each model, we must solve for agents' continuation values, in some cases jointly with asset prices or endogenous risk-sharing constraints. These functions solve systems of highly nonlinear PDEs. Depending on the model, we use either finite-difference based methods or, for larger state spaces, a deep Galerkin method-policy improvement algorithm, incorporating neural net approximations. See Achdou et al. (2022) and d'Avernas et al. (2022) for some

additional macro applications of implicit finite-difference schemes for PDEs, based on the seminal work of Barles and Souganidis (1991). See Al-Aradi et al. (2022), Duarte et al. (2023), Gopalakrishna (2022), and Barnett et al. (2023) for recent developments and discussions of deep neural network methods as an alternative designed to accommodate higher dimensional state spaces.

A Calculations for heterogeneous-agent model

We develop the theoretical model calculations used in the model with agent heterogeneity.

A.1 Setup and HJB equations

For each agent type with discount rate δ, inverse EIS ρ, and risk aversion γ, their HJB equation is given by

$$\begin{aligned} 0 = \max \left(\frac{\delta}{1-\rho}\right)\left[\left(\frac{c}{\exp(\upsilon)}\right)^{1-\rho} - 1\right] + \mu_n - c - \frac{1}{2}|\sigma_n|^2 + \mu_x \cdot \partial_x \upsilon + \frac{1-\gamma}{2}|\sigma_n|^2 \\ +(1-\gamma)\sigma_n \cdot \sigma_x' \partial_x \upsilon + \frac{1}{2}\operatorname{tr}\left(\sigma_x' \partial_{xx'} \upsilon \sigma_x\right) + \frac{1-\gamma}{2}|\sigma_x' \partial_x \upsilon|^2 \end{aligned} \tag{27}$$

Maximizing over consumption c delivers the following consumption-wealth ratios:

$$\begin{aligned} c^e(x) &= \delta_e^{1/\rho_e} \exp\left(\left(1 - \frac{1}{\rho_e}\right)\upsilon^e(x)\right) \\ c^h(x) &= \delta_h^{1/\rho_h} \exp\left(\left(1 - \frac{1}{\rho_h}\right)\upsilon^h(x)\right) \end{aligned}$$

Next, note that the expert and household expected return-on-capital are given by

$$\mu_R^e = \frac{\alpha_e - i^*}{Q_t} + \mu_q + \Phi(i^*) + \beta_k z_1 - \eta_k + \sqrt{z_2}\sigma_k \cdot \sigma_q \tag{28}$$

$$\mu_R^h = \frac{\alpha_h - i^*}{Q_t} + \mu_q + \Phi(i^*) + \beta_k z_1 - \eta_k + \sqrt{z_2}\sigma_k \cdot \sigma_q \tag{29}$$

The only difference is the type-specific productivity α_j. The investment-to-capital ratio i^* only shows up in agents' HJBs through μ_R^j and it does so symmetrically. Thus, maximizing over i^* delivers

$$i^*(x) = (\Phi')^{-1}\left(\frac{1}{q(x)}\right) = \frac{q(x) - 1}{\phi},$$

where the explicit form of i^* uses our specification of the installation function $\Phi(x) = \phi^{-1}\log(1 + \phi i)$.

Finally, notice that the capital holding K^j and derivatives positions θ^j only show up in the HJB equation through the net worth drift and diffusion terms (μ_n, σ_n), leading to problem (26). Households maximize the portfolio problem (26) over all possible choices of

their risk exposure vector $\sigma_{n,t}^h = \frac{Q_t K_t^h}{N_t^h}\sigma_{R,t} + \theta_t^h$ by choice of $K_t^h \geqslant 0$ and $\theta_t^h \in \mathbb{R}^3$, while experts maximize (26) over all possible choices of $\sigma_{n,t}^e = \frac{Q_t K_t^e}{N_t^e}\sigma_{R,t} + \theta_t^e = \chi_t \frac{Q_t K_t^e}{N_t^e}\sigma_{R,t}$ such that $K_t^e \geqslant 0$ and $\chi_t \geqslant \underline{\chi}$. In the next subsections, we will solve these portfolio choice problems.

In this appendix, we will sometimes work with the risk premium "wedges" Δ^e and Δ^h, which are defined as the agent-specific gap between capital returns and market returns:

$$\Delta^e \stackrel{\text{def}}{=} \underline{\chi}^{-1}\big(\mu_R^e - r - \pi \cdot \sigma_R\big) \tag{30}$$

$$\Delta^h \stackrel{\text{def}}{=} \mu_R^h - r - \pi \cdot \sigma_R \tag{31}$$

We will also write households' and experts' shadow risk prices by π^h and π^e, respectively. Because households face complete markets, $\pi^h = \pi$ (i.e., their shadow risk price equals the traded risk price). Because experts face incomplete markets, $\pi^e \neq \pi$ generally speaking.

A.2 Household portfolio choice

The necessary conditions for optimality for households can be summarized as follows:

$$\begin{aligned} \mu_R^h - r + (1-\gamma_h)(\sigma_x\sigma_R)\cdot\partial_x v^h &\leqslant \gamma_h \sigma_R \cdot \sigma_n^h \\ \pi^h + (1-\gamma_h)\sigma_x'\partial_x v^h &= \gamma_h \sigma_n^h. \end{aligned}$$

Combining these equations, we have households' Euler equation,

$$\begin{cases} \mu_R^h - r \leqslant \pi^h \cdot \sigma_R, & \text{if} \quad K^h = 0 \\ \mu_R^h - r = \pi^h \cdot \sigma_R, & \text{if} \quad K^h > 0. \end{cases} \tag{32}$$

In other words, when households' expected capital return is below what they can earn with exposure to aggregate risk via futures contracts, they do not hold any capital. When they do hold capital, the expected return on such capital is equal to compensation for aggregate risk (via $\pi^h \cdot \sigma_R$). Households' optimal risk allocations are given by

$$\sigma_n^h = \frac{QK^h}{N^h}\sigma_R + \theta_h = \frac{\pi^h}{\gamma_h} + \frac{1-\gamma_h}{\gamma_h}\sigma_x'\partial_x v^h \tag{33}$$

A.3 Expert portfolio choice

Experts' portfolio choice is similar. Their first-order conditions

$$\begin{aligned}\mu_R^e - r - (1-\chi)\pi^h \cdot \sigma_R + \chi(1-\gamma_e)(\sigma_x \sigma_R) \cdot \partial_x \upsilon^e &= \gamma_e \chi \sigma_R \cdot \sigma_n^e \\ \pi^h \cdot \sigma_R + (1-\gamma_e)(\sigma_x \sigma_R) \cdot \partial_x \upsilon^e &\leqslant \gamma_e \sigma_R \cdot \sigma_n^e,\end{aligned}$$

can be combined to yield an Euler equation:

$$\begin{cases} \pi^h \cdot \sigma_R \leqslant \mu_R^e - r, & \text{if} \quad \chi = \underline{\chi} \\ \pi^h \cdot \sigma_R = \mu_R^e - r, & \text{if} \quad \chi > \underline{\chi}. \end{cases} \tag{34}$$

In other words, if the risk-premium $\pi_t^h \cdot \sigma_{R,t}$ required to be paid to the market for issuing equity is lower than the expected excess return that experts earn on their capital, they will issue as much equity as they can, and bounce against their skin-in-the-game constraint $\underline{\chi}$. Experts' optimal leverage is given by

$$\frac{\chi Q K^e}{N^e} = \frac{1}{\gamma_e |\sigma_R|^2} \Big[\Delta^e + \pi^h \cdot \sigma_R + (1-\gamma_e)(\sigma_x \sigma_R) \cdot \partial_x \upsilon^e \Big], \tag{35}$$

and because they take all aggregate risks in equal proportions, $\sigma_n^e = \frac{\chi Q K^e}{N^e} \sigma_R$. The "wedge" Δ_t^e is the incremental risk premium attained by experts, per unit of equity investment. To see that Δ^e represents an incremental private risk premium for experts, use the definition of Δ^e and experts' Euler equation to obtain the following equation: $\mu_R^e - r = \chi(\pi^h \cdot \sigma_R + \Delta^e) + (1-\chi)\pi^h \cdot \sigma_R$. In particular, $\chi(\pi^h \cdot \sigma_R + \Delta^e)$ represents the experts' excess return to "inside equity" whereas $(1-\chi)\pi^h \cdot \sigma_R$ represents the excess return to "outside equity" held by households. These sum to the excess return on assets, and Δ^e can thus be interpreted as the bonus return per unit of inside equity, of which there are χ units.

A.4 Equilibrium capital and risk distribution

Define expert's capital share

$$\kappa \stackrel{\text{def}}{=} \frac{K^e}{K}, \tag{36}$$

which fully summarizes the capital distribution. The Euler equations (32) and (34) can be used to determine κ and equity-retention share χ. Since households are less productive, it is often efficient for experts to manage all capital ($\kappa = 1$) and exhaust their equity-issuance

capacity ($\chi = \underline{\chi}$). Thus, the solutions for κ and χ describe the nature of *occasionally-binding constraints* in this model.

Lemma A.1. *The equilibrium expert capital share κ_t and equity retention χ_t satisfy the following complementary slackness conditions:*

$$0 = \min(1 - \kappa_t, -\Delta_t^h) \tag{37}$$

$$0 = \min(\chi_t - \underline{\chi}, \Delta_t^e). \tag{38}$$

When households hold capital ($\kappa_t < 1$), experts are equity-issuance constrained ($\chi_t = \underline{\chi}$).

Lemma A.1 also shows how Δ^e and Δ^h play the roles of a Lagrange multipliers on equity-issuance and shorting constraints: Δ^e measures the shadow value of loosening the equity-issuance constraint (decreasing $\underline{\chi}$), whereas $-\Delta^h$ measures the shadow value of allowing households to short some of the capital stock.

Proof of Lemma A.1. Begin with Euler equations (32) and (34), use the definitions of Δ^h and Δ^e in (31)-(30), and use the definition of κ to immediately obtain (37)-(38). To verify the claim that $\kappa < 1$ implies $\chi = \underline{\chi}$, use the definitions of μ_R^e and μ_R^h which differ only in their dividend yields $(\alpha_e - i^*)/Q$ and $(\alpha_h - i^*)/Q$. Therefore, $\underline{\chi}\Delta^e = \Delta^h + \mu_R^e - \mu_R^h = \Delta^h + (\alpha_e - \alpha_h)/Q$. If $\kappa < 1$, then $\Delta^h = 0$ by (37). If $\Delta^h = 0$, then $\Delta^e > 0$ by the previous result, which implies $\chi = \underline{\chi}$ by (38). □

A.5 Price of capital

The goods market clearing condition can be written

$$\alpha_e K_t^e + \alpha_h K_t^h = C_t^e + C_t^h + I_t^e + I_t^h.$$

In other words, aggregate consumption plus aggregate investments by households and experts must equal aggregate output. Dividing the equation above by aggregate wealth $Q_t K_t$ in the economy, and remembering the definition of $\kappa = K^e/K$, we obtain

$$(1 - w)c^h + wc^e + \frac{i^*(q)}{q} = \frac{(1 - \kappa)\alpha_h + \kappa\alpha_e}{q} \tag{39}$$

Equation (39) relates q and κ to the state variables, conditional on knowing the wealth-normalized value functions v^h and v^e. One can show that this equation in q has a unique

positive root. We also notice that in the unitary IES case, when all the capital in the economy is held by experts (i.e. $\kappa = 1$), the price of capital is invariant to the driving processes (z_1, z_2), and simply equal to the ratio of the dividend yield $\alpha_e - i^*(q)$ divided by the wealth-weighted average rate of time preference $w\delta_e + (1-w)\delta_h$. With our functional form assumed for the installation function Φ, we obtain the following price of capital:

$$q = \frac{(1-\kappa)\alpha_h + \kappa\alpha_e + 1/\phi}{(1-w)\delta_h^{1/\rho_h}\exp\left(\left(1-\frac{1}{\rho_h}\right)\upsilon^h\right) + w\delta_e^{1/\rho_e}\exp\left(\left(1-\frac{1}{\rho_e}\right)\upsilon^e\right) + 1/\phi} \tag{40}$$

A.6 Law of motion of K, W, and Q

Because experts and households utilize a common investment rate $i^*(q)$, aggregate capital dynamics are particularly simple:

$$\frac{dK_t}{K_t} = \mu_{K,t}dt + \sigma_{K,t}\cdot dB_t \tag{41}$$

$$\mu_{K,t} \doteq \beta_k Z_t^1 + \Phi[i^*(Q_t)] - \eta_k \tag{42}$$

$$\sigma_{K,t} \doteq \sqrt{Z_t^2}\sigma_k \tag{43}$$

The law of motion of the wealth distribution W is derived below. Note in deriving these equations, we are allowing for an overlapping generations (OLG) structure with a birth/death rate of λ_d and a fraction ν of newborns exogenously designated experts. Dying agent wealth is automatically redistributed to newborns on a per-capita basis.

Lemma A.2. *The drift $\mu_{w,t}$ and diffusion $\sigma_{w,t}$ of the wealth share W_t are given by*

$$\mu_{w,t} = W_t(1-W_t)\left[c_t^h - c_t^e + \frac{\chi_t\kappa_t}{W_t}\Delta_t^e\right] + \sigma_{w,t}\cdot(\pi_t^h - \sigma_{R,t}) + \lambda_d(\nu - W_t) \tag{44}$$

$$\sigma_{w,t} = (\chi_t\kappa_t - W_t)\,\sigma_{R,t}. \tag{45}$$

Proof of Lemma A.2. Combine agents' dynamic budget constraints with their portfolio choices to obtain the evolution of aggregate households' and aggregate experts' wealth N_t^h and N_t^e:

$$\frac{dN_t^h}{N_t^h} = \left[r_t - c^h - \lambda_d + \sigma_{n,t}^h\cdot\pi_t^h + \frac{1-\kappa_t}{1-W_t}\Delta_t^h + \frac{(1-\nu)\lambda_d}{1-W_t}\right]dt + \sigma_{n,t}^h\cdot dB_t \tag{46}$$

$$\frac{dN_t^e}{N_t^e} = \left[r_t - c^e - \lambda_d + \sigma_{n,t}^e\cdot\pi_t^h + \frac{\chi_t\kappa_t}{W_t}\Delta_t^e + \frac{\nu\lambda_d}{W_t}\right]dt + \sigma_{n,t}^e\cdot dB_t, \tag{47}$$

and where

$$\sigma_n^h = \frac{1-\chi\kappa}{1-w}\sigma_R \tag{48}$$

$$\sigma_n^e = \frac{\chi\kappa}{w}\sigma_R. \tag{49}$$

The terms containing λ_d represent contributions from OLG. The key observation in obtaining the risk exposures (e.g., terms involving $\chi\kappa$ and $1-\chi\kappa$) is that experts hold $\chi\kappa$ fraction of total capital risk in the economy (after equity-issuance), so households must hold the balance $1-\chi\kappa$ by market clearing. The terms involving Δ^h and Δ^e come from recalling their definitions along with that of κ and w; e.g., households earn excess return Δ^h on their capital holdings, which equal $\frac{1-\kappa}{1-w}$ per unit of their net worth.

By Itô's formula, the wealth share $W_t = \frac{N_t^e}{N_t^e+N_t^h}$ evolves as

$$dW_t = W_t(1-W_t)\left(\frac{dN_t^e}{N_t^e}-\frac{dN_t^h}{N_t^h}\right)-W_t(1-W_t)\left(W_t\frac{d[N_t^e]}{(N_t^e)^2}-(1-W_t)\frac{d[N_t^h]}{(N_t^h)^2}+(1-2W_t)\frac{d[N_t^e,N_t^h]}{N_t^eN_t^h}\right)$$

Using (46)-(47) and (48)-(49), and making several simplifications, the result is

$$\mu_w = w(1-w)\Big[c^h - c^e + \frac{\chi\kappa}{w}\Delta^e - \frac{1-\kappa}{1-w}\Delta^h\Big] + (\chi\kappa - w)\sigma_R\cdot(\pi^h-\sigma_R) + \lambda_d(\nu - w) \tag{50}$$

$$\sigma_w = (\chi\kappa - w)\sigma_R. \tag{51}$$

The result of Lemma A.2 is obtained by using Lemma A.1 to get $(1-\kappa)\Delta^h = 0$. □

Finally, by Itô's formula, the drift and diffusion coefficients of Q_t are

$$\mu_q = \mu_x\cdot\partial_x\log q + \frac{1}{2}\left[\mathrm{tr}\left(\sigma_x'\partial_{xx'}\log(q)\sigma_x\right) + |\sigma_x'\partial_x\log q|^2\right] \tag{52}$$

$$\sigma_q = \sigma_x'\partial_x\log q. \tag{53}$$

On the other hand, σ_x depends on σ_q, constituting a two-way feedback loop. We can solve this loop by substituting the expression for σ_x into the formula for σ_q, using $\sigma_R = \sqrt{z_2}\sigma_k + \sigma_q$ to obtain:

$$\sigma_q = \frac{(\chi\kappa - w)\left(\partial_w\log q\right)\sqrt{z_2}\sigma_k + \sigma_z'\partial_z\log q}{1-(\chi\kappa-w)\partial_w\log q}, \tag{54}$$

where recall $z \stackrel{\text{def}}{=} (z_1, z_2)'$ and $\sigma_z = \sqrt{z_2}(\sigma_1, \sigma_2)'$. Conditional on knowing χ and κ, if we know the price function q across the state space, we know the capital price volatility vector σ_q, as well as the wealth share volatility vector σ_w. Note that this generates capital return volatility equal to

$$\sigma_R = \frac{\sqrt{z_2}\sigma_k + \sigma_z' \partial_z \log q}{1 - (\chi\kappa - w)\partial_w \log q}. \tag{55}$$

A.7 Equilibrium risk-free rate and risk prices

We solve for the risk-free rate r as well as the households' and experts' risk-prices π^h, π^e. To do this, we use the fact that $Q_t K_t = N_t^h + N_t^e$, which we time-differentiate. Using the dynamic evolution equations for N^h and N^e in (46) and (47), and for K in (41), by equating the drift terms we obtain:

$$r + (1-w)\left(\sigma_n^h \cdot \pi^h + \frac{1-\kappa}{1-w}\Delta^h - c^h\right) + w\left(\sigma_n^e \cdot \pi^h + \frac{\chi\kappa}{w}\Delta^e - c^e\right) = \mu_q + \mu_K + \sigma_K \cdot \sigma_q \tag{56}$$

By equating the diffusion terms:

$$(1-w)\sigma_n^h + w\sigma_n^e = \sigma_R. \tag{57}$$

To solve for r, substitute (57) into (56), use the result from Lemma A.1 that $(1-\kappa)\Delta^h = 0$, and rearrange:

$$r = \mu_q + \mu_K + \sigma_K \cdot \sigma_q - \sigma_R \cdot \pi^h + wc^e + (1-w)c^h - \chi\kappa\Delta^e \tag{58}$$

To solve for π^h, substitute optimal exposure σ_n^h from (33) with its equilibrium value from (48) to obtain:

$$\pi^h = \gamma_h \frac{1-\chi\kappa}{1-w}\sigma_R + (\gamma_h - 1)\sigma_x' \partial_x \upsilon^h. \tag{59}$$

Since experts face incomplete markets, there is in theory an infinite number of stochastic discount factors that can price claims for which the expert is marginal. We thus focus on the marginal utility of consumption process, which for any agent with recursive preferences

takes the following form (see for example Duffie and Epstein (1992b)):

$$S_t = \exp\left[\int_0^t \left(\left(\frac{\rho-\gamma}{1-\rho}\right)\delta^{1/\rho}\exp\left(\left(1-\frac{1}{\rho}\right)\upsilon_s\right) - \delta\left(\frac{1-\gamma}{1-\rho}\right)\right)ds\right] N_t^{-\gamma}\exp\left((1-\gamma)\upsilon_t\right)$$

In the case of time- and state-separability (i.e. when $\rho = \gamma$), we obtain the familiar formula $S_t/S_0 = e^{-\delta t}\left(C_t/C_0\right)^{-\gamma}$. Remember that we have for households and experts:

$$\frac{dN_t^j}{N_t^j} = \left(\mu_{n,t}^j - c_t^j\right)dt + \sigma_{n,t}^j \cdot dB_t$$

This leads to the key equation defining the vector of shadow risk prices faced by an investor:

$$\frac{dS_t^j}{S_t^j} - \mathbb{E}_t\left[\frac{dS_t^j}{S_t^j}\right] = -\left[\gamma_j\sigma_{n,t}^j + (\gamma_j - 1)\sigma_{\upsilon,t}^j\right]\cdot dB_t \stackrel{\text{def}}{=} -\pi_t^j \cdot dB_t \tag{60}$$

In the above, the k^{th} coordinate of π_t^j is the expected excess return investor j gets paid per unit of risk exposure to the k^{th} shock of B_t. Substituting formula (49) for σ_n^e into (60), we have

$$\pi^e = \gamma_e\frac{\chi\kappa}{w}\sigma_R + (\gamma_e - 1)\sigma_x'\partial_x\upsilon^e \tag{61}$$

This means that experts' equilibrium expected excess return compensation is equal to:

$$\begin{aligned}\pi^e \cdot \sigma_R &= \gamma_e\frac{\chi\kappa}{w}|\sigma_R|^2 + (\gamma_e - 1)\left(\sigma_x\sigma_R\right)\cdot\partial_x\upsilon^e \\ &= \Delta^e + \pi^h \cdot \sigma_R,\end{aligned}$$

where π^h is the vector of aggregate risk prices faced by households.[23]

[23]Note that we could follow these same steps for households but would obtain an equivalent result to our equilibrium risk price vector. Substitute formula (48) for σ_n^h into the shadow risk-price definition (60) to get

$$\pi^h = \gamma_h\frac{1-\chi\kappa}{1-w}\sigma_R + (\gamma_h - 1)\sigma_x'\partial_x\upsilon^h \tag{62}$$

Notice that π^h in (62) is identical to (59).

A.8 Deriving the functional equation for χ

We first note that the experts' aggregate risk choice (35) can be re-arranged to express the expected return premium Δ^e as follows:

$$\Delta^e = \gamma_e \frac{\chi\kappa}{w}|\sigma_R|^2 - \gamma_h \frac{1-\chi\kappa}{1-w}|\sigma_R|^2 - (\sigma_x\sigma_R)\cdot\left[(\gamma_h-1)\partial_x\upsilon^h - (\gamma_e-1)\partial_x\upsilon^e\right] \tag{63}$$

Substituting (63) into the complementary slackness condition for experts' skin-in-the-game constraint (38),

$$0 = \min\Big\{\chi - \underline{\chi}, (1-w)\gamma_e\chi\kappa|\sigma_R|^2 - w\gamma_h(1-\chi\kappa)|\sigma_R|^2 \\ - w(1-w)\,(\sigma_x\sigma_R)\cdot\left[(\gamma_h-1)\partial_x\upsilon^h - (\gamma_e-1)\partial_x\upsilon^e\right]\Big\}.$$

Since all the capital is held by experts whenever their skin-in-the-game constraint is not binding, we may substitute $\kappa = 1$ everywhere in this equation, as shown in Lemma A.1. The above equation is actually an algebraic equation for χ, which can be solved by substituting σ_x and σ_R into the second term in the minimum, obtaining

$$0 = \min\Big\{\chi - \underline{\chi}, \Big[((1-w)\gamma_e + w\gamma_h)|D_z|^2 + (\partial_w \log q)D_{\upsilon,z} - D_{\upsilon,w}\Big](\chi - w) \\ + w(1-w)(\gamma_e-\gamma_h)|D_z|^2 - D_{\upsilon,z}\Big\}. \tag{64}$$

In the above, we have defined[24]

$$D_z \doteq \sqrt{z_2}\sigma_k + \sigma_z'\partial_z \log q \tag{65}$$

$$D_{\upsilon,w} \doteq w(1-w)|D_z|^2\partial_w\big[(\gamma_h-1)\upsilon^h - (\gamma_e-1)\upsilon^e\big] \tag{66}$$

$$D_{\upsilon,z} \doteq w(1-w)\,(\sigma_z D_z)\cdot\partial_z\big[(\gamma_h-1)\upsilon^h - (\gamma_e-1)\upsilon^e\big]. \tag{67}$$

When $\chi > \underline{\chi}$, the second term of the minimum operator in equation (64) is linear in $\chi - w$, holding fixed the functions $(q, \upsilon^e, \upsilon^h)$.

The analysis is simpler in one special case. If risk aversions are identical ($\gamma_e = \gamma_h = \gamma$),

[24]The notation above is helpful, since it allows us to write $|D_z|^2 = \left(1 - (\chi\kappa - w)\,\partial_w \log q\right)^2|\sigma_R|^2$, and simplify the expression for $\sigma_x\sigma_R$ as follows:

$$\sigma_x\sigma_R = \frac{1}{1-(\chi\kappa-w)\,\partial_w\log q}\begin{pmatrix}\frac{\chi\kappa-w}{1-(\chi\kappa-w)\partial_w\log q}|D_z|^2 \\ \sigma_z D_z\end{pmatrix}$$

the second term of the minimum operator in equation (64) simplifies substantially. Then, we may prove the following proposition, which says for many parameters that the skin-in-the-game constraint is either always-binding or never-binding.

Proposition A.3. *Suppose agents have identical risk aversions ($\gamma_e = \gamma_h = \gamma$). Experts' optimal risk retention χ is*

$$\chi = \max(\underline{\chi}, w). \tag{68}$$

For $w \geqslant \underline{\chi}$, the skin-in-the-game constraint is slack and the wealth share evolves (locally) deterministically, i.e., $\sigma_w = 0$. At $w = \underline{\chi}$, when the skin-in-the-game constraint just binds, the formula for the drift of the expert wealth share is

$$\mu_w(\underline{\chi}, z) = \underline{\chi}(1 - \underline{\chi})\left[c^h(\underline{\chi}, z) - c^e(\underline{\chi}, z)\right] + \lambda_d(\nu - \underline{\chi}).$$

The following hold:

(i) If $W_t \leqslant \underline{\chi}$ for some time t and $\sup_z \mu_w(\underline{\chi}, z) < 0$, then $\chi_t = \underline{\chi}$ with probability one.

(ii) If $W_t \geqslant \underline{\chi}$ for some time t and $\inf_z \mu_w(\underline{\chi}, z) > 0$, then $\chi_t > \underline{\chi}$ with probability one.

Proof of Proposition A.3. If $\gamma_e = \gamma_h = \gamma$, then the second term in the minimum operator in equation (64) becomes

$$\mathcal{M}(\chi) \doteq \Big[\gamma|D_z|^2 + (\partial_w \log q)D_{v,z} - D_{v,w}\Big](\chi - w) - D_{v,z}. \tag{69}$$

Whenever $\chi > \underline{\chi}$, we solve for χ from $\mathcal{M}(\chi) = 0$. Therefore, $\chi = \max(\underline{\chi}, \chi^*)$, where $\chi^* \in \{y : \mathcal{M}(y) = 0\}$. As a preliminary, we show that $\chi^* = w$ solves $\mathcal{M}(\chi^*) = 0$, such that (68) holds. To prove this, conjecture (and later verify) that $\pi^e = \pi^h$ on $\chi > \underline{\chi}$. Using (61) and (62), this conjecture implies

$$\gamma\frac{\chi\kappa}{w}\sigma_R + (\gamma - 1)\sigma_x'\partial_x v^e = \gamma\frac{1 - \chi\kappa}{1 - w}\sigma_R + (\gamma - 1)\sigma_x'\partial_x v^h, \quad \text{if} \quad \chi > \underline{\chi}. \tag{70}$$

Since $\kappa = 1$ when $\chi > \underline{\chi}$ (Lemma A.1), and since $\sigma_w = (\chi\kappa - w)\sigma_R = (\chi - w)\sigma_R$, equation (70) reduces to

$$(\gamma - 1)\sigma_z'\partial_z\left(v^h - v^e\right) = (\chi - w)\frac{\gamma - (\gamma - 1)w(1 - w)\partial_w(v^h - v^e)}{w(1 - w)}\sigma_R, \quad \text{if} \quad \chi > \underline{\chi}. \tag{71}$$

Substituting (71) into (67) and (69), we obtain

$$\mathcal{M}(\chi) = (\chi - w)\Big[\gamma|D_z|^2 + (\partial_w \log q)D_{v,z} - D_{v,w} - \Big(\gamma - (\gamma-1)w(1-w)\partial_w(\upsilon^h - \upsilon^e)\Big)D_z'\sigma_R\Big].$$

Consequently, $\chi^* = w$ is one solution to $\mathcal{M}(\chi^*) = 0$.

Under this solution, we may verify $\pi^e = \pi^h$ as follows. First, use $\sigma_w = (\chi - w)\sigma_R = 0$ when $\chi = \chi^* = w$ to find from (48)-(49) that this equilibrium features

$$\sigma_n^e = \sigma_n^h = \sigma_R, \quad \text{if} \quad \chi > \underline{\chi}. \tag{72}$$

Second, introduce to all agents, for a short period of time, zero-net-supply Arrow-Debreu claims on each of the Brownian shocks. Let σ_n^{e*} and σ_n^{h*} denote agents' risk exposures in this modified economy. In the modified equilibrium, there is a single traded risk price π^* on these shocks, and both expert and household risk prices coincide with π^*. Also, since these Arrow-Debreu assets are only introduced for an arbitrarily short period of time, agents value processes υ^e and υ^h are unaffected. Putting these results together, and using formulas (61) and (62), we have

$$\begin{aligned}
\gamma\sigma_n^e &= \pi^e + (1-\gamma)\sigma_x'\partial_x\upsilon^e \\
\gamma\sigma_n^h &= \pi^h + (1-\gamma)\sigma_x'\partial_x\upsilon^h \\
\gamma\sigma_n^{e*} &= \pi^* + (1-\gamma)\sigma_x'\partial_x\upsilon^e \\
\gamma\sigma_n^{h*} &= \pi^* + (1-\gamma)\sigma_x'\partial_x\upsilon^h.
\end{aligned}$$

By repeating the arguments leading to (72), we know that the modified equilibrium also features $\sigma_n^{e*} = \sigma_n^{h*} = \sigma_R$. Therefore, $\pi^e = \pi^h = \pi^*$.

Finally, because $\mathcal{M}(\chi^*) = 0$ in (69) is a linear equation in χ^*, it admits a unique solution, so $\chi^* = w$ must be the only solution. This proves (68).

Next, to demonstrate cases (i) and (ii), compute the drift μ_w. We have already shown that $\sigma_w = 0$ when $\chi > \underline{\chi}$, so it suffices to show that $\mu_w < 0$ when $\chi \geqslant \underline{\chi}$ in case (i) and $\mu_w > 0$ when $\chi \leqslant \underline{\chi}$ in case (ii). For case (i), the condition $W_t \leqslant \underline{\chi}$ implies that we need only show $\mu_w < 0$ when $\chi = \underline{\chi}$. Similarly for case (ii), the condition $W_t \geqslant \underline{\chi}$ implies that we need only show $\mu_w > 0$ when $\chi = \underline{\chi}$. These are implied by $\sup_z \mu_w(\underline{\chi}, z) < 0$ and $\inf_z \mu_w(\underline{\chi}, z)$, respectively. □

A.9 Deriving the functional equation for κ

First, note that (63) is an equation relating χ, κ, and Δ^e. Second, by taking the difference $\mu_R^e - \mu_R^h = \mu_R^e - r - \pi \cdot \sigma_R + \pi \cdot \sigma_R - (\mu_R^h - r)$, using the definitions of μ_R^e and μ_R^h, along with the definitions of Δ^e and Δ^h in (30)-(31), we obtain:

$$\Delta^h = \underline{\chi}\Delta^e - \frac{a_e - a_h}{q}. \tag{73}$$

Now, combine the complementary-slackness condition for households' capital holdings (37) from Lemma A.1, with (63) and (73) to obtain

$$\begin{aligned} 0 = \min \Big\{ & 1 - \kappa,\ w\gamma_h(1-\chi\kappa)|\sigma_R|^2 - (1-w)\gamma_e\chi\kappa|\sigma_R|^2 \\ & + w(1-w)\frac{\alpha_e - \alpha_h}{\underline{\chi} q} + w(1-w)\left(\sigma_x\sigma_R\right)\cdot\left[(\gamma_h - 1)\partial_x \upsilon^h - (\gamma_e - 1)\partial_x \upsilon^e\right] \Big\}. \end{aligned} \tag{74}$$

We may substitute $\chi = \underline{\chi}$ everywhere in this equation, due to Lemma A.1. Given (υ^e, υ^h), equation (74) is actually a standalone variational inequality (differential equation wrapped inside of a min operator) for κ, since q can be expressed solely as a function of $(\kappa, \upsilon^e, \upsilon^h)$ through (39), and since both σ_x and σ_R can be expressed solely in terms of χ, κ, q, and $\partial_x q$ through (51) and (55). By inspection, the boundary condition $\kappa(0, z) = 0$ will be satisfied automatically as long as $\alpha_h > -\infty$.

A.10 Asymptotic analysis as $w \to 0$

In this section, we work in a one-dimensional model (no shocks to Z), so assume $\sigma_z = 0$. We will allow the birth/death (OLG) process with rate λ_d but will assume all newborn agents are born as households, so $\nu = 0$. We will make following assumption on the nature of equilibrium and analyze the two cases separately.

Assumption A.4. *One of the following two assumptions hold as $w \to 0$. Either (i) $\chi\kappa/w \to C \in (1, \infty)$ or (ii) $\chi\kappa \to C \in (0, 1]$.*

Our goal is to prove the following proposition:

Proposition A.5. *Suppose $\rho_e = \rho_h = 1$, $\nu = 0$, $\delta_e \geqslant \delta_h$, and $\gamma_h \geqslant \gamma_e$. Shut down growth and volatility shocks, $\sigma_z = 0$. Models satisfying case (ii) of Assumption A.4 feature a*

stationary wealth density that decays quadratically, i.e.,

$$f(w) \sim G_0 w^2 \quad as \quad w \to 0, \quad some\ constant \quad G_0.$$

Models satisfying case (i) of Assumption A.4 feature a stationary wealth density that decays at rate ζ, i.e.,

$$f(w) \sim G_0 w^{\zeta} \quad as \quad w \to 0, \quad some\ constant \quad G_0,$$

where

$$\zeta \stackrel{\text{def}}{=} \frac{2[\delta_h - \delta_e - \lambda_d + (\gamma_e C^2 - \gamma_h - (C-1))\sigma_k^2]}{(C-1)^2\sigma_k^2} - 2,$$

and where $C \geqslant 1$ is given below in equations (77) or (78), depending on parameters. Consequently, the lower tail of models in case (i) is thicker than that of case (ii) models if and only if $\delta_h - \delta_e - \lambda_d < [(C-1)(2C-1) - \gamma_e C^2 + \gamma_h]\sigma_k^2$.

Remark 1. *Proposition A.5 imposes $\nu = 0$ (experts are never exogenously "reborn") in order to make a stark comparison between two classes of models. If $\nu > 0$, then the formula for the tail index ζ will change, because these economies feature $\mu_w(0) = \nu\lambda_d > 0$ and $\sigma_w(0) = 0$. A particular implication is that, if $\nu > 0$, the density $f(w)$ can never have an asymptote as $w \to 0$, whereas an asymptote is possible if $\nu = 0$. That said, the point of Proposition A.5 is to provide guidance on features that generically "thicken" the tail of the wealth share density, and these features remain the same in economies with $\nu > 0$.*

Proof of Proposition A.5. Below, we will use the notation $g_1(w) \sim g_2(w)$ to mean $g_1(w)/g_2(w) \to 1$ as $w \to 0$. For expedience, we assume, but do not verify (although it can be verified), that $\mu_q \sim \bar{\mu}_q$ and $\sigma_q \sim \bar{\sigma}_q$ for bounded constants $\bar{\mu}_q$ and $\bar{\sigma}_q$.[25] This assumption, in particular, implies $\sigma_R \sim \sigma$ for some constant σ. From Lemma A.2 and the form of π^e, π^h in (61) and (62), we have the following asymptotic state dynamics:

$$\begin{aligned}\mu_w \sim\ & (\delta_h - \delta_e - \lambda_d)w + \chi\kappa\sigma^2[\gamma_e\frac{\chi\kappa}{w} + (\gamma_e - 1)(\chi\kappa - w)\frac{d}{dw}\upsilon^e - \gamma_h(1 - \chi\kappa) - (\gamma_h - 1)(\chi\kappa - w)\frac{d}{dw}\upsilon^h] \\ & + (\chi\kappa - w)\sigma^2[\gamma_h(1 - \chi\kappa) + (\gamma_h - 1)(\chi\kappa - w)\frac{d}{dw}\upsilon^h - 1] \qquad (75)\end{aligned}$$

[25] In either case, we would conjecture $q \sim A_q + B_q w$ and derive the aforementioned facts by solving A_q and B_q both from goods market clearing, e.g., (40). After determining A_q and B_q, the values of $\bar{\mu}_q$ and $\bar{\sigma}_q$ could be obtained by applying Itô's formula to q.

$$\sigma_w \sim (\chi\kappa - w)\sigma \tag{76}$$

In the one-dimensional model, agents' HJB equations take the following form:

$$0 = \max\left\{\delta(\log\delta - 1 - \upsilon) + \mu_n - \frac{\gamma}{2}\sigma_n^2 + [\mu_w + (1-\gamma)\sigma_n\sigma_w]\upsilon' + \frac{1}{2}\sigma_w^2\upsilon'' + \frac{1-\gamma}{2}\sigma_w^2(\upsilon')^2\right\},$$

where

$$\begin{aligned}
\mu_n^e &\sim r + \frac{\chi\kappa}{w}\Big[\gamma_e(\chi\kappa/w) + (\gamma_e - 1)(\chi\kappa - w)\frac{d}{dw}\upsilon^e\Big]\sigma^2 \\
\mu_n^h &\sim r + (1-\chi\kappa)\Big[\gamma_h(1-\chi\kappa) + (\gamma_h - 1)(\chi\kappa - w)\frac{d}{dw}\upsilon^h\Big]\sigma^2 \\
\sigma_n^e &\sim \frac{\chi\kappa}{w}\sigma \quad \text{and} \quad \sigma_n^h \sim (1-\chi\kappa)\sigma
\end{aligned}$$

Now, we consider the two cases of Assumption A.4.

Case 1: $\chi\kappa/w \to C$**.** Conjecture state dynamics of the asymptotic form

$$\mu_w \sim B_\mu w \quad \text{and} \quad \sigma_w \sim B_\sigma w.$$

Conjecture also value functions take the asymptotic form

$$\upsilon^e \sim A_e + B_e w^{\zeta_e} \quad \text{and} \quad \upsilon^h \sim A_h + B_h w^{\zeta_h} \quad \text{where} \quad \zeta_e, \zeta_h > 0.$$

Substituting these assumptions into (75)-(76) shows that

$$\begin{aligned}
B_\mu &= \delta_h - \delta_e - \lambda_d + [\gamma_e C^2 - \gamma_h - (C-1)]\sigma^2 \\
B_\sigma &= (C-1)\sigma
\end{aligned}$$

At this point, we have the dynamics of w, independently of the value functions, but we still must verify the conjecture.

Asymptotically, the HJBs require the following dominant-term equations to hold,

$$\begin{aligned}
0 &= \delta_e[\log\delta_e - 1 - A_e] + r + \gamma_e C^2\sigma^2 - \frac{\gamma_e}{2}C^2\sigma^2 \\
0 &= \delta_h[\log\delta_h - 1 - A_h] + r + \gamma_h\sigma^2 - \frac{\gamma_h}{2}\sigma^2.
\end{aligned}$$

We substitute r which must take the form

$$r \sim \delta_h + \Phi(i^*(q)) - \eta_k + \bar{\mu}_q + \bar{\sigma}_q \sigma_k - \gamma_h \sigma^2,$$

which is bounded (and equals the representative-agent risk-free rate when households dominate the economy). Substituting this into the HJB equations, we obtain explicit expressions for A_e, A_h. For the terms of order w^{ζ_e}, w^{ζ_h}, the HJB equations say

$$\begin{aligned}
\delta_e &= B_\mu \zeta_e + \frac{1}{2} B_\sigma^2 \zeta_e (\zeta_e - 1) \\
\delta_h &= B_\mu \zeta_h + \frac{1}{2} B_\sigma^2 \zeta_h (\zeta_h - 1),
\end{aligned}$$

whereby B_e, B_h have dropped out (these constants are determined by the right boundary $w = 1$). These quadratic equations each have one positive and one negative root. Taking the positive root, we verify that $\zeta_e, \zeta_h > 0$.

It remains to determine C. The solution depends on the separate asymptotics of κ and χ, not only their product. If $\kappa \to 0$ while $\chi \to \underline{\chi} \neq 0$, then the following analysis holds. Using the definition of μ_R^j, the relationship $\mu_R^e = \sigma_R \cdot [\chi \pi^e + (1-\chi)\pi^h]$, and previous results on asymptotics as $w \to 0$, we have that

$$\frac{\alpha_e - \alpha_h}{q} \sim \chi(\gamma_e C - \gamma_h)\sigma^2.$$

Using the goods market clearing condition (39), we see that $q(0)$ is independent of C. Hence,

$$C = \frac{\gamma_h}{\gamma_e} + \frac{\alpha_e - \alpha_h}{\underline{\chi} \sigma^2 q(0)} \geqslant 1. \tag{77}$$

On the other hand, if $\kappa \to 1$ while $\chi \to 0$ (e.g., this occurs if $\alpha_h = -\infty$ and $\underline{\chi} = 0$), then we may use equation (64) to obtain[26]

$$C = \frac{\gamma_h}{\gamma_e} \geqslant 1. \tag{78}$$

The cases of interest, where $C > 1$ strictly, are when either (a) $\gamma_h > \gamma_e$ and $\alpha_e = \alpha_h$ as in Gârleanu and Panageas (2015); or (b) $\gamma_h = \gamma_e$ and $\alpha_e > \alpha_h$ as in Brunnermeier and

[26]Note that these equations for C agree if $\alpha_e = \alpha_h$ and $\underline{\chi} = 0$, which shows that a frictionless economy in the spirit of Gârleanu and Panageas (2015) can be implemented in our model by equivalently allowing one of either χ or κ to adjust.

Sannikov (2014).

Returning to the dynamics of w, we have the Kolmogorov Forward Equation, which reads

$$0 = -\frac{d}{dw}[\mu_w f] + \frac{1}{2}\frac{d^2}{dw^2}[\sigma_w^2 f].$$

Integrating from an interior point w to 1, and using the fact that $\mu_w(1) < 0$ and $\sigma_w(1) = 0$ in all models we consider, implying f and σ_w both vanish at the upper boundary, we obtain

$$0 = -\mu_w f + \frac{1}{2}\frac{d}{dw}[\sigma_w^2 f].$$

Asymptotically, as $w \to 0$, we have

$$0 = -B_\mu w f + \frac{1}{2} B_\sigma \frac{d}{dw}[w^2 f] + o(w).$$

Solving this equation shows that, asymptotically,

$$f(w) \sim G_0 w^{2(B_\mu/B_\sigma^2 - 1)}, \quad \text{some constant} \quad G_0 > 0. \tag{79}$$

This equation determines the existence (non-degeneracy) and asymptotic shape of the stationary density.[27]

Case 2: $\chi\kappa \to C$**.** In this case, it suffices to consider parameters $\underline{\chi} > 0$ and $\alpha_h = -\infty$, in which case $\chi \sim \underline{\chi}$ and $\kappa \sim 1$. Then, $C = \underline{\chi} \in (0, 1]$ as desired. Mimicking the previous analysis, conjecture that

$$\mu_w \sim B_\mu / w \quad \text{and} \quad \sigma_\mu \sim A_\sigma$$

and for the value functions

$$v^e \sim A_e + B_e \log(w) \quad \text{and} \quad v^h \sim A_h + B_h w.$$

[27] As long as $2B_\mu > B_\sigma^2$, a non-degenerate density exists. This condition is

$$2[\delta_h - \delta_e - \lambda_d] > [3(C-1)^2 - 2\gamma_e C^2 + 2\gamma_h]\sigma^2.$$

The shape is given by the exponent $2(B_\mu/B_\sigma^2 - 1)$. If, as in Brunnermeier and Sannikov (2014), $\frac{1}{2}B_\sigma^2 < B_\mu < B_\sigma^2$, then the density has an asymptotic spike.

These conjectures imply

$$\begin{aligned} A_\sigma &= C\sigma \\ B_\mu &= (C\sigma)^2[\gamma_e + (\gamma_e - 1)B_e] \\ \pi^e &\sim (C\sigma/w)[\gamma_e + (\gamma_e - 1)B_e] \\ \pi^h &\sim \sigma[(1-C)\gamma_h + C(\gamma_h - 1)B_h] \\ r &\sim A_r + (1/w)B_r \end{aligned}$$

for constants $A_r \doteq \delta_h + \Phi(i^*(q(0))) - \eta_k + \frac{q'(0)}{q(0)}A_\sigma\sigma_k - (1-C)\sigma[(1-C)\gamma_h + C(\gamma_h - 1)B_h]$ and

$$B_r \doteq \frac{q'}{q}B_\mu - (C\sigma)^2(\gamma_e + (\gamma_e - 1)B_e)].$$

Note that equation (39) with $\kappa = 1$ shows that q'/q is bounded. Indeed, we have

$$\frac{q'(0)}{q(0)} = -\frac{\delta_e - \delta_h}{\delta_h + 1/\phi_1}, \quad \text{some constant} \quad \phi_1 > 0.$$

which is the same equation one would obtain for the specific functional form leading to (40). In the above, ϕ_1 is to be interpreted as the local elasticity of the accumulation function Φ near $w \sim 0$, whereas this elasticity is assumed globally constant in (40).

Substituting these results into agents' HJB equations, and keeping only the highest-order terms, we obtain

$$\begin{aligned} 0 &= \frac{1}{w^2}\Big[\gamma_e(C\sigma)^2 - \frac{1}{2}\gamma_e(C\sigma)^2 + B_\mu B_e - \frac{1}{2}A_\sigma^2 B_e + \frac{1-\gamma_e}{2}A_\sigma^2 B_e^2\Big] \\ 0 &= \frac{1}{w}\Big[B_r + B_\mu B_h\Big]. \end{aligned}$$

Due to $1/w \to \infty$ as $w \to 0$, the terms in brackets must be 0 for the equations to hold. Substituting previous results and simplifying, we obtain[28]

$$\begin{aligned} B_e &= -1 \\ B_h &= 1 + \frac{\delta_e - \delta_h}{\delta_h + 1/\phi_1}. \end{aligned}$$

Any A_e, A_h are consistent with the HJBs at this boundary.

[28]Note that B_e solves a quadratic equation $0 = \gamma_e + (2\gamma_e - 1)B_e + (\gamma_e - 1)B_e^2$, which has the second solution $B_e = -\gamma_e/(\gamma_e - 1)$. However, substituting this root yields $\pi^e \sim 0$.

The state dynamics are thus given by

$$\mu_w \sim (C\sigma)^2(1/w) \quad \text{and} \quad \sigma_w \sim C\sigma.$$

Hence, repeating the same analysis of the Kolmogorov Forward Equation as in case 1, we obtain asymptotically,

$$f(w) \sim G_0 w^2, \quad \text{some constant} \quad G_0 > 0. \tag{80}$$

Thus, the density has a tail that decays quadratically, irrespective of B_μ, B_σ and by extension the model parameters.

Comparing the cases. Comparing the formulas (79) and (80), we see that case 1 has a thicker tail than case 2, if and only if

$$\delta_h - \delta_e - \lambda_d < [(C-1)(2C-1) - \gamma_e C^2 + \gamma_h]\sigma^2,$$

where C is given either by (77) or (78) depending on the context. This analysis proves Proposition A.5. □

B Computational Appendix

Joseph Huang, Haomin Qin and Chun Hei Hung

B.1 Global solutions using finite difference methods

We solve the single-agent models in Sections 4 as well as the heterogeneous agents model in environment IP in Section 5 using finite difference methods. The single-agent models require solving a PDE of the following form:

$$L_{HJB}(v; x) = 0 \tag{81}$$

Where $x = (z^1, z^2)$ in Section 4.4, $x = (z^1)$ in Section 4.5 and $x = (k^2/k, z^1, z^2)$ in Section 4.6. The heterogeneous agent problems can be summarized using experts' and households' HJB equations, as well as two functional equations for χ and κ that are contained in

Appendix A,[29]

$$
\begin{aligned}
L^e_{HJB}\left(v^e, v^h, \kappa, \chi; x\right) &= \frac{\rho_e}{1-\rho_e}\delta_e^{1/\rho_e}\exp\left[(1-\frac{1}{\rho_e})v^e)\right] - \frac{\delta_e}{1-\rho_e} + r \\
&+ \frac{1}{2\gamma_e}\frac{\left(\Delta^e + \pi^h\cdot\sigma_R\right)^2}{\left\|\sigma_R\right\|^2} + \left[\mu_X + \frac{1-\gamma_e}{\gamma_e}\left(\frac{\Delta^e + \pi^h\cdot\sigma_R}{\left\|\sigma_R\right\|^2}\right)\sigma_X\sigma_R\right]\cdot\partial_X v^e \\
&+ \frac{1}{2}\left[\mathrm{tr}\left(\sigma_X'\partial_{xx'}v^e\sigma_X\right) + \frac{1-\gamma_e}{\gamma_e}\left(\sigma_X'\partial_x v_e\right)'\left[\gamma_e\mathbb{I}_d + (1-\gamma_e)\frac{\sigma_R\sigma_R'}{\left\|\sigma_R\right\|^2}\right]\sigma_X'\partial_x v^e\right] = 0
\end{aligned} \tag{82}
$$

$$
\begin{aligned}
L^h_{HJB}\left(v^e, v^h, \kappa, \chi; x\right) &= \frac{\rho_h}{1-\rho_h}\delta_h^{1/\rho_h}\exp\left[(1-\frac{1}{\rho_h})v^h)\right] - \frac{\delta_h}{1-\rho_h} + r + \frac{1}{2\gamma_h}\|\pi^h\|^2 \\
&+ \left[\mu_X + \frac{1-\gamma_h}{\gamma_h}\sigma_X\pi^h\right]\cdot\partial_x v^h + \frac{1}{2}\left[\mathrm{tr}\left(\sigma_X'\partial_{xx'}v^h\sigma_X\right) + \frac{1-\gamma_h}{\gamma_h}\left\|\sigma_X'\partial_x v^h\right\|^2\right] = 0
\end{aligned} \tag{83}
$$

$$
L_\kappa\left(v^e, v^h, \kappa, \chi; x\right) = 0 \tag{84}
$$

$$
L_\chi\left(v^e, v^h, \kappa, \chi; x\right) = 0 \tag{85}
$$

where $x = (w, z^1, z^2)$.

The PDEs for v in equations (21) and v^e, v^h in equation (82) and (83) have the general quasi-linear form

$$
0 = A^*\left(x, v, \partial_x v\right) + \mu_X\left(x, v, \partial_x v\right)\partial_x v + \mathrm{tr}\left[B\left(x, v, \partial_x v\right)\partial_{xx'}vB\left(x, \phi_k, \partial_x v\right)'\right] \tag{86}
$$

Note that we are able to achieve this form by substituting the minimizing drift adjustment H_t^* into the HJB equation using equation (10) so that the term becomes part of $A^*(x, v, \partial_x v)$ in (86).

To solve, we augment (86) with a false time-derivative $\partial_t v$, known as a "false transient". Since the time-derivative appears on the right-hand-side of the PDE, the equation to solve is

$$
0 = \partial_t v + A^*\left(x, v, \partial_x v\right) + \mu_X\left(x, v, \partial_x v\right)\partial_x v + \mathrm{tr}\left[B\left(x, v, \partial_x v\right)\partial_{xx'}vB\left(x, \phi_k, \partial_x v\right)'\right] \tag{87}
$$

Thus, the original PDE (86) is the stationary solution to the augmented PDE (87), i.e., $\partial_t v = 0$ holds in (87). We solve (87) iteratively until $\partial_t v \approx 0$.

We break down our approach into three algorithms. Algorithm 1 updates the value

[29]The experts and households HJB equations for the heterogeneous-agent models in Section 5 share the general form in equation (27). Additionally, L_κ can be formulated using equation (74) and L_χ can be formulated using equation (64).

function given a generic set of equilibrium objects $\hat{c}, \hat{i}, \hat{\kappa}$ etc. - this is called the "outer loop". Algorithm 2 describes how we compute the equilibrium objects for the single-agent models while Algorithm 3 describes the same for environment IP in section 5 (the "inner loop").

Algorithm 1 Finite difference methods for PDEs

1: Form a guess for $\phi_0(x) := v(x, T)$, which is the terminal condition.
2: Generate a grid of time points $\{T, T - \Delta t, \ldots\}$ and a grid of space points $\mathcal{X}$.
3: Given a candidate function $\phi_k(x)$ for $v(x, T - k\Delta t)$ restricted to $\mathcal{X}$, compute finite difference approximations to all derivatives. The time derivative is approximated with the backward difference

$$\partial_t v(x, T - k\Delta t) \approx \frac{v(x, T - k\Delta t) - v(x, T - (k+1)\Delta t)}{\Delta t} = \frac{\phi_k(x) - \phi_{k+1}(x)}{\Delta t}$$

Denote the finite-difference approximations of the spatial derivatives, i.e. the derivatives of the value function with respect to the state variables, by

$$\hat{\partial}_x \phi_k(x) \approx \partial_x v(x, T - k\Delta t)$$
$$\hat{\partial}_{xx'} \phi_k(x) \approx \partial_{xx'} v(x, T - k\Delta t).$$

We apply these approximations to (87) to solve for ϕ_{k+1} given ϕ_k, using one of the schemes in (88) and (89).
4: Using ϕ_{k+1}, calculate

$$\text{error}_{k+1} := \max_{x \in \mathcal{X}} \frac{|v(x, T - k\Delta t) - v(x, T - (k+1)\Delta t)|}{\Delta t} = \max_{x \in \mathcal{X}} \frac{|\phi_{k+1}(x) - \phi_k(x)|}{\Delta t}.$$

Given a tolerance for convergence $\text{tol} > 0$, repeat this step until $\text{error}_{k+1} < \text{tol}$. The function $\phi_{k+1}(x)$ is the approximate solution to (86).

There are several considerations when applying Algorithm 1:

Discrete grid: We use $\Delta_t = 1.0$ when possible to reduce time to convergence, but reduce Δ_t to 0.01 and 0.001 in two cases (Model IP and the two capital model with $\tau = 1$) where we would otherwise experiences problems in convergence. For the models where we use $\Delta_t = 1.0$, we find that lowering Δ_t does not alter our converged solutions. We also experiment with different sizes and densities for our state space grids and find no difference in the results (other than computational time).

Approximation of spatial derivatives: We can find ϕ_{k+1} explicitly or implicitly and assume ϕ_k is known. The explicit method approximates the spatial derivatives in (87)

using ϕ_k, so that ϕ_{k+1} only appears on the left-hand side of the equation:

$$\begin{aligned}\phi_{k+1} =& \phi_k + \Big\{ A^* \left(x, v, \hat{\partial}_x \phi_k\right) + \mu_X \left(x, \phi_k, \hat{\partial}_x \phi_k\right) \hat{\partial}_x \phi_k \\ &+ \operatorname{tr}\left[B \left(x, \phi_k, \hat{\partial}_x \phi_k\right) \hat{\partial}_{xx'} \phi_k B \left(x, \phi_k, \hat{\partial}_x \phi_k\right)' \right] \Big\} \Delta t.\end{aligned} \tag{88}$$

Notice the right-hand side of (88) can be written as a matrix-vector product (recall that ϕ_k and its partial derivatives are known).

The implicit scheme solves for ϕ_{k+1} in (89). Notice how ϕ_{k+1} (rather than ϕ_k) appears in (89):

$$\begin{aligned}\phi_{k+1} - \phi_k =& \Big\{ A^* \left(x, v, \hat{\partial}_x \phi_k\right) + \mu_X \left(x, \phi_k, \hat{\partial}_x \phi_k\right) \hat{\partial}_x \phi_{k+1} \\ &+ \operatorname{tr}\left[B \left(x, \phi_k, \hat{\partial}_x \phi_k\right) \hat{\partial}_{xx'} \phi_{k+1} B \left(x, \phi_k, \hat{\partial}_x \phi_k\right)' \right] \Big\} \Delta t.\end{aligned} \tag{89}$$

Recall that ϕ_{k+1} and its partial derivatives are unknown. (89) is a linear partial differential equation that can be solved using a finite difference method. In summary, the explicit scheme requires us to compute matrix-vector products whereas the implicit scheme requires us solving a linear system.

The advantage of the implicit scheme is that it tends to work robustly even for larger Δ_t, whereas the explicit scheme typically requires a sufficiently small Δ_t (Achdou et al. (2022)). As such, the implicit scheme provides faster convergence and greater numerical stability. Therefore, we opt for the implicit scheme.

Approximation of drift terms: In (88), we approximate the term $\mu_X \left(x, \phi_k, \hat{\partial}_x \phi_k\right) \hat{\partial}_x \phi_k$ using an upwinding scheme. For each state X_i we compute its contribution to the above term as:

$$\begin{aligned}\mu_{X_i} \left(x, \phi_k, \hat{\partial}_x \phi_k\right) \hat{\partial}_x \phi_k =& \max\{\mu_{X_i}, 0\} \frac{v(x_i + \Delta x_i, x_{-i}, T - k\Delta t) - v(x_i, x_{-i}, T - k\Delta t)}{\Delta x_i} \\ &+ \min\{\mu_{X_i}, 0\} \frac{v(x_i, x_{-i}, T - k\Delta t) - v(x_i - \Delta x_i, x_{-i}, T - k\Delta t)}{\Delta x_i} \\ =& \mu^+_{X_i}(x, \phi_k, \hat{\partial}_x \phi_k) \hat{\partial}^{(+)}_x(\phi_k) + \mu^-_{X_i}(x, \phi_k, \hat{\partial}_x \phi_k) \hat{\partial}^{(-)}_x(\phi_k)\end{aligned}$$

Where x_i denotes the value of state X_i at x, x_{-i} denotes the values of the rest of the state variables at x, $\hat{\partial}^{(+)}_x$and $\hat{\partial}^{(-)}_x$ are forward and backward differences, while $\mu^+_{X_i}$ and $\mu^-_{X_i}$

denote the positive and negative parts of μ_{X_i}. Barles and Souganidis (1991) show that this ensures that under certain regularity conditions, the numerical scheme converges to the unique viscosity solution of the underlying partial differential equation, though we do not verify whether these conditions have been satisfied here.

Solving the linear system: The linear system in (88) can be expressed as:

$$Av = u$$

where v is the stacked vector $\phi_{k+1}(x)$ at each point in the state-space grid, u is the flow term and A is a sparse square matrix with dimension equal to the product of the dimensions of the state space grid. In the single-agent models, we solve this using Julia's base function for solving linear systems, which uses an LU decomposition and back-substitution to solve the system.

For Model IP, to solve the linear systems repeatedly, we use a conjugate gradient method, an iterative method that efficiently solves large, sparse, symmetric positive definite linear systems by constructing a sequence of orthogonal search directions to minimize the residual and converge to the solution. There are two advantages associated with conjugate gradient for our solution method. First, notice that for a given linear system, conjugate gradient requires that the user provides an initial guess. In our model, as ϕ_k converges to the true solution, one can reasonably suspect that the distance between ϕ_{k+1} and ϕ_k shrinks as ϕ_k converges. We can then use a "smart guess" approach where, when solving for ϕ_{k+1}, we use ϕ_k as the initial guess. Second, when constructing the finite difference matrix, a smaller Δ_t increases the diagonal of the matrix, making the matrix better-conditioned. This is particularly useful when we solve for models that require smaller Δ_t, because the time required to solve each linear system declines as Δ_t drops.

Now we apply Algorithm 1 to the single and heterogeneous agent models:

Algorithm 2 Numerical Procedure for Single Agent Models using FDM

Given $v^{(n)}$, we would like to update $v^{(n+1)}$ by iterating one time-step in its PDE.

1: **Inner loop: update equilibrium objects iteratively.** For any equilibrium object y, let the sequence of iterants for this loop be $\left\{\hat{y}^{(l)} : l = 0, 1, \ldots\right\}$. Form some initial guess for $v^{(0)}$. At the n^{th} step in the iteration process:

   1. Solve for the consumption and investment policy functions $\hat{c}^{(n)}$, $\hat{i}^{(n)}$ by applying $v^{(n)}$ to equations (22), (17). Solve also for the drift distortion term $\frac{1-\gamma}{2} z^2 |\sigma_x' \frac{\partial v}{\partial x}|$ described in (10).

   2. When structural ambiguity exists, solve additionally for the robust control variable $\hat{s}^{(n)}$ following Hansen and Sargent (2022).

   3. Construct the drift and diffusion terms in (21).

2: **Outer loop: update value function using PDE.** Update the value functions $v^{(n+1)}$ using **Algorithm 1**

Algorithm 3 Numerical Procedure for Heterogeneous Agent Models using FDM

Given $v^{e,(n)}$ and $v^{h,(n)}$, we would like to update $v^{e,(n+1)}$ and $v^{h,(n+1)}$ by iterating one time-step in their PDEs.

1: **Inner loop: update equilibrium objects iteratively.**

For any equilibrium object y, let the sequence of iterants for this inner loop be $\{\hat{y}^{(l)} : l = 0, 1, \ldots\}$

1. If $n \geqslant 1$, initialize $\hat{y}^{(0)} = y^{(n-1)}$. If $n = 0$, use the guess $\hat{\kappa}^{(0)} = w$, $\hat{\chi}^{(0)} = 1$, $\hat{q}^{(0)}$ from equation (40), $\hat{\Delta}^{h,(0)} = 0$, and $\hat{\Delta}^{e,(0)} = \underline{\chi}^{-1}[\hat{\Delta}^{h,(0)} + \frac{a_e - a_h}{\hat{q}^{(0)}}]$ from equation (31).
2. For each $l \geqslant 0$, do the following:
   (a) Update all other $\hat{y}^{(l)}$ objects as follows.
      i. Set $\hat{\beta}_e^{(l)} = \hat{\chi}^{(l)}\hat{\kappa}^{(l)}/w$ and $\hat{\beta}_h^{(l)} = (1 - \hat{\kappa}^{(l)})/(1 - w)$.
      ii. Set $\hat{\sigma}_K^{(l)}$, $\hat{\sigma}_q^{(l)}$, $\hat{\sigma}_R^{(l)}$, and $\hat{\pi}^{(l)}$ (in that order) using equations (18), (54), (55), and (59).
      iii. Set $\hat{\mu}_K^{(l)}$, $\hat{\mu}_q^{(l)}$, and $\hat{r}^{(l)}$ (in that order) using equations (18), (52), and (58). Get $\hat{\mu}_R^{e,(l)}$ and $\hat{\mu}_R^{h,(l)}$ from equations (28) and (29), respectively..
   (b) Define $\hat{\kappa}^{(l+1)} = \hat{\kappa}^{(l)} + H^{(l)} \times dt$, where dt is a small enough time-step, and $H^{(l)}$ is defined by the right-hand-side of equation (74), computed using $\chi = \underline{\chi}$ and $\hat{y}^{(l)}$ for all other objects.
   (c) Denote the linear expression in the second argument of the minimum in equation (64) by
   $$G(w, \chi) := A_0(w) + A_1(w)(\chi - w)$$
   Define $\tilde{q}$ according to equation (40) with $\kappa = 1$. Using $\tilde{q}$ and its derivatives in place of q, as well as $\kappa = 1$ and $\hat{y}^{(l)}$, compute A_0, A_1. Solve the equation $G(w, \chi) = 0$ for χ at each w. Denote the solution by $\tilde{\chi}$. If $\tilde{\chi} \geqslant \underline{\chi}$, set $\hat{\chi}^{(l+1)} = \tilde{\chi}$. Otherwise, there are two cases:
   - If $G(w, \underline{\chi}) > 0$, then set $\hat{\chi}^{(l+1)} = \underline{\chi}$.
   - If $G(w, \underline{\chi}) < 0$, then set $\hat{\chi}^{(l+1)} = +\infty$ (or some very large number).

   (d) Use equation (63) to solve for $\hat{\Delta}^{e,(l+1)}$, then set $\hat{\Delta}^{h,(l+1)}$ by (73). Use $\hat{\kappa}^{(l+1)}$ and $\hat{\chi}^{(l+1)}$ but $\hat{y}^{(l)}$ for everything else in this step.
   (e) Set $\hat{q}^{(l+1)}$ by equation (40), using $\hat{\kappa}^{(l+1)}$ and $(v^{e,(n)}, v^{h,(n)})$.
3. Iterate on (b). When $\|\hat{\kappa}^{(l+1)} - \hat{\kappa}^{(l)}\| + \|\hat{\chi}^{(l+1)} - \hat{\chi}^{(l)}\|$ is small, stop iterating.
4. Put $y^{(n)} = \hat{y}^{(l)}$.

2: **Outer loop: update value functions using PDEs.** Update the experts and households value functions $v^{e,(n+1)}, v^{h,(n+1)}$ separately using **Algorithm 1**

B.2 Approximate global solutions using neural networks

We globally solve the heterogeneous agents models in environments RF, PR, SG in section 5 using machine learning methods. Amidst the backdrop of rapid advancements in deep learning, Sirignano and Spiliopoulos (2018) proposed the deep Galerkin method (DGM) to solve partial differential equations using neural networks without relying on mesh generation. Al-Aradi et al. (2022) handled HJB equations in their original, unsimplified form, solving for the value function and optimal control by representing each with deep neural networks, and proceed with policy iteration algorithm (DGM-PIA). Barnett et al. (2023) systematically review the recent development for deep learning algorithms in scientific computing.

Contrast with the DGM-PIA algorithm used in Al-Aradi et al. (2022), we approximate expert value function, v^e, households value function, v^h, and expert's capital share κ simultaneously using a single neural network with 3-dimensional outputs. The algorithm avoids any iteration among equilibrium variables to achieve efficiency. We explicitly solve χ using (85) due to its embedded linear structure, and rewrite the system to be solved as

$$\begin{aligned} L^e_{HJB}\left(v^e, v^h, \kappa; x\right) &= 0 \\ L^h_{HJB}\left(v^e, v^h, \kappa; x\right) &= 0 \\ L_\kappa\left(v^e, v^h, \kappa; x\right) &= 0 \end{aligned} \tag{90}$$

Our single neural network has 1 input layer, 2 hidden layers, and 1 final output layer. The input layer takes a 3-dimensional vector, (w, z^1, z^2), as inputs. The final layer has 3-dimensional outputs, which are used to approximate v^e, v^h, κ respectively. Each hidden layer has 16 neurons[30]. tanh activation functions are used in each neuron except for the final layer. In the final layer, we choose no activation function for v^e and v^h, and use a sigmoid activation function for κ to constrain the expert's capital share between 0 and 1. Our neural net approximation F can be characterized as

$$[v^e, v^h, \kappa] = F(x; \boldsymbol{\theta}) \tag{91}$$

where $\boldsymbol{\theta}$ are neural net parameters.

[30]Our results are robust across various neural network architectures. Increasing the number of hidden layers and units do not impact our results.

Algorithm 4 Training Procedure

We use a Glorot normal initializer[1] to initialize our neural nets paramamters $\boldsymbol{\theta}_0$. Then given $\boldsymbol{\theta}_i$, $i = 0, 1, 2, ..n$[31], at each iteration we

1: Uniformly draw (w, z^1, z^2) from the state space N times. The formulated training set $\boldsymbol{x_i} = (\boldsymbol{w_i}, \boldsymbol{z_i^1}, \boldsymbol{z_i^2})$ is a $N \times 3$ matrix.[2]

2: Evaluate the neural nets on the training set

$$[\boldsymbol{v_i^e}, \boldsymbol{v_i^h}, \boldsymbol{\kappa_i}] = F(\boldsymbol{x_i}; \boldsymbol{\theta}_i)$$

and calculate the loss functions

$$\begin{aligned} &\boldsymbol{L}^e_{HJB}\left(\boldsymbol{v_i^e}, \boldsymbol{v_i^h}, \boldsymbol{\kappa_i}; \boldsymbol{x_i}, \boldsymbol{\theta}_i\right) \\ &\boldsymbol{L}^h_{HJB}\left(\boldsymbol{v_i^e}, \boldsymbol{v_i^h}, \boldsymbol{\kappa_i}; \boldsymbol{x_i}, \boldsymbol{\theta}_i\right) \\ &\boldsymbol{L}_{\kappa}\left(\boldsymbol{v_i^e}, \boldsymbol{v_i^h}, \boldsymbol{\kappa_i}; \boldsymbol{x_i}, \boldsymbol{\theta}_i\right) \end{aligned} \tag{92}$$

3: Calculate the mean square error for each loss function

$$\begin{aligned} \mathcal{L}^e_{HJB}\left(\boldsymbol{x_i}, \boldsymbol{\theta}_i\right) &= \frac{1}{N}\|\boldsymbol{L}^e_{HJB}\left(\boldsymbol{v_i^e}, \boldsymbol{v_i^h}, \boldsymbol{\kappa_i}; \boldsymbol{x_i}, \boldsymbol{\theta}_i\right)\|^2 \\ \mathcal{L}^h_{HJB}\left(\boldsymbol{x_i}, \boldsymbol{\theta}_i\right) &= \frac{1}{N}\|\boldsymbol{L}^h_{HJB}\left(\boldsymbol{v_i^e}, \boldsymbol{v_i^h}, \boldsymbol{\kappa_i}; \boldsymbol{x_i}, \boldsymbol{\theta}_i\right)\|^2 \\ \mathcal{L}_{\kappa}\left(\boldsymbol{x_i}, \boldsymbol{\theta}_i\right) &= \frac{1}{N}\|\boldsymbol{L}_{\kappa}\left(\boldsymbol{v_i^e}, \boldsymbol{v_i^h}, \boldsymbol{\kappa_i}; \boldsymbol{x_i}, \boldsymbol{\theta}_i\right)\|^2 \end{aligned} \tag{93}$$

where $\mathcal{L}^e_{HJB}, \mathcal{L}^h_{HJB}, \mathcal{L}_{\kappa}$ are all scalars.

4: Construct the composite objective loss function as

$$\mathcal{L} = \mathcal{L}^e_{HJB} + \mathcal{L}^h_{HJB} + \lambda_{\mathcal{L}}\mathcal{L}_{\kappa}$$

where $\lambda_{\mathcal{L}}$ is a weighting coefficient.[3]

5: Update $\boldsymbol{\theta}_i$ using the standard scipy Broyden–Fletcher–Goldfarb–Shanno optimization algorithm[45] in each iteration till $\boldsymbol{\theta}_n$ and $\mathcal{L}$ below the tolerance[6].

$$\boldsymbol{\theta}_{i+1} = \arg\min \mathcal{L} \tag{94}$$

B.3 Computing Shock Elasticities

The shock elasticities are computed by solving:

$$\varepsilon_M(t,x) = \nu(x) \cdot \Big\{ \sigma_M(x) + \sigma_X(x) \cdot \frac{\partial}{\partial x} \log \mathbb{E}\Big[\Big(\frac{M_t}{M_0} \Big) \mid X_0 = x \Big] \Big\}. \tag{95}$$

where μ_M, σ_M are the drift and diffusion term of $d \log M_t$. We compute this in two ways: 1) by solving a PDE using finite differences, and 2) using simulations.

First, we can compute the conditional expectations in (95) using finite differences as follows. Define $f_M(t,x) := \mathbb{E}[\frac{M_t}{M_0} f_M(0, X_t) \mid X_0 = x]$. Then, using the law of iterated expectations, followed by the definition of f_M, we have $f_M(t,x) = \mathbb{E}[\frac{M_u}{M_0} \mathbb{E}[\frac{M_t}{M_u} f_M(0, X_t) \mid X_u] \mid X_0 = x] = \mathbb{E}[\frac{M_u}{M_0} f_M(t-u, X_u) \mid X_0 = x]$. Hence, $\{M_t f_M(T-t, X_t)\}_{t \in [0,T]}$ is a martingale and must have zero drift. Applying Itô's formula gives a PDE for f_M in (t,x), i.e.,

$$0 = -\frac{\partial f_M}{\partial t} + \Big(\mu_M + \frac{1}{2} \|\sigma_M\|^2 \Big) f_M + \big(\mu_X + \sigma_M \cdot \sigma_X \big) \frac{\partial f_M}{\partial x} + \frac{1}{2} \|\sigma_X\|^2 \frac{\partial^2 f_M}{\partial x^2}. \tag{96}$$

The initial condition is $f_M(0,x) \equiv 1$, which allows us to recover the desired conditional expectation. The PDE in (96) is solved using finite difference methods. We obtain $\varepsilon_M(t,x)$ by numerically differentiating $f_M(t,x)$ and substituting it into (95).

Alternatively, we can compute the expectation term by simulating M using μ_M and σ_M and taking the mean across simulations for each (t,x). We find that both methods generate the same results for the figures used in the paper. However, discrepancies arise when we initialize the state variable near the boundaries of the state space grid. In these cases, the simulation method shows strong mean reversion, as illustrated in 16.

The term structure of uncertainty prices is formed as a second type of shock elasticity, which differs conceptually from the first type described above. While $\varepsilon_M(t,x)$ measures the expected response of M_t to a shock at time 0, we could also compute the expected response

[1] Further details on TensorFlow's Glorot normal initializer are available here.

[2] Our results are robust after increasing the number of points in each individual training set.

[3] In our training, we prioritize ensuring that first-order conditions are met by setting $\lambda_{\mathcal{L}} = 10,000$. This penalization effectively reduces L_κ to a range between 10^{-11} and 10^{-14}.

[4] A detailed explanation of the BFGS algorithm implemented in SciPy can be found here.

[5] We choose the BFGS algorithm over Adam due to its higher efficiency in our tests. BFGS achieves a rapid reduction in composite loss and attains lower validation errors across three models.

[6] We choose $n = 5$ and set tolerance as 10^{-4}. Our results are robust for $n \geqslant 5$.

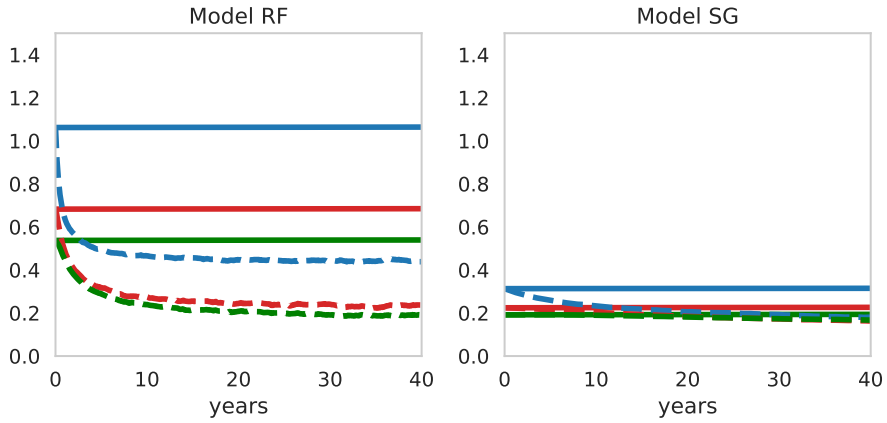

Figure 16: Capital shock price elasticities for RF and SG. The solid lines represent elasticities computed using finite differences, while the dashed lines represent elasticities computed using simulations. The green curve gives elasticities when W is initialized at the 0.02, the red curve at the 0.016 and the blue curve at the 0.012. The difference between the two methods increases as the initial point moves closer to the boundary at zero

of M_t to a shock at the same time t. We can compute this alternative shock elasticity via

$$\tilde{\varepsilon}_M(t,x) = \nu(x) \cdot \frac{\mathbb{E}[\frac{M_t}{M_0}\sigma_M(X_t) \mid X_0 = x]}{\mathbb{E}[\frac{M_t}{M_0} \mid X_0 = x]}, \tag{97}$$

The calculation of term structure of uncertainty prices requires solving the PDE (96) with initial conditions $f_M(0,x) \equiv \sigma_M(x)$ to obtain the numerator. Note that the denominator is 1 due to the martingale property.

References

Achdou, Yves, Jiequn Han, Jean-Michel Lasry, Pierre-Louis Lions, and Benjamin Moll. 2022. Income and wealth distribution in macroeconomics: A continuous-time approach. *The Review of Economic Studies* 89 (1):45–86.

Al-Aradi, Ali, Adolfo Correia, Gabriel Jardim, Danilo de Freitas Naiff, and Yuri Saporito. 2022. Extensions of the deep Galerkin method. *Applied Mathematics and Computation* 430:127287.

Andrei, Daniel, Michael Hasler, and Alexandre Jeanneret. 2019. Asset Pricing with Persistence Risk. *The Review of Economic Studies* 32:2809–2849.

Bansal, R. and A. Yaron. 2004. Risks for the Long Run: A Potential Resolution of Asset Pricing Puzzles. *The Journal of Finance* 59 (4):1481–1509.

Barles, Guy and Panagiotis E Souganidis. 1991. Convergence of approximation schemes for fully nonlinear second order equations. *Asymptotic Analysis* 4 (3):271–283.

Barnett, Michael, William Brock, Lars Peter Hansen, Ruimeng Hu, and Joseph Huang. 2023. A Deep Learning Analysis of Climate Change, Innovation, and Uncertainty. SSRN.

Basak, Suleyman and Domenico Cuoco. 1998. An equilibrium model with restricted stock market participation. *The Review of Financial Studies* 11 (2):309–341.

Bianchi, Javier. 2011. Overborrowing and systemic externalities in the business cycle. *The American Economic Review* 101 (7):3400–3426.

Borovička, Jaroslav, Lars Peter Hansen, and Jose A Scheinkman. 2014. Shock Elasticities and Impulse Responses. *Mathematics and Financial Economics* 8.

Brock, W and L Mirman. 1972. Optimal Economic Growth and Uncertainty: The Discounted Case. *Journal of Economic Theory* 4:479–513.

Brock, William A and Michael JP Magill. 1979. Dynamics under uncertainty. *Econometrica: Journal of the Econometric Society* 843–868.

Brunnermeier, Markus K and Yuliy Sannikov. 2014. A macroeconomic model with a financial sector. *The American Economic Review* 104 (2):379–421.

———. 2015. International credit flows and pecuniary externalities. *American Economic Journal: Macroeconomics* 7 (1):297–338.

———. 2016. The I theory of money. Tech. rep., National Bureau of Economic Research.

Cerreia-Vioglio, Simone, Lars Peter Hansen, Fabio Maccheroni, and Massimo Marinacci. 2024. Making Decisions under Model Misspecification. Bocconi University and University of Chicago.

Chen, Hui, Winston Wei Dou, and Leonid Kogan. 2024. Measuring "Dark Matter" in Asset Pricing Models. *The Journal of Finance* 79 (2):843–902.

Chen, Zengjing and Larry Epstein. 2002. Ambiguity, Risk, and Asset Returns in Continuous Time. *Econometrica* 70:1403–1443.

Christiano, Lawrence J, Roberto Motto, and Massimo Rostagno. 2014. Risk shocks. *The American Economic Review* 104 (1):27–65.

Cochrane, John, Francis A. Longstaff, and Pedro Santa-Clara. 2008. Two Trees. *Review of Financial Studies* 21:347–385.

Cox, John C, Jonathan E Ingersoll Jr, and Stephen A Ross. 1985. An intertemporal general equilibrium model of asset prices. *Econometrica: Journal of the Econometric Society* 363–384.

Crouzet, Nicolas, Janice C. Eberly, Andrea L. Eisfeldt, and Dimitris Papanikolaou. 2022. The Economics of Intangible Capital. *Journal of Economic Perspectives* 36:29 –52.

Di Tella, Sebastian. 2017. Uncertainty shocks and balance sheet recessions. *Journal of Political Economy* 125 (6):2038–2081.

———. 2019. Optimal Regulation of Financial Intermediaries. *The American Economic Review* 109 (1):271–313.

Dou, Winston W., Andrew W. Lo, Ameya Muley, and Harald Uhlig. 2020. Macroeconomic Models for Monetary Policy: A Critical Review from a Finance Perspective. *Annual Review of Financial Economics* 12:95–140.

Drechsler, Itamar, Alexi Savov, and Philipp Schnabl. 2018. A model of monetary policy and risk premia. *The Journal of Finance* 73 (1):317–373.

Duarte, Victor, Diogo Duarte, and Dejanir Silva. 2023. Machine learning for continuous-time finance. *SSRN, 2023a. URL https://ssrn. com/abstract=* 3012602.

Duffie, D. and L. G. Epstein. 1992a. Stochastic Differential Utility. *Econometrica* 60 (2):353–394.

Duffie, Darrell and Larry G Epstein. 1992b. Asset pricing with stochastic differential utility. *The Review of Financial Studies* 5 (3):411–436.

Dumas, Bernard, Raman Uppal, and Tan Wang. 2000. Efficient Intertemporal Allocations with Recursive Utility. *Journal of Economic Theory* 93:240–259.

d'Avernas, Adrien, Damon Petersen, and Quentin Vandeweyer. 2022. A Solution Method for Continuous-Time Models. Unpublished working paper.

Eberly, Janice C and Neng Wang. 2009. Capital Reallocation and Growth. *American Economic Review* 99 (2):560–566.

Eberly, Janice C. and Neng Wang. 2011. Reallocating and Pricing Illiquid Capital: Two Productive Trees. Workingpaper, Columbia Unversity and Northwestern University.

Eberly, Janice C and Neng Wang. 2012. Reallocating and Pricing Illiquid Capital: Two Productive Trees.

Fournié, Eric, Jean-Michel Lasry, Jérôme Lebuchoux, Pierre-Louis Lions, and Nizar Touzi. 1999. Applications of Malliavin calculus to Monte Carlo methods in finance. *Finance and Stochastics* 3 (4):391—412.

Gallant, A. Ronald, Peter E. Rossi, and George Tauchen. 1993. Nonlinear Dynamic Structures. *Econometrica* 61:871–907.

Gârleanu, Nicolae and Stavros Panageas. 2015. Young, old, conservative, and bold: The implications of heterogeneity and finite lives for asset pricing. *Journal of Political Economy* 123 (3):670–685.

Garleanu, Nicolae and Lasse Heje Pedersen. 2011. Margin-based asset pricing and deviations from the law of one price. *The Review of Financial Studies* 24 (6):1980–2022.

Gertler, Mark and Peter Karadi. 2011. A model of unconventional monetary policy. *Journal of monetary Economics* 58 (1):17–34.

Gertler, Mark and Nobuhiro Kiyotaki. 2010. Financial intermediation and credit policy in business cycle analysis. In *Handbook of monetary economics*, vol. 3, 547–599. Elsevier.

———. 2015. Banking, liquidity, and bank runs in an infinite horizon economy. *The American Economic Review* 105 (7):2011–43.

Good, Irving J. 1952. Rational Decisions. *Journal of the Royal Statistical Society. Series B (Methodological)* 14.

Gopalakrishna, Goutham. 2022. A Macro-Finance Model with Realistic Crisis Dynamics. Unpublished working paper.

Gromb, Denis and Dimitri Vayanos. 2002. Equilibrium and welfare in markets with financially constrained arbitrageurs. *Journal of Financial Economics* 66 (2-3):361–407.

Haddad, Valentin. 2014. Concentrated ownership and equilibrium asset prices. Princeton University.

Hansen, L P, B Szőke, L S Han, and T J Sargent. 2020. Twisted probabilities, uncertainty, and prices. *Journal of Econometrics* 216:151–174.

Hansen, Lars Peter. 2007. Beliefs, Doubts and Learning: Valuing Macroeconomic Risk. *American Economic Review* 97:1–30.

———. 2014. Nobel lecture: Uncertainty outside and inside economic models. *Journal of Political Economy* 122:945–987.

Hansen, Lars Peter and Thomas J Sargent. 2021. Macroeconomic uncertainty prices when beliefs are tenuous. *Journal of Econometrics* 223:222–250.

———. 2022. Structured Ambiguity and Model Misspecification. *Journal of Economic Theory* 199:1–32.

Hansen, Lars Peter and Thomas J. Sargent. 2023. Risk, Ambiguity, and Misspecification: Decision Theory, Robust Control, and Statistics. *Journal of Applied Econometrics* online:1–31.

Hayashi, Fumio. 1982. Tobin's marginal q and average q: A neoclassical interpretation. *Econometrica: Journal of the Econometric Society* 213–224.

He, Zhiguo and Arvind Krishnamurthy. 2011. A model of capital and crises. *The Review of Economic Studies* 79 (2):735–777.

———. 2013. Intermediary asset pricing. *The American Economic Review* 103 (2):732–70.

———. 2019. A macroeconomic framework for quantifying systemic risk. *American Economic Journal: Macroeconomics* 11 (4):1–37.

Hugonnier, Julien. 2012. Rational asset pricing bubbles and portfolio constraints. *Journal of Economic Theory* 147 (6):2260–2302.

Jacobson, David H. 1973. Optimal Stochastic Linear Systems with Exponential Performance Criteria and Their Relation to Deterministic Differential Games. *IEEE Transactions for Automatic Control* AC-18:1124–1131.

James, Matthew R. 1992. Asymptotic Analysis of Nonlinear Stochastic Risk-Sensitive Control and Differential Games. *Mathematics of Control, Signals and Systems* 5:401–417.

Jermann, Urban J. 1998. Asset pricing in production economies. *Journal of Monetary Economics* 41:257–275.

Jones, Larry E and Rodolfo Manuelli. 1990. A convex model of equilibrium growth: Theory and policy implications. *Journal of Political Economy* 98 (5, Part 1):1008–1038.

Khorrami, Paymon. 2020. The Risk of Risk-Sharing: Diversification and Boom-Bust Cycles. Imperial College, London.

———. 2021. Entry and slow-moving capital: using asset markets to infer the costs of risk concentration. Available at SSRN 2777747.

Khorrami, Paymon and Fernando Mendo. 2023. Rational sentiments and financial frictions.

Klimenko, Nataliya, Sebastian Pfeil, Jean-Charles Rochet, and Gianni De Nicolo. 2016. Aggregate bank capital and credit dynamics.

Koop, Gary, M. Hashem Pesaran, and Simon M. Potter. 1996. Impulse response analysis in nonlinear multivariate models. *Journal of Econometrics* 74:119–147.

Kozak, Serhiy. 2022. Dynamics of bond and stock returns. *Journal of Monetary Economics* 126:188–209.

Kreps, D. M. and E. L. Porteus. 1978. Temporal Resolution of Uncertainty and Dynamic Choice. *Econometrica* 46 (1):185–200.

Krishnamurthy, Arvind and Wenhao Li. 2021. Dissecting Mechanisms of Financial Crises: Intermediation and Sentiment. Tech. rep., NBNER Working 27088.

Lucas, R E. 1978. Asset Prices in an Exchange Economy. *Econometrica* 46:1429–1445.

Lucas, Robert E and Edward C Prescott. 1971. Investment Under Uncertainty. *Econometrica* 39:659–681.

Maccheroni, Fabio, Massomp Marinacci, and Aldo Rustichini. 2006. Ambiguity Aversion, Robustness, and the Variational Representation of Preferences. *Econometrica* 74:1147–1498.

Martin, Ian. 2013. Lucas Orchard. *Econometrica* 81:55–111.

Maxted, Peter. 2024. A macro-finance model with sentiment. *Review of Economic Studies* 91 (1):438–475.

Mendo, Fernando. 2018. Risk to control risk. Unpublished working paper.

Mendoza, Enrique G. 2010. Sudden stops, financial crises, and leverage. *The American Economic Review* 100 (5):1941–66.

Merton, Robert C. 1973. An intertemporal capital asset pricing model. *Econometrica: Journal of the Econometric Society* 867–887.

Moreira, Alan and Alexi Savov. 2017. The macroeconomics of shadow banking. *The Journal of Finance* 72 (6):2381–2432.

Panageas, Stavros. 2020. The implications of heterogeneity and inequality for asset pricing. *Foundations and Trends® in Finance* 12 (3):199–275.

Petersen, Ian R., Matthew R. James, and Paul Dupuis. 2000. Minimax Optimal Control of Stochastic Uncertain Systems with Relative Entropy Constraints. *IEEE Transactions on Automatic Control* 45:398–412.

Phelan, Gregory. 2016. Financial intermediation, leverage, and macroeconomic instability. *American Economic Journal: Macroeconomics* 8 (4):199–224.

Schorfheide, Frank, Dongho Song, and Amir Yaron. 2018. Identifying Long-Run Risks: A Bayesian Mixed-Frequency Approach. *Econometrica* 86:617–654.

Silva, Dejanir H. 2016. The risk channel of unconventional monetary policy. Tech. rep., Working Paper, MIT.

Sirignano, Justin and Konstantinos Spiliopoulos. 2018. DGM: A deep learning algorithm for solving partial differential equations. *Journal of Computational Physics* 375:1339–1364.

Whittle, Peter. 1981. Risk Sensitive Linear Quadratic Gaussian Control. *Advances in Applied Probability* 13:764–777.